



SILVER-CATALYZED CASCADE CONVERSIONS OF CO₂ INTO HETEROCYCLES

Xuetong Li

ADVERTIMENT. L'accés als continguts d'aquesta tesi doctoral i la seva utilització ha de respectar els drets de la persona autora. Pot ser utilitzada per a consulta o estudi personal, així com en activitats o materials d'investigació i docència en els termes establerts a l'art. 32 del Text Refós de la Llei de Propietat Intel·lectual (RDL 1/1996). Per altres utilitzacions es requereix l'autorització prèvia i expressa de la persona autora. En qualsevol cas, en la utilització dels seus continguts caldrà indicar de forma clara el nom i cognoms de la persona autora i el títol de la tesi doctoral. No s'autoritza la seva reproducció o altres formes d'explotació efectuades amb finalitats de lucre ni la seva comunicació pública des d'un lloc aliè al servei TDX. Tampoc s'autoritza la presentació del seu contingut en una finestra o marc aliè a TDX (framing). Aquesta reserva de drets afecta tant als continguts de la tesi com als seus resums i índexs.

ADVERTENCIA. El acceso a los contenidos de esta tesis doctoral y su utilización debe respetar los derechos de la persona autora. Puede ser utilizada para consulta o estudio personal, así como en actividades o materiales de investigación y docencia en los términos establecidos en el art. 32 del Texto Refundido de la Ley de Propiedad Intelectual (RDL 1/1996). Para otros usos se requiere la autorización previa y expresa de la persona autora. En cualquier caso, en la utilización de sus contenidos se deberá indicar de forma clara el nombre y apellidos de la persona autora y el título de la tesis doctoral. No se autoriza su reproducción u otras formas de explotación efectuadas con fines lucrativos ni su comunicación pública desde un sitio ajeno al servicio TDR. Tampoco se autoriza la presentación de su contenido en una ventana o marco ajeno a TDR (framing). Esta reserva de derechos afecta tanto al contenido de la tesis como a sus resúmenes e índices.

WARNING. Access to the contents of this doctoral thesis and its use must respect the rights of the author. It can be used for reference or private study, as well as research and learning activities or materials in the terms established by the 32nd article of the Spanish Consolidated Copyright Act (RDL 1/1996). Express and previous authorization of the author is required for any other uses. In any case, when using its content, full name of the author and title of the thesis must be clearly indicated. Reproduction or other forms of for profit use or public communication from outside TDX service is not allowed. Presentation of its content in a window or frame external to TDX (framing) is not authorized either. These rights affect both the content of the thesis and its abstracts and indexes.



UNIVERSITAT
ROVIRA I VIRGILI

Silver-Catalyzed Cascade Conversions of CO₂ into Heterocycles

Xuetong Li



DOCTORAL THESIS

2023

UNIVERSITAT ROVIRA I VIRGILI
SILVER-CATALYZED CASCADE CONVERSIONS OF CO₂ INTO HETEROCYCLES
Xuetong Li

UNIVERSITAT ROVIRA I VIRGILI
SILVER-CATALYZED CASCADE CONVERSIONS OF CO₂ INTO HETEROCYCLES
Xuetong Li

UNIVERSITAT ROVIRA I VIRGILI
SILVER-CATALYZED CASCADE CONVERSIONS OF CO₂ INTO HETEROCYCLES
Xuetong Li

PhD Thesis

**“Silver-Catalyzed Cascade Conversions of CO₂ into
Heterocycles”**

Xuetong Li

Supervised by Prof. Dr. Arjan W. Kleij

Tarragona

September 2023



UNIVERSITAT
ROVIRA i VIRGILI



UNIVERSITAT ROVIRA I VIRGILI
SILVER-CATALYZED CASCADE CONVERSIONS OF CO₂ INTO HETEROCYCLES
Xuetong Li



Prof. Dr. Arjan W. Kleij, Group Leader at the Institute of Chemical Research of Catalonia (ICIQ) and Research Professor at the Catalan Institution for Research and Advanced Studies (ICREA):

I STATE that the present Doctoral Thesis, entitled “**Silver-Catalyzed Cascade Conversions of CO₂ into Heterocycles**” presented by Xuetong Li to receive the degree of Doctor, has been carried out under my supervision at the Institute of Chemical Research of Catalonia (ICIQ).

Tarragona, September 2023

Doctoral Thesis Supervisor

Prof. Dr. Arjan W. Kleij

UNIVERSITAT ROVIRA I VIRGILI
SILVER-CATALYZED CASCADE CONVERSIONS OF CO₂ INTO HETEROCYCLES
Xuetong Li

Curriculum Vitae

Xuetong Li was born on the 25th of May in 1993 in Shaanxi province, China. She started studying chemistry at Xianyang Normal University and obtained her BSc degree in July 2016. Then she moved to Shaanxi Normal University in Xi'an, where she received her MSc degree in 2019 with a major in organic chemistry under the supervision of Prof. Tao Wang. During the MSc period, her main research focus was on cascade reactions of (iso)quinoline *N*-oxides with alkynones, resulting in the formation of (iso)quinoline derivatives. Hereafter, she successfully applied for a predoctoral fellowship awarded by Chinese Scholarship Council (CSC). From November 2019 until September 2023, she performed her PhD studies in the group of Prof. Arjan W. Kleij at the Institute of Chemical Research of Catalonia. Here she focused on silver-catalyzed cascade conversions of CO₂ to produce new types of heterocycles, and the results are presented in this thesis. Part of this PhD research was communicated as a poster at the XXV Conference on Organometallic Chemistry (EuCOMC XXV, 2023) in Alcalá de Henares, Spain.

UNIVERSITAT ROVIRA I VIRGILI
SILVER-CATALYZED CASCADE CONVERSIONS OF CO₂ INTO HETEROCYCLES
Xuetong Li

Acknowledgments

Four years have passed in the blink of an eye since I arrived at Tarragona for the first time in October of 2019. At this special and unforgettable moment, I look back and think over my four years of chemistry-related experiences at the Institute of Chemical Research of Catalonia (ICIQ). There is no doubt that my doctoral thesis could not have been achieved in the absence of support and participation from other people. I would like to take this precious opportunity to express my sincerest gratitude to those who have constantly helped me during this process.

First and foremost, I would like to thank my supervisor, Professor **Arjan W. Kleij**, for providing me with this incredible opportunity to pursue my doctoral research under his guidance. Especially I am grateful for his constant confidence, patience and encouragement that he gave me at all stages to accomplish this doctoral dissertation. Furthermore, in our daily communication, his humor, kindness and optimism cheered me up, and provided me with more energy to overcome all difficulties. Unfortunately, I could not finish my third research project because of my health problems. Nonetheless, he still encouraged me to face these things positively and helped me to complete my thesis on time. For me, he is not only my mentor, but also a respectable elder and friend. Some caring words from him keep repeating in my ears and touch me: “Xuetong, don’t worry, trust me, I will help you”. This short but powerful sentence will inspire me in my personal and professional future. I am deeply proud to have been able to grow as a scientist under his supervision.

I also would particularly like to thank my co-authors **Alba Villar, Charlene Ngassam Tounzoua, Jordi Benet-Buchholz, Bruno Grignard, Carles Bo, Christophe Detrembleur and Eduardo C. Escudero-Adán**. Their substantial contributions to the work presented in this thesis is really appreciated and I very much enjoyed the scientific collaborations.

Many thanks also to all the former and present members of the Kleij group at ICIQ with whom I had the pleasure to spend my PhD: **Jianing Xie, Alèria García, Kun Guo, Debasish Ghorai, Nicola Zanda, Sijing Xue, Chang Qiao, Qian Zeng, Wangyu Shi, Fengyun Gao, Alejandro Delgado, David Lamparelli, Matteo Lanzi, Balázs Tóth, Francesco Della Monica, Bart Limburg, Dimitrios Skoulas, Thirusangumurugan Senthamarai, Àlex Cristòfol, Alba Villar, Jixiang Ni, Diego Meneses, Lorenz Dittrich, Arianna Brandolese, Cristina Maquilón, Ilaria Grimaldi and Aijie Cai**. Because of the emergence of the COVID epidemic, we lost many opportunities to participate in activities together. But I’ll never forget the help and advice you have given to me, it has been a pleasure to work with you guys, many

thanks! I would particularly like to thank **Jianing Xie**, it was an extraordinary experience. Thanks for sharing your knowledge, and helping me to adapt to the new environment. During the year we worked together, I benefitted a lot from your many insightful suggestions and our discussions, I will never forget the first Christmas you spent here with me. **Chang**, I cannot forget the first high pressure reaction I set up here with your help, thank you for sharing your research experience about carbon dioxide with me and helping me to analyze and solve the experimental problems. **Wangyu**, thanks for your countless support when I needed to set up high-pressure reactions, and your care when I faced health problems. I wish you all the best with your research and upcoming thesis completion and defense. **Chenyang**, thanks for joining my last project. Unfortunately, we were not able to work together for a long time due to my health problems. I see you as a positive and optimistic girl, best wishes for your personal life and career.

I would also like to thank ICIQ's research support are: the IT department, HR, maintenance and SHEQ unit. Especially, I would like to express my gratitude to the NMR, X-ray and Mass units. Many thanks to our secretaries/administrative support including **Ingrid, Núria, Eva and Cristina**. Without your support, it would have been much harder for me to complete my PhD work!

I would like to express my gratitude for the financial support from the CSC (China Scholarship Council), as well as the meticulous work of the education group in Spain. With your kind support, I have had the opportunity to experience a completely different research atmosphere while being exposed to the rich Mediterranean culture.

Last but not least, I would like to express my deepest gratitude to my family for all their love and encouragement. Especially, to my parents, because of your company my life is filled with sunshine and happiness allowing me to actively face the challenges in work and life. Our deep love for each other will never be blocked by mountains or oceans. I look forward to our future together full of happiness. The experience of living in Tarragona and working at ICIQ is a precious memory worth cherishing my whole life. In the near future, I will return to my homeland and I will tell the story of this beautiful city to my fellow countrymen.

Xuetong Li, 2023

List of Publications

The results described in this doctoral thesis are based on the following publications:

- **X. Li**, A. Villar-Yanez, C. Ngassam Tounzoua, J. Benet-Buchholz, B. Grignard, C. Bo, C. Detrembleur, A. W. Kleij, “Cascade Transformation of Carbon Dioxide and Alkyne-1,*n*-diols into Densely Substituted Cyclic Carbonates”. *ACS. Catal.* **2022**, *12*, 2854–2860.
- **X. Li**, J. Benet-Buchholz, E. C. Escudero-Adán, A. W. Kleij, “Silver-Mediated Cascade Synthesis of Functionalized 1,4-dihydro-2*H*-Benzo-1,3-Oxazin-2-Ones from Carbon Dioxide”. *Angew. Chem. Int. Ed.* **2023**, *62*, [e202217803](https://doi.org/10.1002/anie.202217803).

Other contribution from the PhD period:

- J. Xie, **X. Li**, A. W. Kleij, “Pd-Catalyzed Stereoselective Tandem Ring-Opening Amination/Cyclization of Vinyl Gamma-Lactones: Access to Caprolactam Diversity”. *Chem. Sci.* **2020**, *11*, 8839–8845.

UNIVERSITAT ROVIRA I VIRGILI
SILVER-CATALYZED CASCADE CONVERSIONS OF CO₂ INTO HETEROCYCLES
Xuetong Li

List of Abbreviations

In this doctoral thesis, the abbreviations and acronyms most commonly used in organic chemistry are based on the recommendations of the ACS “Guidelines for authors” which can be found and consulted at:

<https://www.cas.org/support/documentation/references/cas-standard-abbreviations#listinga>.

UNIVERSITAT ROVIRA I VIRGILI
SILVER-CATALYZED CASCADE CONVERSIONS OF CO₂ INTO HETEROCYCLES
Xuetong Li

Table of Contents

Chapter 1 Introduction.....	1
1.1 Carbon dioxide	1
1.2 Formation of heterocycles compounds	2
1.2.1 CO ₂ -based cyclic carbonates.....	3
1.2.2 CO ₂ -based cyclic carbamates.....	7
1.3 Cascade processes with CO ₂	11
1.4 Main objective and outline of this thesis.....	13
Chapter 2 Cascade Transformation of Carbon Dioxide and Alkyne-1,n-diols into Densely Substituted Cyclic Carbonates	15
2.1 Introduction	17
2.2 Aims of the work.....	18
2.3 Results and discussion.....	20
2.4 DFT studies	27
2.5 Conclusions	30
2.6 Experimental section	31
2.6.1 General information	31
2.6.2 Further screening data of the reaction conditions	32
2.6.3 Experimental procedures and characterization data for substrates	37
2.6.4 Procedures and characterization data for the carbonate products	46
2.6.5 Catalytic screening towards larger ring cyclic carbonates.....	57
2.6.6 Synthetic and analytical details for compound 2.11 and 2.12	67
2.6.7 X-ray details.....	69
2.6.8 DFT details.....	72
Chapter 3 Silver-Mediated Cascade Synthesis of Functionalized 1,4-Dihydro-2H-benzo-1,3-oxazin-2-ones from Carbon Dioxide	75
3.1 Introduction	77
3.2 Aims and objectives	80

3.3	Results and discussion.....	83
3.4	Conclusions	92
3.5	Experimental section	93
3.5.1	General comments	93
3.5.2	Preliminary results with various types of substrates.....	94
3.5.3	Optimization of the reaction condition.....	98
3.5.4	Experimental procedures and characterization data for the substrates	100
3.5.5	Procedures and characterization data for the cyclic carbamate products.....	106
3.5.6	Experimental procedures for the product diversification.....	118
3.5.7	X-ray details.....	122
3.5.8	Additional control experiments and data	126
	<i>Chapter 4 Summary and General Conclusions</i>	<i>129</i>

Chapter 1.

Introduction

UNIVERSITAT ROVIRA I VIRGILI
SILVER-CATALYZED CASCADE CONVERSIONS OF CO₂ INTO HETEROCYCLES
Xuetong Li

1.1 Carbon dioxide

The concentration of carbon dioxide, considered to be a greenhouse gas, has been constantly increasing in the atmosphere over a period of hundreds of years. This has been largely associated to anthropogenic activities, and recently also linked to the occurrence of a more extreme climate.¹ According to the Global Energy & CO₂ Status Report 2019, the emissions of CO₂ into the atmosphere have reached a detrimental level of 33.1 Gt per annum.² This dramatic rise of carbon dioxide emissions endangers the balance within our natural ecosystems and threatens the survival of globally occurring species. To address this escalating amount of CO₂, various initiatives have been proposed among which are “carbon” capture and storage. These are regarded as promising strategies to mitigate CO₂ emissions. While the use of carbon dioxide in chemistry as a carbon feedstock will not have any significant effect on these emissions due to a large off-set between both scales, it may act as a cheap and renewable one-carbon (C1) source to provide high-value-added organic molecules.³

Recently, in the realm of green and sustainable chemistry, carbon dioxide has become a prime source of attention. Compared to products based on petrochemical feedstock, production of chemicals from CO₂ could lead to efficient and economical alternatives to existing chemical intermediates and products and result into a significant contribution to social awareness.^{3a,4,5,6}

¹ (a) A. E. Creamer, B. Gao, *Environ. Sci. Technol.* **2016**, *50*, 7276–7289; (b) M. Meinshausen, N. Meinshausen, W. Hare, S. C. B. Raper, K. Frieler, R. Knutti, D. J. Frame, M. R. Allen, *Nature* **2009**, *458*, 1158–1162; (c) D. Keith, *Science* **2009**, *325*, 1654–1655; (d) M. Cokoja, C. Bruckmeier, B. Rieger, W. A. Herrmann and E. Fritz, *Angew. Chem. Int. Ed.* **2011**, *50*, 8510–8537; (e) L. M. Alsarhan, A. S. Alayyar, N. B. Alqahtani and N. H. Khadry, *Sustainability* **2021**, *13*, 11625–11650; (f) A. Saravan, P. S. Kumar, D. -V. N. Vo, S. Jeevanantham, V. Bhuvaneshwari, V. A. Narayanan, P. R. Yaashikaa, S. Wetha, B. Reshma, *Chem. Eng. Sci.* **2021**, *236*, 116515–116531.

² See: <https://www.iea.org/reports/global-energyco2-statusreport-2019>.

³ (a) M. Aresta, *Carbon Dioxide as Chemical Feedstock*, Wiley-VCH, Weinheim, **2010**, pp. 9–13; (b) K. Huang, C.-L. Sun, Z.-J. Shi, *Chem. Soc. Rev.* **2011**, *40*, 2435–2452; (c) R. Martin, A. W. Kleij, *ChemSusChem* **2011**, *4*, 1259–1263; (d) Y. Tsuji, T. Fujihara, *Chem. Commun.* **2012**, *48*, 9956–9964; (e) W. Zhang, X. Lu, *Chin. J. Catal.* **2012**, *33*, 745–756; (f) L. Zhang, Z. Hou, *Chem. Sci.* **2013**, *4*, 3395–3403; (g) Q. Liu, L. Wu, R. Jackstell, M. Beller, *Nat. Commun.* **2015**, *6*, 5933; (h) B. Yu, L. N. He, *ChemSusChem* **2015**, *8*, 52–62; (i) D. Yu, S. P. Teong, Y. Zhang, *Coord. Chem. Rev.* **2015**, *293–294*, 279–291; (j) S. Wang, G. Du, C. Xi, *Org. Biomol. Chem.* **2016**, *14*, 3666–3676; (k) Q. Zhu, L. Wang, C. Xia, C. Liu, *Chin. J. Org. Chem.* **2016**, *36*, 2813–2821; (l) G. Yuan, C. Qi, W. Wu, H. Jiang, *Curr. Opin. Green Sust. Chem.* **2017**, *3*, 22–27; (m) A. W. Kleij, M. North, A. Urakawa, *ChemSusChem* **2017**, *10*, 1036–1038; (n) Z. Zhang, T. Ju, J.-H. Ye, D.-G. Yu, *Synlett* **2017**, *28*, 741–750.

⁴ L.-N. He, *Carbon Dioxide Chemistry*, Chinese Science Press, Beijing, **2013**.

⁵ D. Riemer, S. Das, in: *CO₂ as a Building Block in Organic Synthesis*, Wiley-VCH, Weinheim, **2020**, pp. 253–285

⁶ L.-N. He, *Chin. Sci. Bull.* **2021**, *66*, 713–715.

For these reasons, this “greenhouse gas” has been long considered an attractive carbon building block in organic synthesis. However, activation of CO₂ represents a huge challenge because of its thermodynamic stability and kinetic inertness and, therefore, suitable methods are required to transform it into useful chemicals.^{5,6}

Faced with this challenging problem and inspired by Nature’s efficiency converting this C1 building block into carbohydrates through photosynthesis, direct activation of carbon dioxide by organometallic was initially explored decades ago. Through the course of time, efficient catalytic methods for C–C and C–O coupling reactions have emerged based on the combination of CO₂ and high-free energy substrates.^{3g,5} In this regard, it is crucial to develop suitable catalysts⁷ that are able to lower the kinetic requirements for the coupling of the involved reaction partners and accelerate the reaction by lowering the activation barrier.

1.2 Formation of heterocycles compounds

Heterocyclic compounds constitute a major class of organic compounds, which are characterized by the fact that some or all of the atoms are joined in rings containing at least one atom of an element other than carbon. The most common heteroatoms are nitrogen, oxygen and sulfur, but heterocyclic rings containing other heteroatoms are also widely known.⁸ Importantly, heterocyclic rings are found in many naturally occurring compounds and pharmaceutically active ingredients. Notably, heterocyclic units can be found in mono- and polysaccharides and in the four DNA bases that make up for genetic codes. According to statistics, more than 85% of all biologically-active chemical compounds contain at least one heterocycle. These observation clearly reflect the key role of heterocycles in modern drug design, biochemistry and natural products.⁹ Furthermore, heterocyclic derivatives are also

⁷ (a) T. Sakakura, J.-C. Choi, H. Yasuda, *Chem. Rev.* **2007**, *107*, 2365–2387; (b) J. Artz, T. E. Müller, K. Thenert, J. Kleinekorte, R. Meys, A. Sternberg, A. Bardow, W. Leitner, *Chem. Rev.* **2018**, *118*, 434–504. See also ref. 3g.

⁸ (a) T. Eicher, S. Hauptmann, A. Speicher, *The Chemistry of Heterocycles: Structures, Reactions, Synthesis, and Applications*, Wiley, Weinheim **2013**; (b) J. A. Joule, K. Mills, *Heterocyclic Chemistry at a Glance*, Wiley, Weinheim **2012**; (c) V. A. Petrov, *Fluorinated Heterocyclic Compounds: Synthesis, Chemistry, and Applications*, Wiley, Weinheim **2009**.

⁹ (a) Q. Jin, X. Wang, S. Li, H. Mikulčić, T. Bešenić, S. Deng, M. Vujanović, H. Tan, B. M. Kumfer, *J. Energy Inst.* **2019**, *92*, 108–117; (b) J. Jampilek, *Molecules* **2019**, *24*, No. 3839; (c) P. N. Kalaria, S. C. Karad, D. K. Raval, *Eur. J. Med. Chem.* **2018**, *158*, 917–936; (d) M. Kidwai, R. Venktaramanan, R. Mohan, P. Sapra, *Curr. Med. Chem.* **2002**, *9*, 1209–1228.

widely applied in agriculture, plastic production, new polymer development and in other fields.¹⁰

CO₂-based cyclic carbonates and carbamates have become a major heterocyclic focus in the area of non-reductive carbon dioxide valorization catalysis, and their relevance and use will be discussed in more detail (*vide infra*).

1.2.1 CO₂-based cyclic carbonates

Cyclic carbonates as small heterocycles that have received increasing attention both at an academic and industrial level, because their synthesis and applications have several attractive features (Figure 1.1). For instance, these heterocyclic structures have been considered as monomers for polycarbonate synthesis. In addition, organic cyclic carbonates also can be applied as green solvents, electrolytes for lithium batteries, and as synthetic intermediates in phenobarbital synthesis.¹¹ Taking the conventional synthesis of cyclic carbonates from diols and triphosgene as a reference, some critical challenges still needed to be solved in terms of (a) finding effective catalysis approaches, (b) increasing process sustainability, and (c) the limitations in the scope of (functional) cyclic carbonates. These challenges have been the focal point of many research groups contributing to the area thereby resulting in a vibrant community. Some of these developments will be discussed below as a prelude to the results described in this thesis.

Until now, the most prominent and effective method for the preparation of cyclic carbonates also at an industrial level is the (3+2) cycloaddition of CO₂ to epoxides. For this reaction, there are several advantages including the use of a renewable, nontoxic and widely available reactant (CO₂), a 100% atom efficiency as all reactants are incorporated in the product, and the possibility to run these processes solvent-free (Figure 1.1).

¹⁰ R. Merten, *Angew. Chem. Int. Ed. Engl.* **1971**, *10*, 294–301; (b) A. F. Pozharskii, A. R. Katritzky, A. T. Soldatenkov, *Heterocycles in Life and Society*, Wiley, Chichester, **2011**.

¹¹ For selected reviews on CO₂-related cyclic carbonate synthesis and utilization, see: (a) L. Guo, K. J. Lamb, M. North, *Green Chem.* **2021**, *23*, 77–118; (b) P. P. Pescarmona, *Curr. Opin. Green Sustain. Chem.* **2021**, *29*, No. 100457; (c) P. Rollin, L. K. Soares, A. M. Barcellos, D. R. Araujo, E. J. Lenardão, R. G. Jacob, G. Perin, *Appl. Sci.* **2021**, *11*, No. 5024; (d) M. Ghasemlou, F. Daver, E. P. Ivanova, B. Adhikari, *Eur. Polym. J.* **2019**, *118*, 668–684; (e) A. J. Kamphuis, F. Picchioni, P. P. Pescarmona, *Green Chem.* **2019**, *21*, 406–448; (f) S. Wang, C. Xi, *Chem. Soc. Rev.* **2019**, *48*, 382–404.

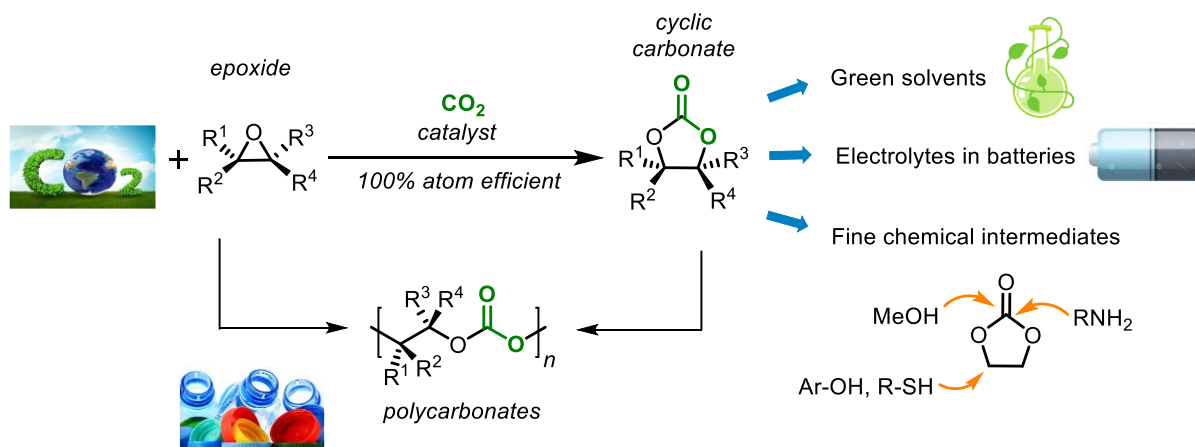


Figure 1.1 Synthesis of cyclic carbonates from CO₂ and epoxides and selected applications.

In order to expand the synthetic repertoire of CO₂-derived cyclic carbonates, additional approaches have been presented by Trost,¹² Gagosz,¹³ and Nishizawa¹⁴ individually (Scheme 1.1). Whereas these approaches are not necessarily atom-economic or sustainable, unique classes of unexplored cyclic alkylidene carbonates could be prepared by using silver catalysis empowered by bulky ligands such as DavePhos or *N*-heterocyclic carbenes¹⁵ and using propargylic alcohols and CO₂ as starting materials. These specific catalytic systems achieved the direct carboxylation cyclization of propargylic alcohols. Apart from using silver catalysts,

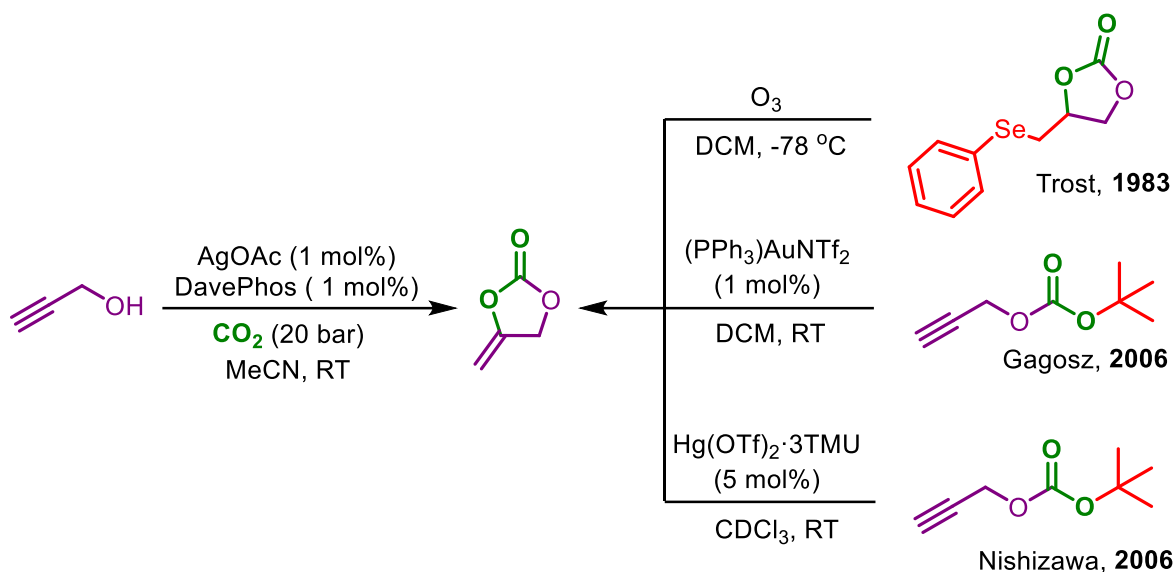
¹² B. M. Trost, D. M. T. Chan, *J. Org. Chem.* **1983**, *48*, 3346–3347.

¹³ (a) A. Buzas, F. Gagosz, *Org. Lett.* **2006**, *8*, 515–518; (b) A. K. Buzas, F. M. Istrate, F. Gagosz, *Tetrahedron* **2009**, *65*, 1889–1901.

¹⁴ H. Yamamoto, M. Nishiyama, H. Imagawa, M. Nishizawa, *Tetrahedron Lett.* **2006**, *47*, 8369–8373.

¹⁵ (a) S. Dabral, B. Bayarmagnai, M. Hermsen, J. Schießl, V. Mormul, A. S. K. Hashmi, T. Schaub, *Org. Lett.* **2019**, *21*, 1422–1425. For some other Ag-based catalytic processes related to the coupling of propargylic alcohols and CO₂, see (b) Q.-W. Song, L.-N. He, *Adv. Synth. Catal.* **2016**, *358*, 1251–1258; (c) S. Kikuchi, S. Yoshida, Y. Sugawara, W. Yamada, H.-M. Cheng, K. Fukui, K. Sekine, I. Iwakura, T. Ikeno, T. Yamada, *Bull. Chem. Soc. Jpn.* **2011**, *84*, 698–717, (d) Q. Song, W. Chen, R. Ma, A. Yu, Q. Li, Y. Chang, L. He, *ChemSusChem* **2015**, *8*, 821–827; (e) W. Yamada, Y. Sugawara, H. Cheng, T. Ikeno, T. Yamada, *Eur. J. Org. Chem.* **2007**, 2604–2607; (f) X. Yu, Z. Yang, F. Zhang, Z. Liu, P. Yang, H. Zhang, B. Yu, Y. Zhao, Z. Liu, *Chem. Commun.*, **2019**, *55*, 12475–12478.

copper complexes,¹⁶ ionic liquids¹⁷ and organic bases¹⁸ also promote the formation of this type of 5-membered cyclic alkylidene carbonate.



Scheme 1.1 Synthetic routes to 5-membered cyclic alkylidene carbonates. TMU stands for tris(tetramethylurea).

Compared to the well-studied formation of *5-membered* cyclic carbonates, literature examples on the preparation of *larger-ring* homologues are relatively scarce. Traditional routes towards the preparation of 6-membered or even larger cyclic carbonates are related to the utilization of phosgene¹⁹ and CO (Scheme 1.2a).²⁰ Due to the toxic nature of these reagents, these processes are not sustainable in terms of environmental impact and safety. With an increasing need for green, economical and sustainable chemical processes, using CO₂ as a C1-

¹⁶ (a) A. Cervantes-Reyes, K. Farshadfar, M. Rudolph, F. Rominger, T. Schaub, A. Ariafard, A. S. K. Hashmi, *Green Chem.* **2021**, *23*, 889–897; (b) H. Jiang, A. Wang, H. Liu, C. Qi, *Eur. J. Org. Chem.* **2008**, 2309–2312; (c) L. Ouyang, X. Tang, H. He, C. Qi, W. Xiong, Y. Ren, H. Jiang, *Adv. Synth. Catal.* **2015**, *357*, 2556–2565; (d) Y. Hu, J. Song, C. Xie, H. Wu, T. Jiang, G. Yang, B. Han, *ACS Sustainable Chem. Eng.* **2019**, *7*, 5614–5619.

¹⁷ Y. Wu, Y. Zhao, R. Li, B. Yu, Y. Chen, X. Liu, C. Wu, Xi. Luo, Z. Liu, *ACS Catal.* **2017**, *7*, 6251–6255.

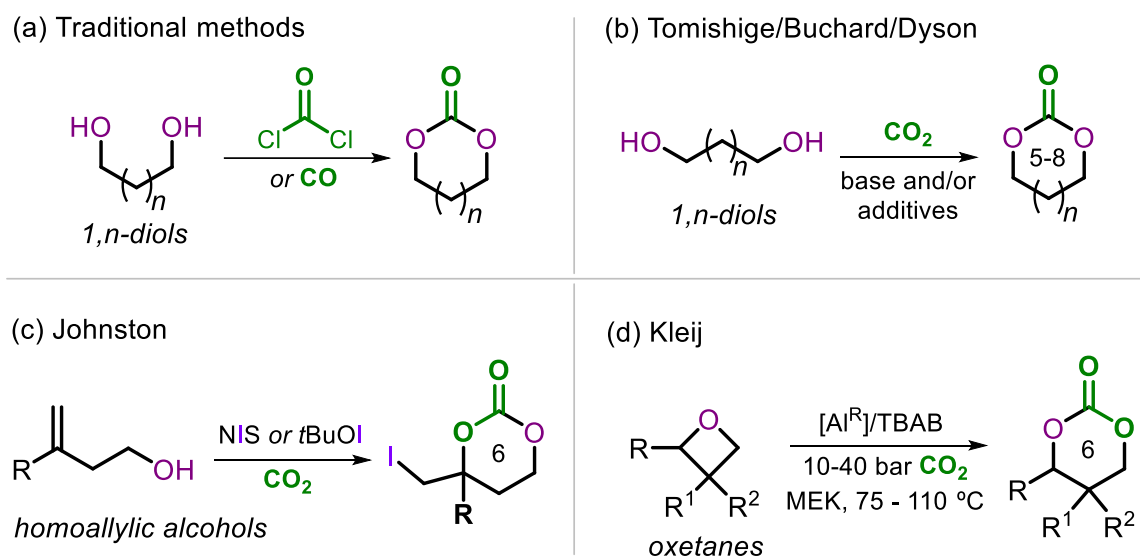
¹⁸ N. Della Ca, B. Gabriele, G. Ruffolo, L. Veltri, T. Zanetta, M. Costaa, *Adv. Synth. Catal.* **2011**, *353*, 133–146

¹⁹ (a) A.-A. G. Shaikh, S. Sivaram, *Chem. Rev.* 1996, *96*, 951–976; (b) G. Rokicki, *Prog. Polym. Sci.* **2000**, *25*, 259–342; (c) A. G. Davies, P. Hua-de, J. A. A. Hawari, *J. Organomet. Chem.* **1983**, *256*, 251–260.

²⁰ (a) B. Gabriele, R. Mancuso, G. Salerno, L. Veltri, M. Costa, A. Dibenedetto, *ChemSusChem* **2011**, *4*, 1778–1786; (b) D. M. Pearson, N. R. Conley, R. M. Waymouth, *Adv. Synth. Catal.* **2011**, *353*, 3007–3013; (c) B. Gabriele, R. Mancuso, G. Salerno, G. Ruffolo, M. Costa, A. Dibenedetto, *Tetrahedron Lett.* **2009**, *50*, 7330–7332.

carbonation agent is an attractive alternative. In this context, efficient procedures have been reported for the synthesis of larger cyclic carbonates which build on the use of CO₂ as a carbonation agent instead of phosgene and CO, see Scheme 1.2b and 1.2c. The examples provided under Scheme 1.2b combine 1,*n*-diols²¹ and CO₂ in the presence of stoichiometric additives, whereas in Scheme 1.2c the preparation of cyclic carbonates with iodo substituents attached to sp³-hybridized carbon atoms is reported using either *N*-iodo-succinimide (NIS) or *tert*-butyl hypoiodite a stoichiometric reactants.²² The final example in Scheme 1.2d is a synthetic methodology that uses oxetanes which are coupled with CO₂ at elevated reaction temperatures/pressures under Al-catalysis.²³

Based on the success attained in the formation of cyclic carbonates from CO₂ as a reagent, cyclic carbamates also appeared on the radar of synthetic chemists as a result of their wide presence in natural compounds and pharmaceuticals. In this sub-area of carbon dioxide valorization space, also new concepts were required to advance the access to these interesting synthons (see section 1.2.2 below).



Scheme 1.2 Reported methods for the synthesis of larger ring cyclic carbonates.

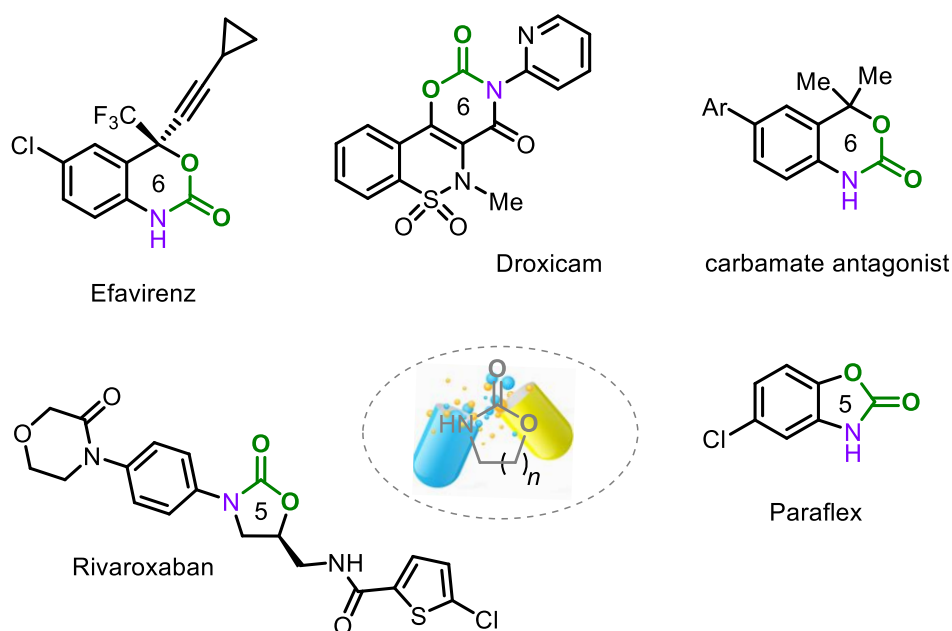
²¹ (a) G. L. Gregory, M. Ulmann, A. Buchard, *RSC Adv.* **2015**, *5*, 39404–39408; (b) M. Honda, M. Tamura, K. Nakao, K. Suzuki, Y. Nakagawa, K. Tomishige, *ACS Catal.* **2014**, *4*, 1893–1896; (c) F. D. Bobbink, W. Gruszka, M. Hulla, S. Das, P. J. Dyson, *Chem. Commun.* **2016**, *52*, 10787–10790.

²² (a) S. Minakata, I. Sasaki, T. Ide, *Angew. Chem. Int. Ed.* **2010**, *49*, 1309–1311; (b) B. A. Vara, T. J. Struble, W. Wang, M. C. Dobish, J. N. Johnston, *J. Am. Chem. Soc.* **2015**, *137*, 7302–7305.

²³ J. Rintjema, W. Guo, E. Martin, E. C. Escudero-Adán, A. W. Kleij, *Chem. Eur. J.* **2015**, *21*, 10754–10762.

1.2.2 CO₂-based cyclic carbamates

Cyclic carbamates represent another family of heterocyclic compounds which are not only useful as building blocks in organic synthesis, but also as small-molecule therapeutics in medicinal chemistry.^{24,25} These scaffolds offer a constrained hydrogen-bond acceptor that is both polar and sterically small. In particular, five-membered and six-membered cyclic carbamates such as five-membered oxazolidinones and six-membered benzoxazine-2-one derivatives exhibit potent biological activity and some examples are shown in Scheme 1.3.²⁶ Benzoxazine-2-one derivatives (i.e., six-membered cyclic carbamates with a fused aryl group) are a specific class of cyclic carbamates with high pharmaceutical relevance as these cores are frequently found in drug molecules such as Efavirenz and Droxicam. Because of their high chemical and proteolytic stability together with the ability to easily penetrate into cells, the carbamate motif has been considered as a very important peptide bond surrogate in drug discovery and development processes.²⁷



Scheme 1.3 Selected drugs containing a cyclic carbamate unit.

²⁴ (a) D. J. Ager, I. Prakash, D. R. Schaad, *Chem. Rev.* **1996**, *96*, 835-876; (b) L. Aurelio, R. T. C. Brownlee, A. B. Hughes, *Chem. Rev.* **2004**, *104*, 5823-5846; (c) T. A. Mukhtar, G. D. Wright, *Chem. Rev.* **2005**, *105*, 529-542.

²⁵ (a) M. R. Barbachyn, *Oxazolidinone Antibacterial Agents*, Springer, Boston, **2012**; (b) A. K. Ghosh, M. Brindisi, *J. Med. Chem.* **2015**, *58*, 2895-2940.

²⁶ (a) M. R. Barbachyn, C. W. Ford, *Angew. Chem. Int. Ed.* **2003**, *42*, 2010-2023; (b) C. A. Correia, K. Gilmore, D. T. McQuade, P. H. Seeberger, *Angew. Chem. Int. Ed.* **2015**, *54*, 4945-4948; (c) M. G. Russell and T. F. Jamison, *Angew. Chem. Int. Ed.* **2019**, *58*, 7678-7681.

²⁷ A. K. Ghosh, M. Brindisi, *J. Med. Chem.* **2015**, *58*, 2895-2940.

There have been many synthetic efforts to establish such heterocyclic structures. These compounds are commonly prepared by using hazardous and/or expensive reagents such as isocyanides and phosgene.²⁸ As a convenient alternative to these highly toxic starting materials, carbon dioxide has also been successfully used as a carbonylating agent toward the synthesis of cyclic carbamates. Notable progress was reported for the structurally more basic 1,3-oxazinan-2-one analogues using 1,3-aminoalcohols as starting materials as shown in Scheme 1.4a.²⁹ Apart from these partially stoichiometric conversions, a carboxylative cyclization of propargylic amines with CO₂ under metal catalysts (M = Ru,³⁰ Pd,³¹ Au,³² Ag³³ or Cu³⁴) were also developed by various groups (Scheme 1.4b). The utilization of CO₂ to generate similar heterocycles with concomitant incorporation of a CF₃ group has additionally been reported. The Yu group reported a copper-catalyzed highly selective oxy-trifluoromethylation of diverse allylamines with carbon dioxide to allow access to CF₃-containing 2-oxazolidones under redox-

²⁸ (a) S. J. Brickner, *Curr. Pharm. Des.* **1996**, *2*, 175–194; (b) V. Famiglini, R. Silvestri, *Molecules* **2016**, *21*, 1–18; (c) M. S. Newman, A. Kutner, *J. Am. Chem. Soc.* **1951**, *73*, 4199–4204; (d) M. E. Dyen, D. Swern, *Chem. Rev.* **1967**, *67*, 197–246.

²⁹ (a) J. Paz, C. Pérez-Balado, B. Iglesias, L. Muñoz, *J. Org. Chem.* **2010**, *75*, 3037–3046; (b) T. Niemi, I. Fernández, B. Steadman, J. K. Mannisto, T. Repo, *Chem. Commun.* **2018**, *54*, 3166–3169; (c) J. R. Khusnutdinova, J. A. Garg, D. Milstein, *ACS Catal.* **2015**, *5*, 2416–2422; (d) M. Tamura, M. Honda, K. Noro, Y. Nakagawa, K. Tomishige, *J. Catal.* **2013**, *305*, 191–203; (e) R. Juárez, P. Concepción, A. Corma, H. García, *Chem. Commun.* **2010**, *46*, 4181–4183; (f) C. J. Dinsmore, S. P. Mercer, *Org. Lett.* **2004**, *6*, 17, 2885–2888.

³⁰ T. Mitsudo, Y. Hori, Y. Yamakawa, Y. Watanabe, *Tetrahedron Lett.* **1987**, *28*, 4417–4418.

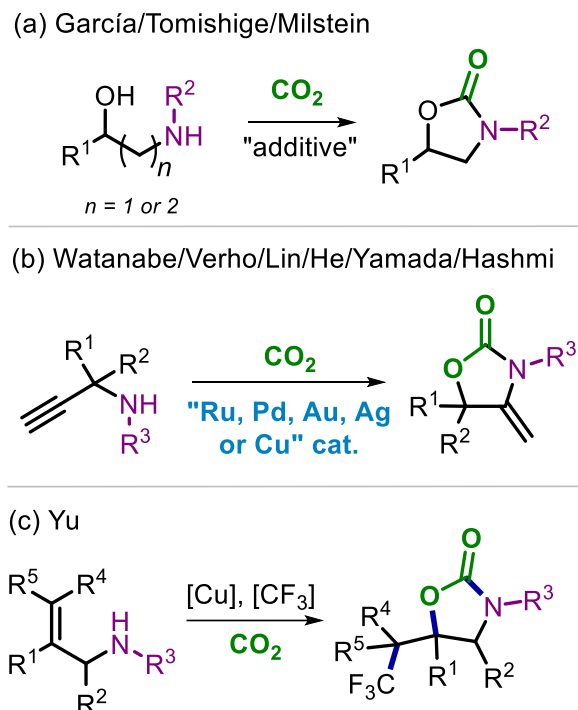
³¹ (a) M. Oschmann, C. Placais, A. Nagendiran, J.-E. Backvall, O. Verho, *Chem. Eur. J.* **2019**, *25*, 6295–6299; (b) P. García-Domínguez, L. Fehr, G. Rusconi, C. Nevado, *Chem. Sci.* **2016**, *7*, 3914–3918; (c) M. Shi, Y.-M. Shen, *J. Org. Chem.* **2002**, *67*, 16–21; (d) A. Bacchi, G. Paolo Chiusoli, M. Costa, B. Gabriele, C. Righi, G. Salerno, *Chem. Commun.* **1997**, 1209–1212.

³² (a) R. Yuan, Z. Lin, *ACS Catal.* **2015**, *5*, 2866–2872; (b) S. Hase, Y. Kayaki, T. Ikariya, *Organometallics* **2013**, *32*, 5285–5288; (c) R. Robles-Machín, J. Adrio, J. C. Carretero, *J. Org. Chem.* **2006**, *71*, 5023–5026; (d) F. Inagaki, K. Maeda, K. Nakazawa, C. Mukai, *Eur. J. Org. Chem.* **2018**, 2972–2976; (e) E.-S. Lee, H.-S. Yeom, J.-H. Hwang, S. Shin, *Eur. J. Org. Chem.* **2007**, 3503–3507; (f) K.-i. Fujita, K. Inoue, J. Sato, T. Tsuchimoto, H. Yasuda, *Tetrahedron* **2016**, *72*, 1205–1212; (g) K. Sekine, *Gold Bull.* **2017**, *50*, 203–209.

³³ (a) J.-F. Qin, B. Wang, G.-Q. Lin, *Green Chem.* **2019**, *21*, 4656–4661; (b) X.-T. Gao, C.-C. Gan, S.-Y. Liu, F. Zhou, H.-H. Wu, J. Zhou, *ACS Catal.* **2017**, *7*, 8588–8593; (c) R. Yuan, B. Wei, G. Fu, *J. Org. Chem.* **2017**, *82*, 3639–3647; (d) Q.-W. Song, L.-N. He, *Adv. Synth. Catal.* **2016**, 358, 1251–1258; (e) M. Yoshida, T. Mizuguchi, K. Shishido, *Chem. Eur. J.* **2012**, *18*, 15578–15581; (f) T. Ishida, S. Kikuchi, T. Tsubo, T. Yamada, *Org. Lett.* **2013**, *15*, 848–851; (g) A. Cervantes-Reyes, T. Saxl, P. M. Stein, M. Rudolph, F. Rominger, A. M. Asiri, A. S. K Hashmi, *ChemSusChem* **2021**, *14*, 2367–2374.

³⁴ (a) F. Chen, S. Tao, Q.-Q. Deng, D. Wei, N. Liu, B. Dai, *J. Org. Chem.* **2020**, *85*, 15197–15212; (b) W.-B. Huang, F.-Y. Ren, M.-W. Wang, L.-Q. Qiu, K.-H. Chen, L.-N. He, *J. Org. Chem.* **2020**, *85*, 14109–14120; (c) A. L. Gu, Y.-X. Zhang, Z.-L. Wu, H.-Y. Cui, T. D. Hu, B. Zhao, *Angew. Chem. Int. Ed.* **2022**, *61*, e202114817; (d) Y. Zhao, J. Qiu, L. Tian, Z. Li, M. Fan, J. Wang, *ACS Sustainable Chem. Eng.* **2016**, *4*, 5553–5560.

neutral and mild reaction conditions (Scheme 1.4c).³⁵ In this latter process, carbon dioxide was used to extend the difunctionalization of alkenes from amino- to oxy-trifluoromethylation.



Scheme 1.4 Various synthetic methods to 5-membered cyclic carbamates.

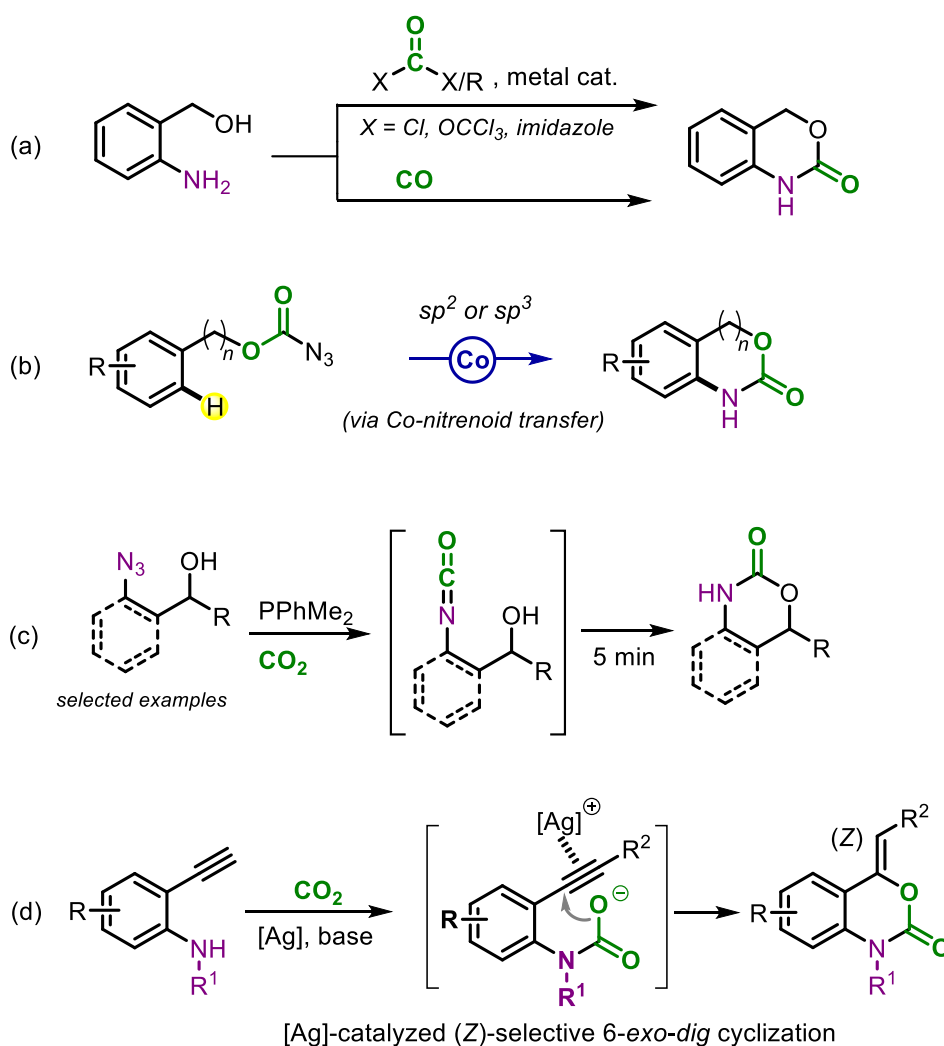
Different from the 5-membered cyclic carbamates, larger ring cyclic carbamates represents more rare structures, and efforts have been made to establish, *inter alia*, benzo-fused cyclic carbamate structures. The most conventional method to construct the carbamate motif in these heterocycles is by using hazardous phosgene and its derivatives,³⁶ which is environmentally unattractive. Alternatively, carbamates can be accessed by reacting CO with amino alcohols such as *o*-aminophenols enabled by transition-metal catalysis.³⁷ In addition, other greener approaches toward carbamate formation have also been developed through the application of

³⁵ J.-H. Ye, L. Song, W.-J. Zhou, T. Ju, Z.-B. Yin, S.-S. Yan, Z. Zhang, J. Li, **D.-G. Yu**, *Angew. Chem. Int. Ed.* **2016**, *55*, 10022–10026.

³⁶ (a) B. Lagu, B. Pio, R. Lebedev, M. Yang, P. D. Pelton, *Bioorg. Med. Chem. Lett.* **2007**, *17*, 3497–3503; (b) E. Hernández, J. M. Vélez, C. P. Vlaar, *Tetrahedron Lett.* **2007**, *48*, 8972–8975.

³⁷ (a) L. Troisi, C. Granito, S. Perrone, F. Rosato, *Tetrahedron Lett.* **2011**, *52*, 4330–4332; (b) Y. Nishiyama, Y. Naitoh, N. Sonoda, *Synlett* **2006**, 109–111; (c) L. Ren, N. Jiao, *Chem. Commun.* **2014**, *50*, 3706–3709.

azide derivatives. In Scheme 1.5b, cyclic carbamate formation is realized under Co-catalysis.³⁸ CO₂ was involved as a key reagent in the reaction depicted in Scheme 1.5c.³⁹ However, the instability of organic azides hampered the realization of a wide product scope. Driven by the inherent synthetic potential of CO₂ as an abundant carbon reagent, a new synthetic method was reported by Yamada and coworkers that produces benzoxazine-2-one derivatives possessing a Z-configured *exo*-olefin (Scheme 1.5d).⁴⁰ These benzo-fused, six-membered carbamate heterocycles were made from *o*-alkynylanilines and carbon dioxide in the presence of a silver catalyst. This latter process is a rare example of a catalytic protocol that enables larger ring cyclic carbamate formation.



Scheme 1.5 Synthetic methods for building carbamate skeletons.

³⁸ J. Lee, J. Lee, H. Jung, D. Kim, J. Park, S. Chang, *J. Am. Chem. Soc.* **2020**, *142*, 12324–12332; (b) P. Dahiya, A. Sarkar, B. Sundararaj, *Adv. Synth. Catal.* **2022**, *364*, 2642–2647.

³⁹ A. Del Vecchio, A. Talbot, F. Caillé, A. Chevalier, A. Sallustrau, O. Loreau, G. Destro, F. Taran, D. Audisio, *Chem. Commun.* **2020**, *56*, 11677–11680.

⁴⁰ T. Ishida, S. Kikuchi, T. Tsubo, T. Yamada, *Org. Lett.* **2013**, *15*, 848–851.

The lack of apparent success while constructing larger ring cyclic carbonates and carbamates calls for new concepts to advance the access to these synthons, and preferably through catalytic approaches. Such methodologies could also accelerate a further development of CO₂-based valorization thereby expanding on structural portfolio. In this sense, the rise of visible-light-driven catalytic carboxylation and the design of multi-step (cascade) processes based on carbon dioxide have the potential for upstream developments into this direction. In the following section, the latter (cascade approaches) are shortly discussed.

1.3 Cascade processes with CO₂

As mentioned, CO₂ can be used for relatively simple transformations such as the formation of cyclic carbonates and carbamates from epoxide and azirines. As a logical extension *en route* to more complex organic carbonates in our group's research program, we focused recently on two approaches that involve multiple steps towards the target products.

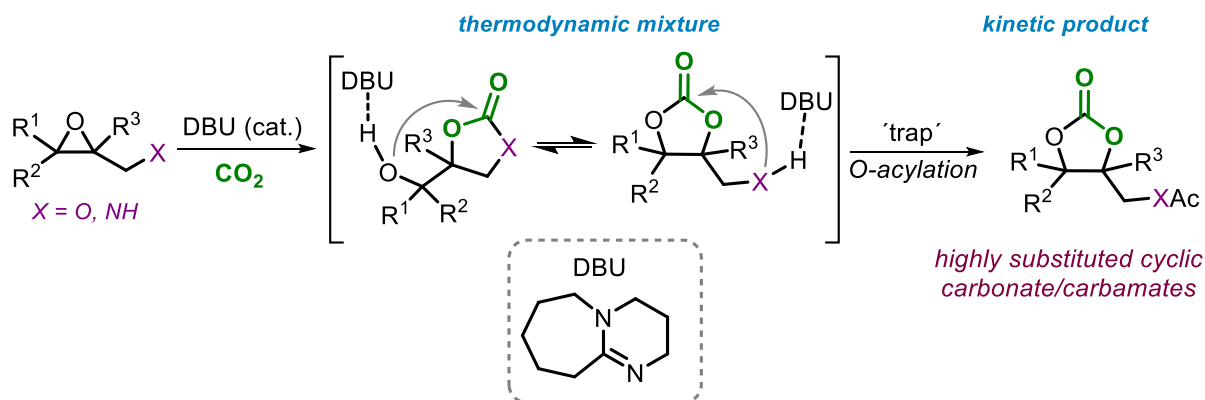
In the first approach, more complex five-membered cyclic carbonates can be obtained using an organocatalyzed domino [3+2] cycloaddition/Payne-type rearrangement. Unlike in the classical mechanism for the cycloaddition of CO₂ to epoxides that builds on the presence of an external (halide) nucleophile, in 2016 our group reported a substrate-controlled divergent synthesis of cyclic carbonates and carbamates from epoxy alcohols and amines,⁴¹ respectively, under Al-catalysis. In this catalytic process, carbon dioxide is initially activated through either the amine or alcohol unit, thereby providing internal nucleophiles for intramolecular epoxy ring opening under mild reaction conditions. Inspired by the Payne rearrangement of epoxy alcohols,⁴² an organocatalytic strategy towards highly substituted cyclic carbonates/carbamates from tri- and tetra-substituted oxiranes and carbon dioxide was eventually achieved (Scheme 1.6).⁴³ A less substituted carbonate/carbamate product is initially formed in this process, which is in equilibrium with a more substituted one through activation of the pendent alcohol that thus enables a thermodynamic mixture of both carbonates. The most substituted carbonate features a primary alcohol which can be selective protected providing a kinetically controlled process that gives access to the most substituted cyclic carbonate with high level of synthetic efficiency. This process constituted a unique example in which epoxy-based substrates are

⁴¹ J. Rintjema, R. Epping, G. Fiorani, E. Martín, E. C. Escudero-Adán, A. W. Kleij, *Angew. Chem. Int. Ed.* **2016**, *55*, 3972–3976.

⁴² G. B. Payne, *J. Org. Chem.* **1962**, *27*, 3819–3822.

⁴³ S. Sopena, M. Cozzolino, C. Maquilón, E. C. Escudero-Adán, Marta Martínez Belmonte, A. W. Kleij, *Angew. Chem. Int. Ed.* **2018**, *57*, 11203–11207.

formally coupled with CO₂ leading to tri- and even tetra-substituted cyclic carbonates/carbamates.

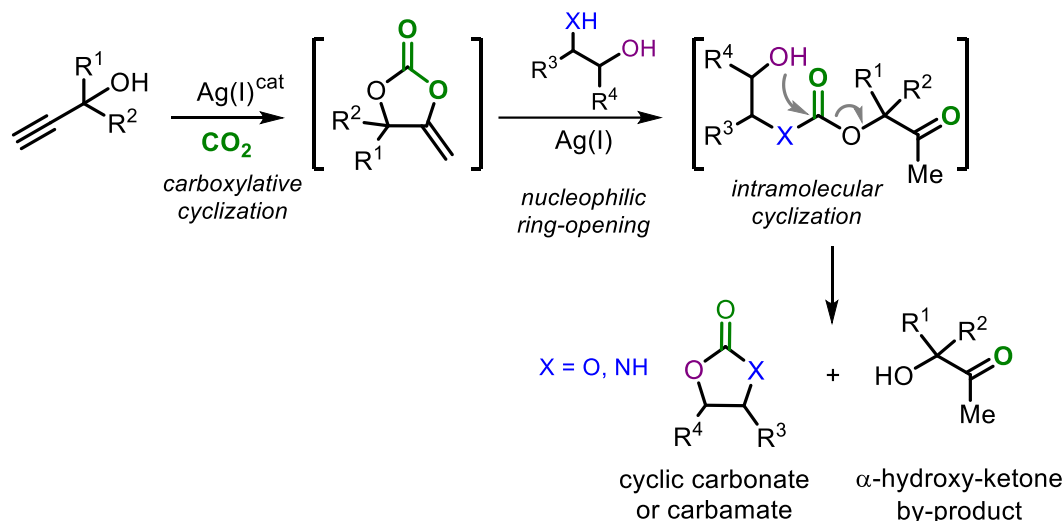


Scheme 1.6 Epoxy alcohol/amine-based cascade processes with a Payne-type cyclic carbonate isomerization step.

The second example of a cascade process is a transformation mediated by Ag-catalysis, and more specifically a reaction between a propargylic alcohol and carbon dioxide which have received increasingly attention over the years. More recently, various groups reported that an intermediate α -alkylidene carbonate (furnished by a known carboxylative cyclization) can be further reacted with nucleophiles such as alcohols (Scheme 1.7) thereby enabling a series of steps culminating into the formation of a final carbonate or carbamate heterocycle and an α -hydroxy-ketone as a secondary product. The combination of terminal propargylic alcohols, carbon dioxide and vicinal diols or 2-aminoethanol (Scheme 1.7)^{44,45} in the presence of a Ag(I)-catalyst leads to either substituted cyclic carbonates or carbamates. These processes, compared with direct condensation of CO₂ with diols/2-aminoethanols, provide thermodynamically favorable routes to cyclic carbonates/carbamates and α -hydroxyl ketones without the addition of dehydration agents. Up to the moment of the development of this thesis work, only *intermolecular* versions of these cascades had been reported and we are not aware of any example where an *internal* nucleophile enables carbonate isomerization by attacking the activated carbonate ring.

⁴⁴ (a) Z.-H. Zhou, Q.-W. Song, L.-N. He, *ACS Omega* **2017**, 2, 337–345; (b) J.-Y. Li, L.-H. Han, Q.-C. Xu, Q.-W. Song, P. Liu, K. Zhang, *ACS Sustainable Chem. Eng.* **2019**, 7, 3378–3388; (c) H. Zhou, H. Zhang, S. Mu, W.-Z. Zhang, W.-M. Ren, X.-B. Lu, *Green Chem.* **2019**, 21, 6335–6341.

⁴⁵ Q.-W. Song, Z.-H. Zhou, M.-Y. Wang, K. Zhang, P. Liu, J.-Y. Xun, L.-N. He, *ChemSusChem* **2016**, 9, 2054–2058.



Scheme 1.7 Reported intermolecular cascade reactions leading to cyclic carbonates or carbamates under Ag catalysis.

1.4 Main objective and outline of this thesis

Section 3 shows that in the last five years, catalytic cascade reactions using CO₂ as a reagent have gained interest as they can lead to more complex structures resembling (parts of) pharmaceutical compounds. Cascade processes offer a way to combine several process steps into a one-pot procedure while having the opportunity to quickly assemble complex and functional scaffolds of interest in pharmaceutical discovery and development studies. Another observation in the area of CO₂ catalysis is the privileged nature of Ag-catalysis to convert propargylic alcohols and CO₂ into activated α-alkylidene carbonates which have potential to undergo further reactions provided that suitable nucleophiles are present that can induce isomerization of the heterocyclic structure. In view of these features and notions, we envisioned that combining all these aspects would deliver a powerful approach to new types of heterocyclic compounds derived from CO₂. The **main objective** of this doctoral thesis is the development of novel Ag-catalyzed cascade conversions of carbon dioxide into new types of heterocycles with a high level of functionality, substitution degree and further extending these procedures to larger ring carbonates and carbamates.

This thesis consists of four chapters. In **Chapter 1**, a general background is given for the experimental chapters of the thesis illustrating the most pertinent aspects of CO₂ utilization, the synthetic and application potential of CO₂-based heterocycles and generic features of some

examples of cascade processes carried out with CO₂. These introductory remarks are followed by two experimental chapters and a summary/general conclusion section.

In **Chapter 2** a new and efficient domino process promoted by a silver/phosphine-based catalyst is reported that involves the use of modular alkyne-1,*n*-diols and carbon dioxide providing access to keto-functionalized cyclic carbonates. The scope of these carbonates included the preparation of functional di-, tri- and even tetra-substituted heterocyclic rings. Detailed computational analysis (DFT) of this complex manifold showed, among other aspects, that the key feature of this keto-carbonate formation is the thermodynamically induced isomerization of an *enol-into-keto* fragment after nucleophilic ring-opening. This specific cascade protocol allows for the construction of larger ring carbonates (i.e., six- and seven-membered ones) through the intermediacy of an α -alkylidene carbonate, and expands the synthetic potential of carbon dioxide.

In **Chapter 3**, a conceptually novel catalytic cascade approach towards the formation of highly functional 1,4-dihydro-2*H*-1,3-benzoxazine-2-one derivatives is presented. In particular, the chemo-selectivity was greatly influenced by the structure of the substrate precursor. We finally found that the presence of a tertiary propargylic carbonate in the precursor is key to override parasitic cyclization processes while empowering the formation of the desired product through Thorpe–Ingold (angle-compression) effects. The formation of a wide range of CO₂-based benzo-fused six-membered cyclic carbamates demonstrates the synthetic diversity of this domino process. The isolation of one of the reaction intermediates and its separately studied conversion into the final product supports an unusual ring-expansion sequence from an α -alkylidene, five-membered cyclic carbonate to a six-membered cyclic carbamate by *N*-induced isomerization.

Finally, in **Chapter 4** a short summary of the silver catalytic cascade processes reported in chapters 2 and 3 is provided together with a general conclusion of the thesis work that puts the entire content into context. A future outlook and remaining challenges are also briefly discussed to serve as an inspiration for follow-up research activities in this area.

Chapter 2.

Cascade Transformation of Carbon Dioxide and Alkyne-1,n-diols into Densely Substituted Cyclic Carbonates

The results described in this chapter have been published in:

X. Li, A. Villar-Yanez, C. N. Tounzoua, J. Benet-Buchholz, B. Grignard, C. Bo, C. Detrembleur, A. W. Kleij, *ACS Catal.* **2022**, *12*, 2854–2860.

UNIVERSITAT ROVIRA I VIRGILI
SILVER-CATALYZED CASCADE CONVERSIONS OF CO₂ INTO HETEROCYCLES
Xuetong Li

2.1 Introduction

The reutilization of carbon-containing waste into value-added products through catalysis provides an attractive route in the context of circular chemistry.¹ The implication of circular principles will realize an improved usage of our natural resources, thereby embracing a sustainable future and a more efficient carbon management.² Carbon dioxide (CO₂) represents the most simple carbon-based reagent available for the fabrication of various products including pharmaceuticals,³ polymerizable monomers,⁴ synthetic intermediates,⁵ and bulk chemicals.⁶ Despite the difficulties encountered in the catalytic transformation of CO₂, much progress has been noted in the last 10 years with outstanding advances in both reductive⁷ and nonreductive conversions.⁸ A prominent, nonreductive conversion process is (3 + 2) cycloaddition of CO₂ to epoxides providing cyclic carbonates as products. These compounds have gained a great deal of synthetic importance over the last few years as suitable starting

¹ a) T. Keijer, V. Bakker, J. C. Slootweg, *Nat. Chem.* **2019**, *11*, 190–195; b) J. Cantzler, F. Creutzig, E. Ayargarnchanakul, A. Javaid, L. Wong, W. Haas, *Environ. Res. Lett.* **2020**, *15*, No. 123001; c) E. C. D. Tan, P. Lamers, *Front. Sustainability* **2021**, *2*, No, 701509.

² *Advances in Carbon Management Technologies*, In S. K. Sikdar, F. Princiotta, Eds., CRC Press: Boca Raton, 2020.

³ a) C. Lescot, D.U. Nielsen, I. S. Makarov, A. T. Lindhardt, K. Daasbjerg, T. Skrydstrup, *J. Am. Chem. Soc.* **2014**, *136*, 6142–6147; b) W. Guo, V. Laserna, J. Rintjema, A. W. Kleij, *Adv. Synth. Catal.* **2016**, R. Epping, G. Fiorani, E. Martín, E. C. Escudero-Adán, A. W. Kleij, *Angew. Chem., Int. Ed.* **2016**, *55*, 3972–3976.

⁴ T. M. McGuire, C. Pérale, R. Castaing, G. I. Kociok-Köhn, A. Buchard, *J. Am. Chem. Soc.* **2019**, *141*, 13301–13305; b) T. M. McGuire, E. M. López-Vidal, G. L. Gregory, A. Buchard, *J. CO₂ Util.* **2018**, *27*, 283–288; c) C. Qiao, A. Villar-Yanez, J. Sprachmann, B. Limburg, C. Bo, A. W. Kleij, *Angew. Chem., Int. Ed.* **2020**, *59*, 18446–18451; d) C. Maquilón, F. Della Monica, B. Limburg, A. W. Kleij, *Adv. Synth. Catal.* **2021**, *363*, 4033–4040; e) J. Vaitla, Y. Guttormsen, J. K. Mannisto, A. Nova, T. Repo, A. Bayer, *ACS Catal.* **2017**, *7*, 7231–7244.

⁵ a) Q. Liu, L. Wu, R. Jackstell, M. Beller, *Nat. Commun.* **2015**, *6*, No. 5933; b) W. Guo, J. E. Gómez, À. Cristòfol, J. Xie, A. W. Kleij, *Angew. Chem., Int. Ed.* **2018**, *57*, 13735–13747; c) L. Zuo, T. Liu, X. Chang, W. Guo, *Molecules* **2019**, *24*, No. 3930; d) S. Dabral, T. Schaub, *Adv. Synth. Catal.* **2019**, *361*, 223–246; e) V. Laserna, E. Martin, E. C. Escudero-Adán, A. W. Kleij, *ACS Catal.* **2017**, *7*, 5478–5482.

⁶ a) J. Klankermayer, S. Wesselbaum, K. Beydoun, W. Leitner, *Angew. Chem., Int. Ed.* **2016**, *55*, 7296–7343; b) M. Aresta, A. DiBenedetto, A. Angelini, *Chem. Rev.* **2014**, *114*, 1709–1742.

⁷ a) A. Tortajada, F. Juliá-Hernández, M. Börjesson, T. Moragas, R. Martin, *Angew. Chem., Int. Ed.* **2018**, *57*, 15948–15982; b) S. Nitopi, E. Bertheussen, S. B. Scott, X. Liu, A. K. Engstfeld, S. Horch, B. Seger, I. E. L. Stephens, K. Chan, C. Hahn, J. K. Nørskov, T. F. Jaramillo, I. Chorkendorff, *Chem. Rev.* **2019**, *119*, 7610–7672; c) S. R. Lingampalli, M. M. Ayyub, C. N. R. Rao, *ACS Omega* **2017**, *2*, 2740–2748; d) Q.-W. Song, Z.-H. Zhou, L.-N. He, *Green Chem.* **2017**, *19*, 3707–3728.

⁸ a) R. R. Shaikh, V. Pornpraprom, et al., *ACS Catal.* **2018**, *8*, 419–450; b) J. W. Comerford, I. D. V. Ingram, M. North, X. Wu, *Green Chem.* **2015**, *17*, 1966–1987; c) M. Alves, B. Grignard, R. Mereau, C. Jérôme, T. Tassaing, C. Detrembleur, *Catal. Sci. Technol.* **2017**, *7*, 2651–2684; d) B. Yu, L.-N. He, *ChemSusChem* **2015**, *8*, 52–62; e) A. J. Kamphuis, F. Picchioni, P. P. Pescarmona, *Green Chem.* **2019**, *21*, 406–448; f) F. Della Monica, A. W. Kleij, *Catal. Sci. Technol.* **2020**, *10*, 3483–3501; g) B. Limburg, À. Cristòfol, F. Della Monica, A. W. Kleij, *ChemSusChem* **2020**, *13*, 6056–6065.

points for decarboxylative formation of compounds with elusive stereocenters⁹ and the creation of more sustainable CO₂-based polymers and materials.¹⁰ The [3 + 2] cycloaddition strategy for the generation of cyclic carbonates generally works well for mono- and disubstituted epoxides but shows important limitations for even more sterically demanding oxiranes. To overcome this challenge, new conceptual designs have emerged that capitalize on alternative reactivity patterns. For instance, the use of substrate-controlled manifolds such as the one presented in Scheme 2.1a allows for the design of highly elusive and complex carbonate structures through unique cascade processes, provided that a suitable trapping mechanism is available.¹¹

Similar though different in its design is the interception of reactive in or ex situ prepared α -alkylidene carbonates by diol reagents in a formal domino transesterification process (Scheme 2.1b) giving a 1:1 mixture of a new cyclic carbonate and an α -hydroxy ketone.¹² Whereas these cascade designs are able to provide some though a rather limited degree of structural diversity, the conformation of a ketone byproduct renders them atom-inefficient. To expedite new types of cascade processes providing new types of carbonate structures, we sought to merge the presence of an intramolecular alcohol (pro)nucleophile and a reactive exocyclic double bond to promote a new rearrangement process that would give access to keto-functionalized cyclic carbonates while enabling an ample scope in substitution and functionality (Scheme 2.1c).

2.2 Aims of the work

The main objective of the work presented in this chapter was to productively use alkyne-1,2-diol under appropriate reaction conditions thereby inducing a skeletal rearrangement of an

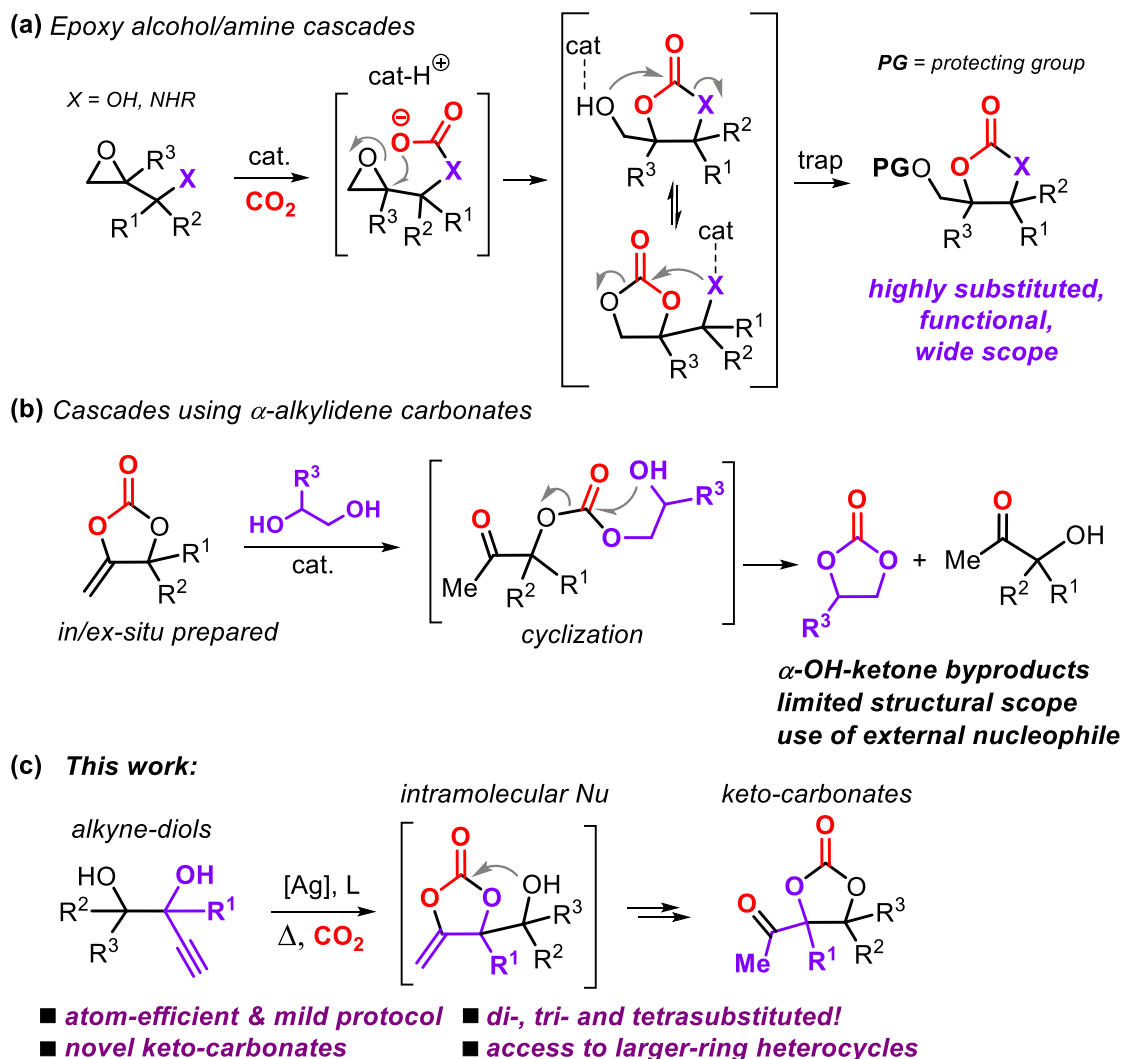
⁹ a) A. Cai, A. W. Kleij, *Angew. Chem., Int. Ed.* **2019**, *58*, 14944–14949; b) I. Cristòfol, B. Limburg, A. W. Kleij, *Angew. Chem., Int. Ed.* **2021**, *60*, 15266–15270.

¹⁰ a) T(a) B. Grignard, S. Gennen, C. Jérôme, A. W. Kleij, C. Detrembleur, *Chem. Soc. Rev.* **2019**, *48*, 4466–4514; b) N. Yadav, F. Seidi, D. Crespy, V. D'Elia, *ChemSusChem* **2019**, *12*, 724–754; c) F. Monie, B. Grignard, J.-M. Thomassin, R. Mereau, T. Tassaing, C. Jérôme, C. Detrembleur, *Angew. Chem., Int. Ed.* **2020**, *59*, 17033–17041; d) G. L. Gregory, G. Kociok-Köhn, A. Buchard, *Polym. Chem.* **2017**, *8*, 2093–2104; e) A. Gomez-Lopez, S. Panchireddy, B. Grignard, I. Calvo, C. Jérôme, C. Detrembleur, H. Sardon, *ACS Sustainable Chem. Eng.* **2021**, *9*, 9541–9562.

¹¹ a) R. Huang, J. Rintjema, J. González-Fabra, E. Martín, E. C. Escudero-Adán, C. Bo, A. Urakawa, A. W. Kleij, *Nat. Catal.* **2019**, *2*, 62–70; b) S. Sopena, M. Cozzolino, C. Maquilón, E. C. Escudero-Adán, M. Martínez Belmonte, A. W. Kleij, *Angew. Chem., Int. Ed.* **2018**, *57*, 11203–11207. See also refs 3, 5, 8.

¹² a) Z.-H. Zhou, Q.-W. Song, L.-N. He, *ACS Omega* **2017**, *2*, 337–345; b) J.-Y. Li, L.-H. Han, Q.-C. Xu, Q.-W. Song, P. Liu, K. Zhang, *ACS Sustainable Chem. Eng.* **2019**, *7*, 3378–3388; c) H. Zhou, H. Zhang, S. Mu, W.-Z. Zhang, W.-M. Ren, X.-B. Lu, *Green Chem.* **2019**, *21*, 6335–6341. See also ref 10.

initially formed α -alkylidene carbonate with the formation of the keto group as a thermodynamic driving force (Scheme 2.1c).



Scheme 2.1. (a) Substrate-controlled cascade reaction leading to highly substituted cyclic carbonates. (b) Domino transesterification process involving external diols. (c) This work: a novel cascade process.

Here, we illustrate the development and mechanistic rationale for this conceptual novel catalytic domino process, thus expanding the current portfolio of highly substituted (saturated) cyclic carbonates. The protocol is characterized by operational simplicity, excellent scope of carbonate-based heterocycles, and mild reaction conditions. *In situ* IR studies, various control experiments, and detailed DFT (density functional theory) analysis of these manifolds reveal the intermediacy of an α -alkylidene cyclic carbonate that is captured by an intramolecular alcohol nucleophile.

2.3 Results and discussion

At the onset of our studies, we selected an alkyne-1,2-diol reagent (**2.1a**) as a model substrate (Tables 2.1)¹³ and AgOAc/DavePhos (*rac*-**L2.1**) as catalyst precursors using CH₃CN as a solvent.¹⁴ Both the Ag salt and phosphine ligand alone are not effective (Table 2.2), but their combination (Table 2.1, entry 1: 10 mol% each) provides a high level of substrate conversion at 35 °C with a moderate yield of **2.2a** (56%). Since the NMR and IR analyses ($\nu = 1803$ and 1729 cm^{-1}) of an isolated sample of **2.2a** were not conclusive and indicated the formation of a product different from an α -alkylidene carbonate, X-ray analysis was performed. This unambiguously confirmed the formation of a keto-substituted cyclic carbonate (*vide infra*, Scheme 2.2).¹⁵ The transformation of **2.1a** into **2.2a** can also be performed at 25 °C (entry 2) but requires a longer reaction time (48 h) to afford a similar yield of **2.2a**. The nature of the phosphine ligand is crucial as simple ligands such as PPh₃, dppe (entries 3 and 4, Table 2.1), and DPEPhos (entry 14, Table 2.2) proved to be unproductive. Then, we decided to examine other bulky monophosphine ligands (**L2.2**–**L2.6**, entries 5–9), with BrettPhos **L2.6** providing the best performance with **2.2a** produced in excellent yield (91% by NMR, 85% isolated; entry 9, Table 2.1).

To make the protocol more attractive, we investigated the use of lower loadings of both the Ag precursor and **L2.6** (entries 10–13, 5.0 mol%). By slightly increasing the reaction temperature to 40 °C, full conversion of **2.1a** could be realized within 6 h while using AgF as a precursor (entry 13), giving **2.2a** in high isolated yield (88%). Lower loadings of AgF/**L2.6** or changing the solvent (entries 14–16, Table 2.1, and Table 2.2) did not further improve the process outcome.¹⁶

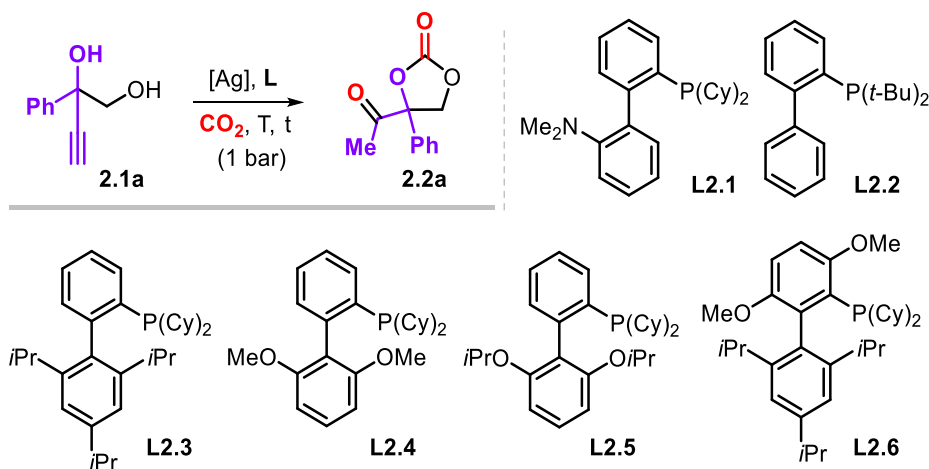
¹³ J. E. Gómez, À. Cristòfol, A. W. Kleij, *Angew. Chem., Int. Ed.* **2019**, *58*, 3903–3907.

¹⁴ The combination of AgOAc and DavePhos **L2.1** was previously reported as a highly effective catalyst system for α -alkylidene carbonate formation, see (a) S. Dabral, B. Bayarmagnai, M. Hermsen, J. Schiebl, V. Mormul, A. S. K. Hashmi, T. Schaub, *Org. Lett.* **2019**, *21*, 1422–1425. For some other Ag-based catalytic processes related to the coupling of propargylic alcohols and CO₂, see (b) Q.-W. Song, L.-N. He, *Adv. Synth. Catal.* **2016**, *358*, 1251–1258; (c) S. Kikuchi, S. Yoshida, Y. Sugawara, W. Yamada, H.-M. Cheng, K. Fukui, K. Sekine, I. Iwakura, T. Ikeno, T. Yamada, *Bull. Chem. Soc. Jpn.* **2011**, *84*, 698–717.

¹⁵ For further details of the structure of **2.2a**, please consult CCDC 2088491. For structure **2.4a**, see CCDC 2088492. For structure **2.7**, see CCDC 2112335.

¹⁶ In the last two reactions of Table 2.1, a much lower chemoselectivity towards the keto-carbonate **2.2a** was observed, with various unidentified products in the crude mixture.

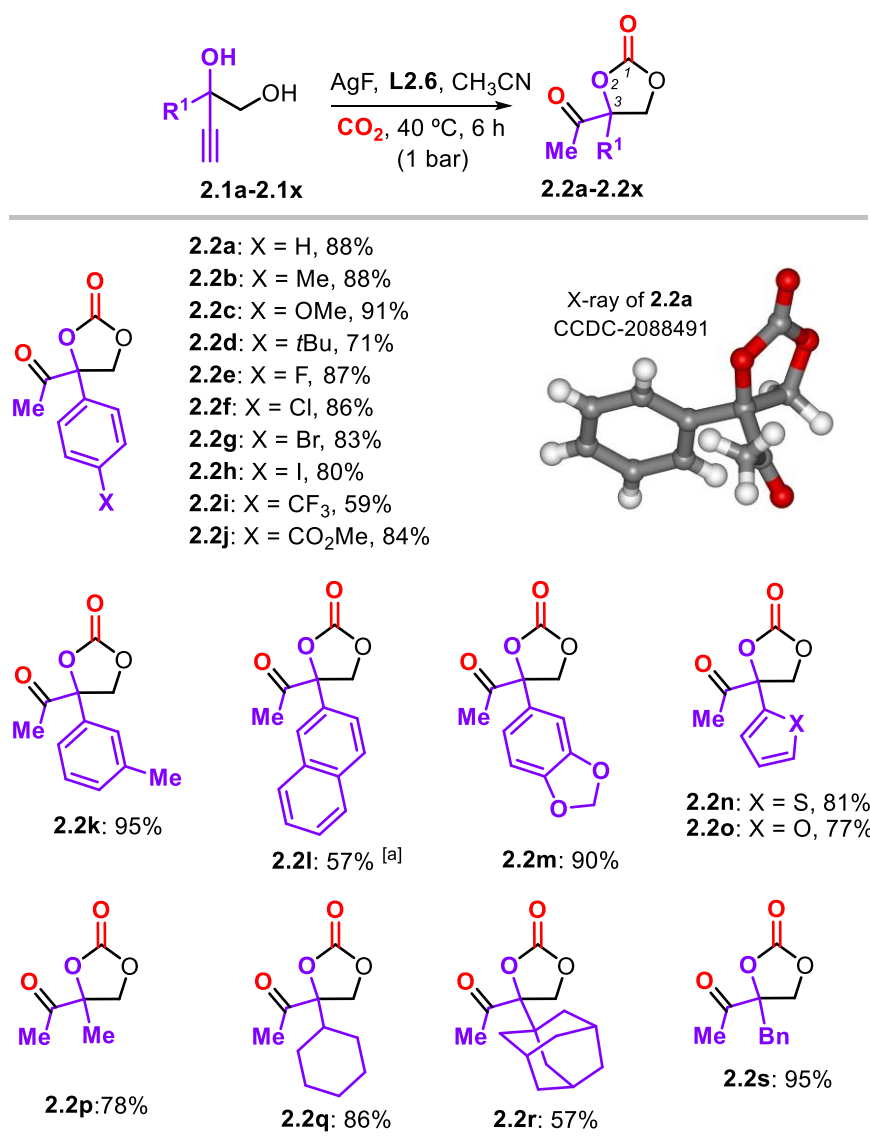
Table 2.1 Screening and optimization of the Ag-catalyzed conversion of alkyne-1,2-diol **2.1a** and CO₂ into keto-substituted cyclic carbonate **2.2a**.^[a]



entry	t, T ^[b]	[Ag] ^[b]	[L] ^[b]	C ^[b,c]	Yield ^[b,c]
1	24, 35	AgOAc, 10	L2.1 , 10	96	56
2	48, 25	AgOAc, 10	L2.1 , 10	83	62
3	24, 25	AgOAc, 10	PPh ₃ , 10	<10	<10
4	24, 25	AgOAc, 10	dppe, 10	0	0
5 ^[d]	24, 25	AgOAc, 10	L2.2 , 10	77	66(63)
6 ^[d]	24, 25	AgOAc, 10	L2.3 , 10	82	74(66)
7 ^[d]	24, 25	AgOAc, 10	L2.4 , 10	84	73(68)
8	24, 25	AgOAc, 10	L2.5 , 10	85	63
9 ^[d]	24, 25	AgOAc, 10	L2.6 , 10	>99	91(85)
10	24, 25	AgOAc, 5	L2.6 , 5.0	73	69
11	24, 40	AgOAc, 5	L2.6 , 5.0	93	85
12	24, 40	AgF, 5	L2.6 , 5.0	>99	90
13 ^[d]	6, 40	AgF, 5	L2.6 , 5.0	>99	91(88)
14	6, 40	AgF, 2.5	L2.6 , 2.5	12	<5
15 ^[e]	6, 40	AgF, 5	L2.6 , 5.0	>99	18
16 ^[f]	6, 40	AgF, 5	L2.6 , 5.0	>99	17

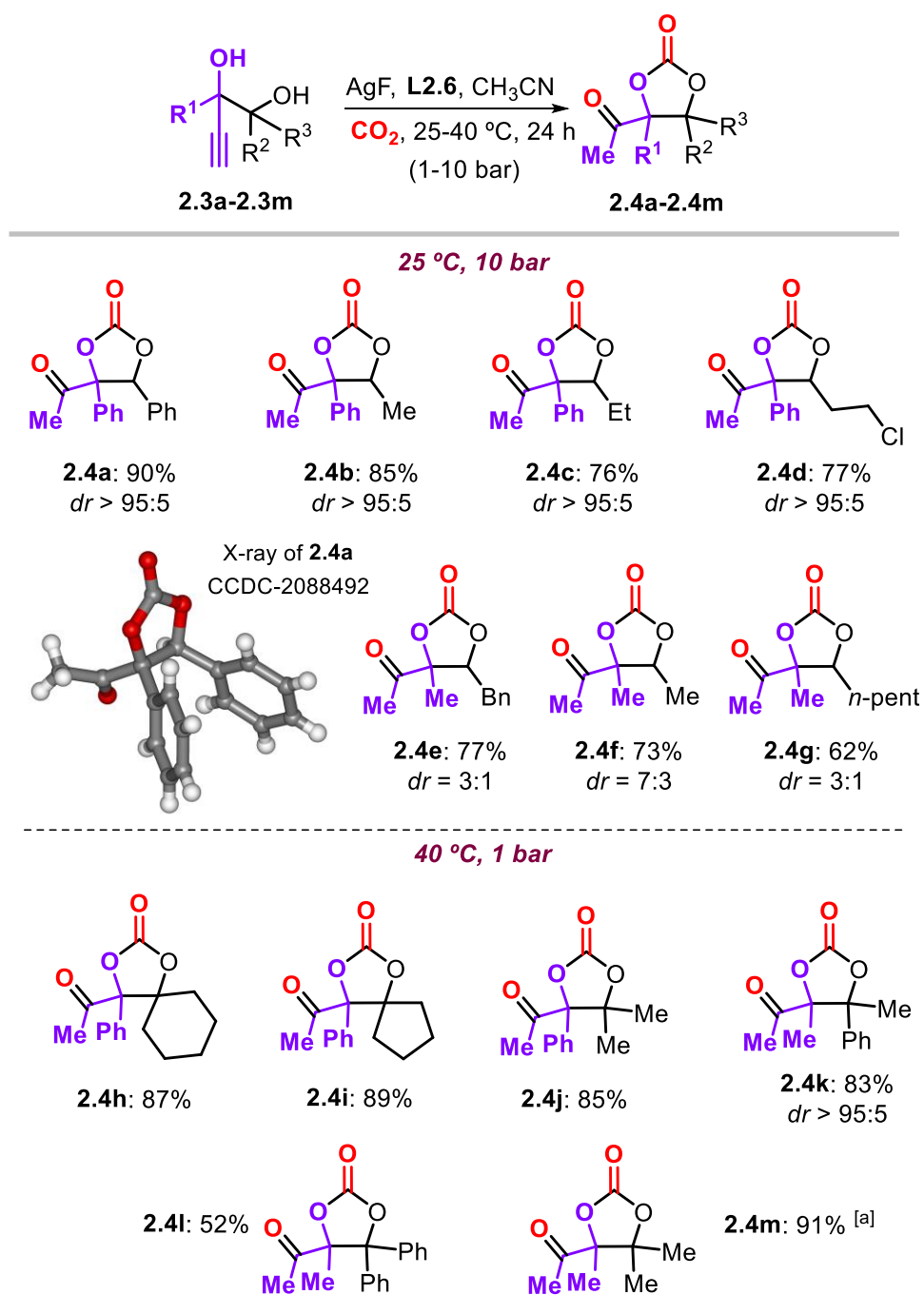
[a] General conditions: **2.1a** (0.30 mmol), CH₃CN (0.60 mL), [Ag]/[L], and T/t as indicated. [b] Time in h, temperature in °C, [Ag] and [L] in mol%, and conversion (C) of **2.1a** and the yield of **2.2a** in %. [c] Conversion and yield based on ¹H NMR (CDCl₃) analysis, using mesitylene as the internal standard. [d] In brackets, the isolated yield of **2.2a**. [e] THF as a solvent. [f] MeOH as a solvent.

The scope of this transformation (Scheme 2.2) was then further explored using the optimized conditions reported in entry 13 of Table 2.1. In general, good-to-excellent isolated yields of the keto-carbonates were achieved under mild temperature (40 °C) and pressure (1 bar) conditions. A wide range of 3-aryl-3-keto-carbonates could be produced (**2.2a–2.2k**) with electronically diverse *para*- and *meta*-substituents. The presence of other (hetero)aryl groups (**2.2l–2.2o**) in the keto-carbonate product is also tolerated, though for naphthyl-substituted **2.2l**, a reaction temperature of 60 °C was required to allow for an appreciable product yield, most likely as a result of increased steric congestion in the intermediate of Scheme 2.1c. Apart from aryl groups, various primary, secondary, and tertiary alkyl groups can also be introduced as illustrated by the successful preparation of **2.2p–2.2s**, with the adamantyl-based **2.2r** (57%) being particularly noteworthy.



Scheme 2.2 Scope of disubstituted keto-based cyclic carbonates (**2.2a–2.2s**) derived from alkyne-1,2-diols **2.1a–2.1s**. [a] The reaction was performed at 60 °C.

Next, we decided to challenge the developed protocol further using substituted (cf., R²) alkynyl-1,2-diols **2.3a–2.3m**. Trisubstituted, aryl-functionalized keto-carbonates **2.4a–2.4d**¹⁵ were obtained in good isolated yields (76–90%) and under high diastereocontrol (*dr* > 95:5), whereas methyl-substituted products **2.4e–2.4g** (62–77%) were produced with lower *dr* values, which is ascribed to an apparent lower degree of diastereocontrol in the intramolecular attack of the secondary alcohol on the α -alkylidene carbonate intermediate (Scheme 2.1c). Encouraged by the low-temperature formation of typically challenging trisubstituted keto-carbonates,^{5c} we then considered alkyne 1,2-diols with three substitutions (R¹–R³, Scheme 2.3, top) to forge sterically more demanding keto-carbonates. Under relatively mild conditions (40 °C, 1 bar), the formation of tetrasubstituted carbonate heterocycles **2.4h–2.4m** could be accommodated in typical good isolated yields of up to 91%. Both spiro-fused cycloalkyl rings (**2.4h** and **2.4i**) and different combinations of aryl/alkyl substituents (**2.4j–2.4m**) are tolerated in the product skeletons, further highlighting the excellent scope of this transformation. It should be noted that the formation of highly substituted cyclic carbonates such as those in Scheme 2.3 represents a huge challenge, and the results described so far thus demonstrate a substantial advance in this area.



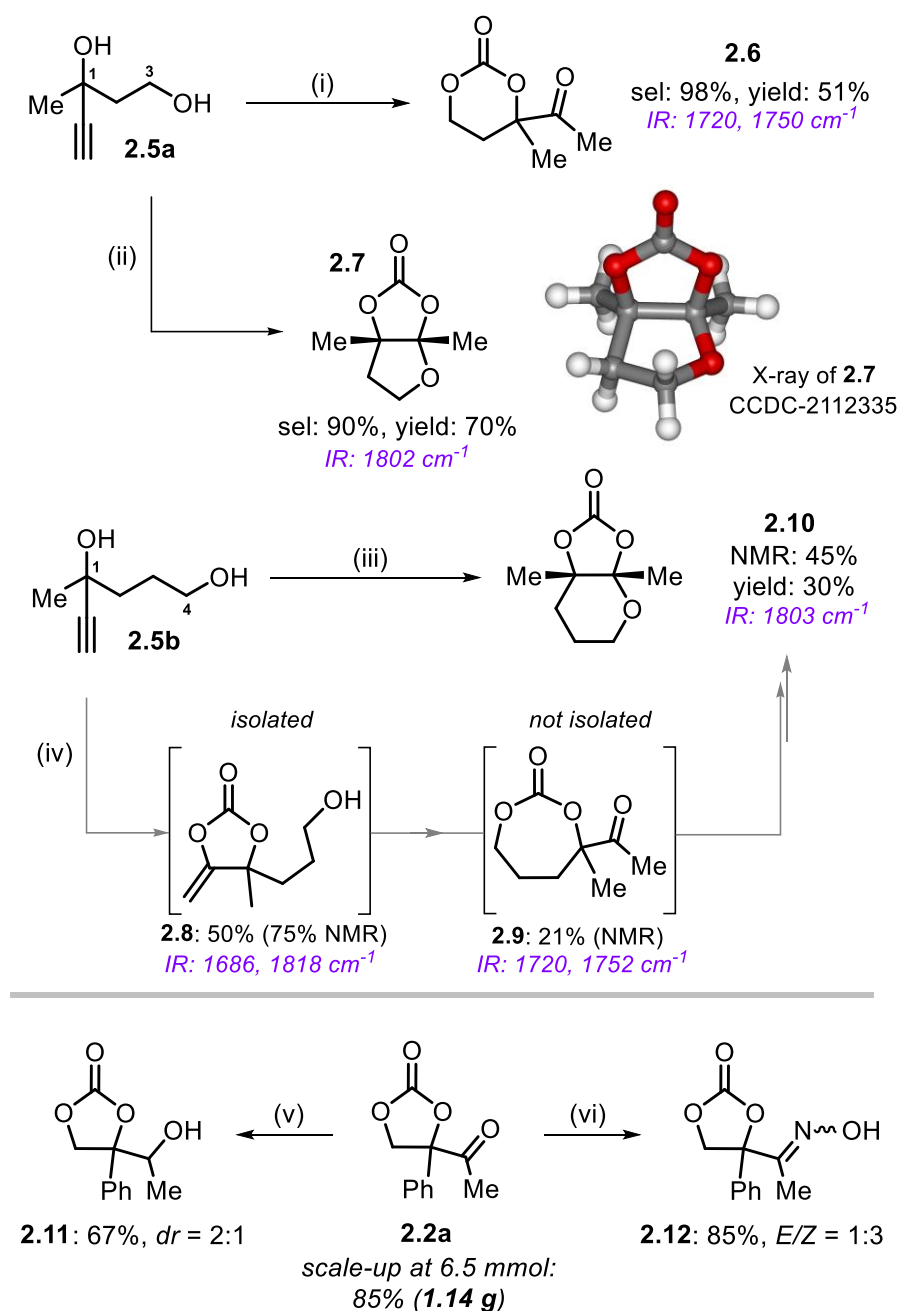
Scheme 2.3 Scope of tri- and tetrasubstituted keto-based cyclic carbonates (**2.4a–2.4m**) derived from substituted alkyne-1,2-diols **2.3a–2.3m**. [a] The reaction time was 48 h. The *dr* values were determined by ¹H NMR.

We then further examined whether the use of higher homologues of the alkyne-1,2-diols would serve as suitable reagents toward larger ring carbonates (Scheme 2.4) and their synthetic utility. The treatment of alkyne-1,3-diol **2.5a** with CO₂ (15 bar) at 25 °C in the presence of the binary catalyst AgI/TBAOPh in DMSO (2.2 M) gave the six-membered keto-carbonate **2.6** with high chemo-selectivity (98%) and appreciable isolated yield (51%, see the Experimental Section for further details; entry 1, Table 2.6).¹⁷ Interestingly, we found that under similar conditions while raising the reaction temperature and changing the solvent to CH₃CN (4.4 M), the chemo-selectivity changed toward a unique, bicyclic tetrasubstituted five-membered cyclic carbonate **2.7** (70%; entry 14, Table 2.6), which was unambiguously identified by X-ray crystallography.¹⁵ Although its formation mechanism is yet unclear, we believe that **2.6** is a viable precursor for **2.7** and ring-opening of **2.6** by the phenolate salt is likely involved, followed by rearrangement into the thermodynamically more stable product **2.7**. To further examine the utility of our cascade protocol, we also subjected alkyne-1,4-diol **2.5b** to a similar carboxylation process. After some optimization (see the Experimental Section, Table 2.7), we found that a bicyclic, tetrasubstituted carbonate **2.10** could be produced in 45% NMR yield (33% isolated) in the presence of AgI/DBU as a binary catalyst (entry 12, Table 2.7). Analogous to the formation of **2.6**, product **2.10** requires the in situ formation of the seven-membered keto-carbonate **2.9** with the alkylidene carbonate **2.8** being the precursor for **2.9**. Both could indeed be observed and identified by both ¹H NMR and operando IR spectroscopy (see the Experimental Section for details). These combined findings indeed suggest further potential of our cascade protocol to access otherwise elusive cyclic carbonate scaffolds.

We then probed whether the keto-based carbonate **2.2a** could be transformed while maintaining the carbonate ring intact (Scheme 2.4, lower part). The scale-up of **2.2a** was easily performed to gram quantities allowing for postsynthetic transformations to be examined. The ketone group could be reduced in the presence of NaBH₄ to afford the corresponding alcohol **2.11** in 67% yield, where the ketone could also be converted into an imine (**2.12**: 85% yield). These results suggest that the carbonate rings in the five-membered keto-carbonates are rather stable.

¹⁷ The choice for AgI/TBAOPh as catalyst came from a screening study, that showed better performance of this system compared to AgF/ **L2.6** that was utilized for the product scope phase. Further to this, carbonate **2.6** proved to be less stable than the five-membered keto-carbonates under the chromatographic conditions and some loss of product was thus noticed upon work up. See the Experimental Section for more details. For the previous use of this catalyst see: C. Ngassam Tounzoua, B. Grignard, A. Brege, C. Jérôme, T. Tassaing, R. Mereau, C. Detrembleur, *ACS Sustainable Chem. Eng.* **2020**, *8*, 9698–9710.

Scheme 2.4 Conversion of alkyne-1,3- and alkyne-1,4-diols **2.5a** and **2.5b** into derivatives **2.6–2.10** with their diagnostic IR data.^[a]



[a] Reaction conditions: (i) AgI/TBAOPh (5 mol%), DMSO (2.2 M), 25 °C, 24 h, 15 bar CO₂; (ii) AgI/TBAOPh (5 mol%), ACN (4.4 M), 80 °C, 24 h, 15 bar CO₂; (iii) AgI/DBU (5 mol%), ACN, 80 °C, 24 h, 15 bar CO₂; (iv) AgI/TBAOPh (5 mol%), DMSO (2.2 M), 25 °C, 24 h, 15 bar CO₂; (v) NaBH₄ (1.1 equiv), THF/MeOH (4:1), 0 °C, 1 h; and (vi) H₂NOH·HCl (2 equiv), pyridine (2 equiv), EtOH, r.t., 16 h.

2.4 DFT studies

To shed light on the formation mechanism of these keto-carbonates, DFT analysis¹⁸ of the benchmark reaction involving **2.1a** and CO₂ was performed using a Ag-catalyst derived from **L2.1** (Figure 2.1).^{19,20,21,22} The reason for this catalyst choice was to be able to directly compare the first part of the manifold with that computed previously¹⁴ in the conversion of a more simple propargylic alcohol precursor by AgOAc/**L2.1**. In our calculations, we used therefore the same complex as a starting point together with substrate **2.1a** and CO₂ as a zero reference (Figure 2.1, denoted as **Reactants**). The phosphine substituents are not symmetric and can rotate at room temperature. All structures were therefore calculated with the same fixed phosphine chiral conformation. Note that substrate **2.1a** has a chiral center giving rise to diastereoisomeric intermediates and transition states for the chosen conformation of the Ag complex derived from **L2.1**. For simplicity, we provide in Figure 2.1 *only* the lowest energetic pathway based on (*R*)-**2.1a** (see the Experimental Section for full details and comments).

The overall mechanistic pathway for the conversion of (*R*)-**2.1a** includes different key stages: initial CO₂ activation by propargylic diol followed by an attack on the triple bond, a carbonate isomerization step involving a pendant alcohol, and a tautomerization step. Notably, all of these steps are facilitated by several proton transfer/H-abstraction sequences that advance the reaction manifold. First, the tertiary alcohol in substrate (*R*)-**2.1a** is deprotonated by the acetate anion bound to Ag(**L2.1**), thereby obtaining an alkoxide species while activating CO₂ via a concerted **TS-1** (19.7 kJ·mol⁻¹) producing the first intermediate **A** located at 15.6 kJ·mol⁻¹ together with a molecule of acetic acid.²² The latter is not involved during the formation of the subsequent intermediates **B**, **C**, and **D**. In intermediate **B** (at -0.2 kJ·mol⁻¹), the initial alkyne coordination is replaced by an *O*-coordination of the formed linear carbonate after CO₂ activation. Then, the alkyne coordination is restored in intermediate **C** (-4.1 kJ·mol⁻¹) giving rise to a bidentate coordination mode. Through intermediate **C**, the system is set up toward the formation of an alkylidene cyclic carbonate going through **TS-2**: in this transition state, the

¹⁸ The Gaussian 16 program was used with implemented functional and basis set PBE0-D3(BJ)/SDD/def2tzv being chosen^{14,18,19} using dispersion correction with Becke–Johnson damping.^{20,21} All calculations were carried out at 298 K using an acetonitrile solvent model SMD. Full access to the computational data is provided through: <http://dx.doi.org/10.19061/iochem-bd-1-214>

¹⁹ T. G. Williams, A. K. Wilson, *J. Chem. Phys.* **2008**, *129*, No. 054108.

²⁰ M. Ernzerhof, G. E. Scuseria, *J. Chem. Phys.* **1999**, *110*, 5029–5036.

²¹ S. Grimme, S. Ehrlich, L. Goerigk, *J. Comput. Chem.* **2011**, *32*, 1456–1465.

²² S. Grimme, J. Antony, S. Ehrlich, H. Krieg, *J. Chem. Phys.* **2010**, *132*, No. 154104.

cyclic carbonate ring that is formed can have two mutual orientations with respect to the fixed conformation of the Ag(**L2.1**) complex, thus producing two different diastereoisomers.²³

In **TS-2** (at 63.0 and 55.1 kJ·mol⁻¹), both **TS-2A** and **TS-2B** differ in the double-bond configuration being *Z* and *E*, respectively. The resultant isomers **D-A** (at -5.0 kJ·mol⁻¹) and **D-B** (at -19.6 kJ·mol⁻¹) mimic the structures reported by Schaub, Hashmi, and co-workers before final protodemetalation affording alkylidene carbonates. Our pathway aligns well with the possibility of having *Z*- and *E*-configured TSs, and the energetic spans related to this first part of the mechanism for the conversion of (*R*)-**2.1a** are 67.1 and 59.2 kJ·mol⁻¹, with the (*E*) isomer being most favored.²⁴

For the other intermediate **E**, located between **TS-2** and **TS-3**, also the *Z* and *E* isomers (designated **A** and **B**) were calculated. For intermediates *E* (at 27.2 and 12.1 kJ·mol⁻¹) also the *Z* isomer is energetically less favored. The only difference compared to intermediates **D** is the presence of a molecule of acetic acid, which enables a protodemetalation through **TS-3A** and **TS-3B** (at 39.3 and 19.2 kJ·mol⁻¹, respectively). The following intermediate **F** located at -61.6 kJ·mol⁻¹ has an OAc ligand coordinating to the metal center, and the stereogenic information around the double bond is erased from this stage on. In **F**, the pendant alcohol of the cyclic carbonate is prepared for deprotonation by the OAc ligand, providing intermediate **G** (at -5.0 kJ·mol⁻¹). It was not possible to determine a transition state structure for this uphill process.

Subsequent decooordination of the carbonate-*O* through intermediate **H** (at -38.8 kJ·mol⁻¹) and rotation and re-coordination of the carbonate via the *O*-atom next to the olefin unit give intermediate **I** (at -20.6 kJ·mol⁻¹). An isomerization process occurs via tetrahedral **TS-4** (at -8.2 kJ·mol⁻¹), and a new five-membered cyclic carbonate is produced with an enol substituent coordinated to the metal via the *O*-center (i.e., intermediate **J** at -93.3 kJ·mol⁻¹). A more stable intermediate **K** (at -103.8 kJ·mol⁻¹) is obtained via an *O*-to-*C* rearrangement that involves the coordinated enolate.

To form the final product, first, a molecule of HOAc approaches the Ag complex in intermediate **L** (-83.1 kJ·mol⁻¹) and a proton transfer from HOAc to the C-atom of the initial

²³ Since the Ag-complex is chiral, diastereoisomeric TSs and intermediates are formed with distinct energies. Though for the chosen chiral conformation of the Ag-complex the conversion of (*R*)-**2.1a** is energetically favored, this is obviously reversed for the other chiral conformation of the Ag-complex making overall the conversion of both substrate enantiomers equally favored.

²⁴ The (*E*)-isomer in **TS-2** and the subsequent intermediate **D** has the carbonate substituents pointing away from the biaryl section of the ligand **L2.1**, and the Ag and carbonate-*O* atom reside on the same side of the C=C bond.

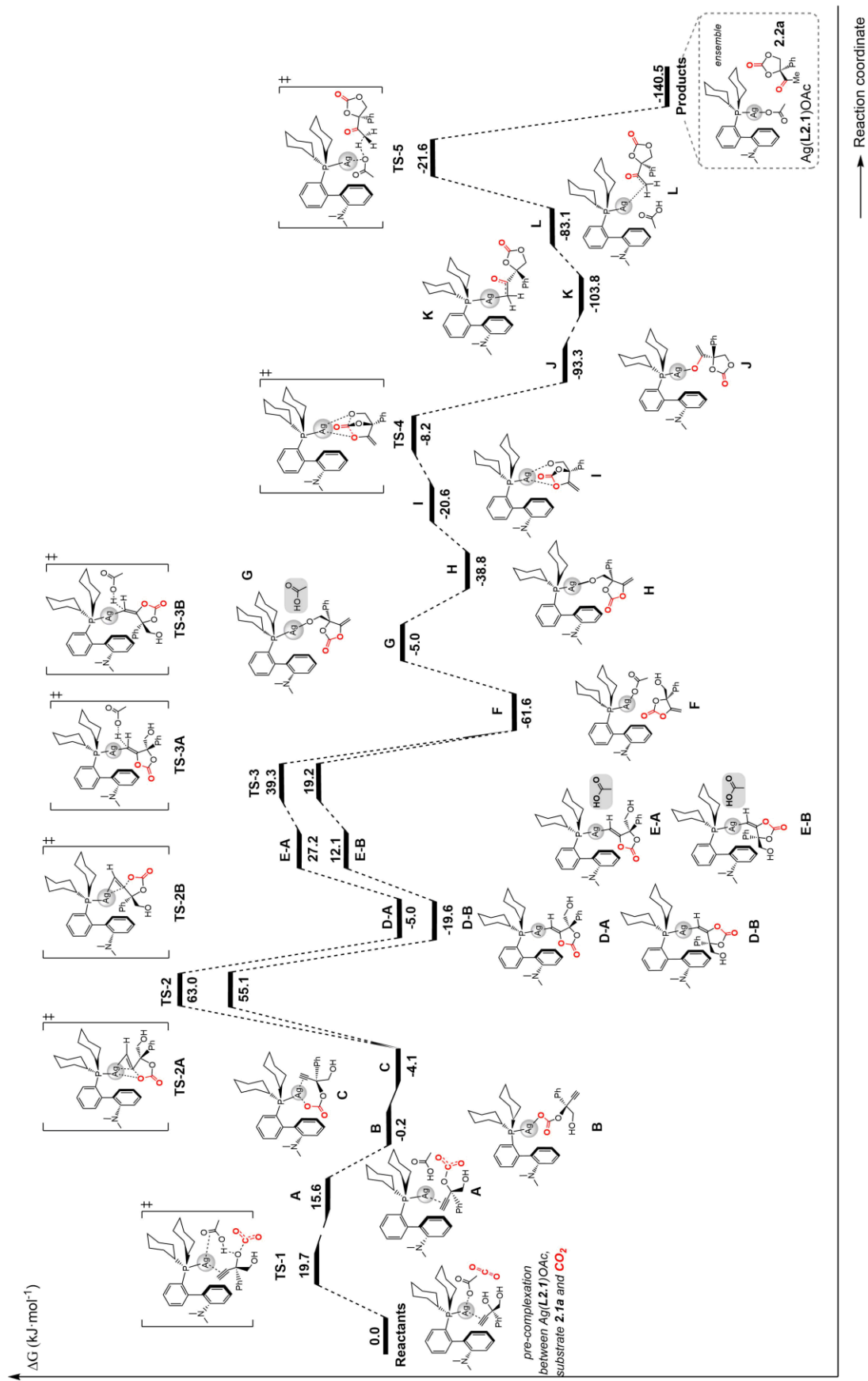


Figure 2.1 DFT-calculated pathway for the conversion of (R)-2.1a into keto-carbonate 2.2a by catalyst $\text{Ag}(\text{L}2.1)\text{OAc}$ in the presence of carbon dioxide.

enolate fragment through **TS-5** (at $-21.6 \text{ kJ}\cdot\text{mol}^{-1}$) releases the ensemble based on the keto-carbonate **2.2a** and the catalyst Ag(**L2.1**)OAc (at $-140.5 \text{ kJ}\cdot\text{mol}^{-1}$). From Figure 2.1, the determining transition state (TDTS) is **TS-2**, with a maximum energetic span of $67.1 \text{ kJ}\cdot\text{mol}^{-1}$ ($16.0 \text{ kcal}\cdot\text{mol}^{-1}$). This data corroborates well with the experimental finding that substrate (*R*)-**2.1a** can be converted into keto-carbonate **2.2a** under ambient conditions, while the same profile holds for (*S*)-**2.1a** using the other catalyst enantiomer.

2.5 Conclusions

In summary, in this chapter we discuss an efficient and new cascade process promoted by a Ag catalyst that involves the use of alkyne-1,2-diols as modular substrates providing access to a wide range of keto-substituted five-membered carbonates with different and unique degrees of substitutional complexity. Detailed computational analysis has shown the key rationale for the formation of these keto-carbonates, which are the most thermodynamically stable products. Preliminary investigations focusing on applying the cascade protocol for the creation of larger ring carbonates demonstrate that these less stable analogues of their five-membered congeners can be used as intermediates of otherwise elusive tetrasubstituted carbonate structures and therefore expand the synthetic importance of cascade approaches in the valorization of carbon dioxide.

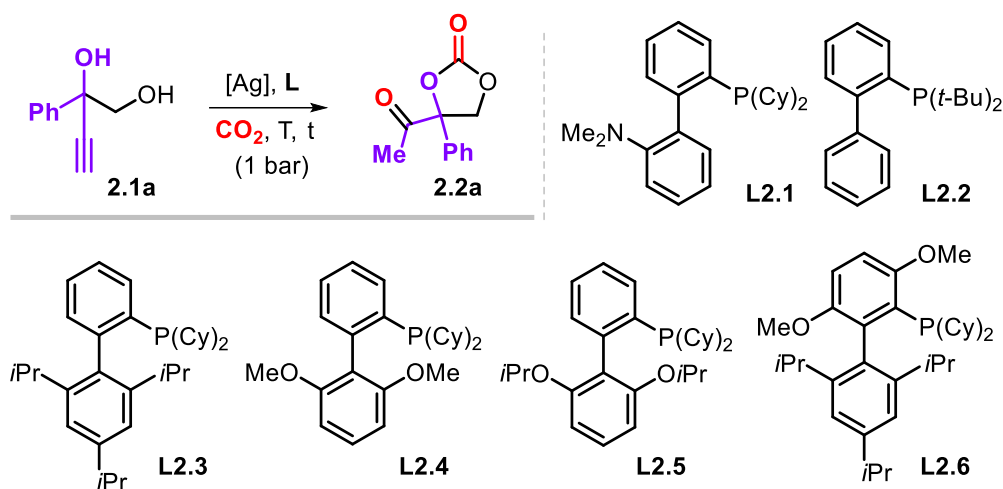
2.6 Experimental section

2.6.1 General information

Unless otherwise noted, all commercially available reagents and solvents were purchased from Sigma-Aldrich, TCI, Strem Chemicals, ABCR GmbH, Acros Organics or Alfa Aesar and were used without further purification. Solvents were dried using an Innovative Technology PURE SOLV solvent purification system. Carbon dioxide was purchased from PRAXAIR and used without further purification. Reactions were performed in a Schlenk tube or a stainless-steel HEL-multireactor under CO₂ atmosphere. Products were purified by flash chromatography or by preparative thin-layer chromatography on silica gel. NMR spectra were recorded on Bruker 400 MHz and Bruker 500 MHz at room temperature (25 °C). The residual solvent signals were used as references for ¹H and ¹³C spectra (CDCl₃: δ_H = 7.26 ppm, δ_C = 77.16 ppm, DMSO-d₆: δ_H = 2.50 ppm, δ_C = 39.52 ppm). ¹⁹F NMR spectra were obtained with ¹H decoupling unless stated otherwise. FT-IR measurements were carried out on a Bruker Optics FTIR-ATR TR0 spectrometer. Exact mass analyses and X-ray diffraction studies were performed by the Research Support Area (RSA) at ICIQ.

2.6.2 Further screening data of the reaction conditions

Table 2.2

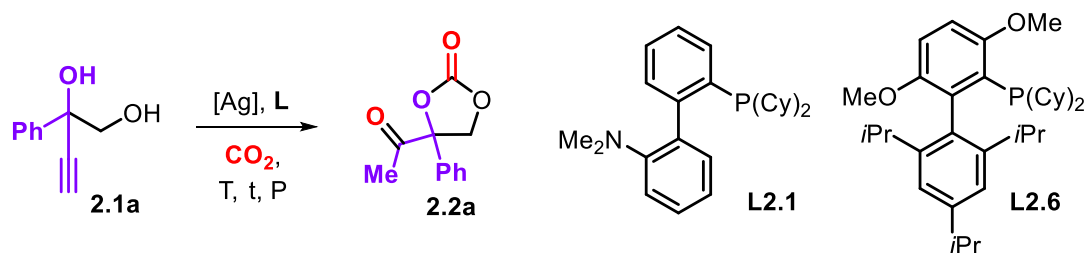


entry ^[a]	[Ag]/[mol%]	[L]/[mol%]	time/[h]	T/[°C]	Conv. [%] ^[b]	Yield [%] ^[b]
1	AgOAc, 10	–	24	35	0	0
2	–	L2.1 , 10	24	35	0	0
3	AgOAc, 10	L2.1 , 5	24	35	50	12
4	AgOAc, 5	L2.1 , 10	24	35	80	50
5	AgOAc, 10	L2.1 , 10	24	35	96	56
6	AgOAc, 10	L2.1 , 10	48	25	83	62
7	AgOAc, 10	PPh ₃ , 10	24	25	<10	<10
8	AgOAc, 10	P(OPh) ₃ , 10	24	25	0	0
9	AgOAc, 10	L2.2 , 10	24	25	77	66(63) ^[c]
10	AgOAc, 10	L2.3 , 10	24	25	82	74(66) ^[c]
11	AgOAc, 10	L2.4 , 10	24	25	84	73(68) ^[c]
12	AgOAc, 10	L2.5 , 10	24	25	85	63
13	AgOAc, 10	L2.6 , 10	24	25	100	91(85) ^[c]
14	AgOAc, 10	L2.7 , 5	24	25	0	0

Table 2.2 continued

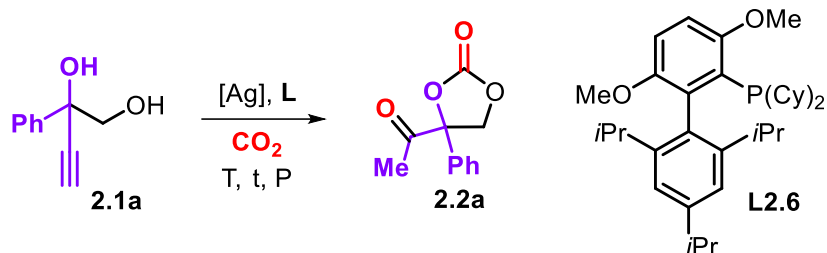
15	AgOAc, 10	L2.8 , 5	24	25	0	0
16	AgOAc, 5	L2.6 , 5	24	25	73	69
17	AgOAc, 25	L2.6 , 25	24	25	88	87
18	AgOAc, 5	L2.6 , 5	24	40	93	85
19	AgOAc, 2.5	L2.6 , 2.5	24	40	58	49
20	AgOAc, 2.5	L2.6 , 2.5	24	50	83	68
21	AgF, 5	L2.6 , 5	24	40	100	90
22	AgOTf, 5	L2.6 , 5	24	40	-	Not detected
23	AgNO ₃ , 5	L2.6 , 5	24	40	0	0
24	Ag ₂ CO ₃ , 5	L2.6 , 5	24	40	67	37
25	AgBF ₄ , 5	L2.6 , 5	24	40	-	Not detected
26	AgF ₆ Sb, 5	L2.6 , 5	24	40	0	0
27	AgF, 5	L2.6 , 5	6	40	100	91(88) ^[c]
28	AgF, 5	L2.6 , 5	12	40	100	89
29	AgF, 5	L2.6 , 5	18	40	100	87
30	AgF, 2.5	L2.6 , 2.5	6	40	12	<5
31	AgF, 5	L2.6 , 5	6	40	100	17 ^[d]
32	AgF, 5	L2.6 , 5	6	40	100	Not detected ^[e]
33	AgF, 5	L2.6 , 5	6	40	100	Not detected ^[f]
34	AgF, 5	L2.6 , 5	6	40	100	18 ^[g]
35	AgF, 5	L2.6 , 5	6	40	100	Not detected ^[h]

[a] Reaction condition: **2.1a** (0.3 mmol), CH₃CN (0.6 mL), [Ag]/[L] as indicated. [b] Determined by ¹H NMR (CDCl₃) analysis using mesitylene as an internal standard. [c] Isolated yield of **2.2a**. [d] Using MeOH as solvent. [e] Using DMF as solvent. [f] Using toluene as solvent. [g] Using THF as solvent. [h] Using DCM as solvent. **L2.7** stands for DPEPhos, **L2.8** for dppe.

Table 2.3

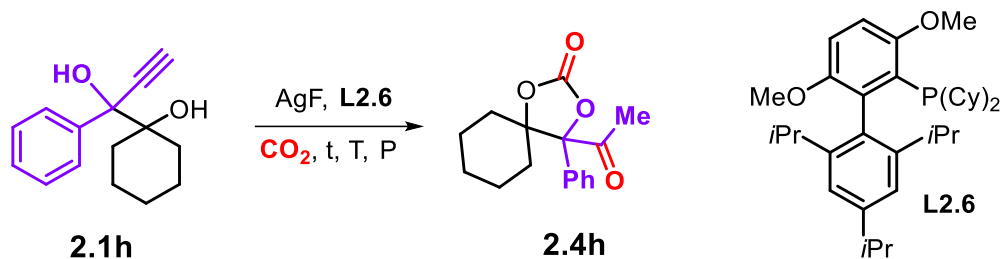
entry ^[a]	[Ag]	[L]	t, P	T	Conv. ^[b]	Yield ^[b]
1	AgF, 5	L2.6, 5	6, 1	40	52	29
2	AgF, 5	L2.6, 5	6, 1	60	22	No detected
3	AgF, 5	L2.6, 5	24, 1	40	83	10
4	AgF, 5	L2.6, 5	24, 10	rt	100	85(90) ^[c]
5	AgOAc, 10	L2.1, 10	24, 1	rt	37	18
6	AgOAc, 10	L2.1, 10	24, 1	50	30	<10
7	AgOAc, 10	L2.1, 10	48, 1	50	77	<10
8	AgOAc, 10	L2.1, 10	24, 10	rt	100	25(19) ^[c]

[a] Reaction conditions: **2.1a** (0.3 mmol), CH₃CN (0.6 mL), [Ag]/[L], t, P and T as indicated: [Ag] and [L] in mol%, time in h, pressure in bar, temperature in °C, conversion of **2.1a** and the yield of **2.2a** in %. [b] Determined by ¹H NMR (CDCl₃) analysis, using mesitylene as the internal standard. [c] Isolated yield of **2.2a** in brackets.

Table 2.4

entry ^[a]	$[\text{Ag}]$	$[\text{L}]$	t, P	T	Conv. ^[b]	Yield ^[b]
1	AgF, 5	L2.6 , 5	6, 1	40	45	Not detected
2	AgF, 5	L2.6 , 5	6, 1	60	42	Not detected
3	AgF, 5	L2.6 , 5	24, 10	rt	51	trace
4	AgF, 10	L2.6 , 10	24, 10	rt	100	<10
5	AgF, 5	L2.6 , 5	24, 30	rt	100	<10

[a] Reaction conditions: **2.1a** (0.3 mmol), CH₃CN (0.6 mL), $[\text{Ag}]/[\text{L}]$, t, P and T as indicated, $[\text{Ag}]$ and $[\text{L}]$ in mol%, time in h, pressure in bar, temperature in °C, conversion of **2.1a** and the yield of **2.2a** in %. [b] Determined by ¹H NMR (CDCl₃) analysis using mesitylene as an internal standard.

Table 2.5Screening data with substrate **2.1h**.

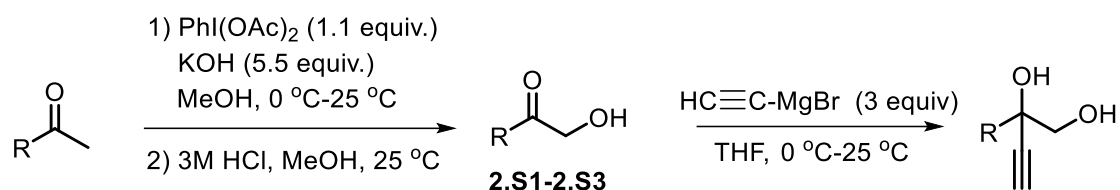
entry ^[a]	[Ag]	[L]	t, P	T	Conv. ^[b]	Yield ^[b]
1	AgF, 10	L2.6 , 10	24, 30	r.t.	100	95
2	AgF, 10	L2.6 , 10	24, 10	r.t.	100	93
3	AgF, 5	L2.6 , 5	6, 1	40	78	74
4	AgF, 5	L2.6 , 5	24, 1	40	100	90(87) ^[c]
5	AgF, 5	L2.6 , 5	24, 1	rt	93	83

[a] Reaction conditions: **2.1h** (0.3 mmol), CH₃CN (0.6 mL), [Ag]/[L], t, P and T as indicated, [Ag] and [L] in mol%, time in h, pressure in bar, temperature in °C, conversion of **2.1h** and the yield of **2.4h** in %. [b] Determined by ¹H NMR (CDCl₃) analysis, using mesitylene as the internal standard. [c] Isolated yield of **2.4h**.

2.6.3 Experimental procedures and characterization data for substrates

The known alkyne-1,2-diols were synthesized as reported in the literature.²⁵ Below the preparation of new alkyne-1,2-diols.

General Procedure A for alkyne-1,2-diol synthesis:

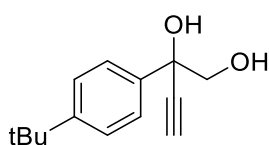


Step1: 2.S1-2.S3 were synthesized according to a literature procedure.²⁶ To a solution of the ketone derivative (30.0 mmol, 1.0 equiv) in MeOH (60 mL), (diacetoxyiodo)benzene (33.0 mmol, 1.1 equiv) and KOH (165.0 mmol, 5.5 equiv) were slowly added at 0 °C in an open round-bottomed flask. After the mixture had been stirred for 0.5 h at the same temperature it was allowed to reach room temperature over night after which TLC analysis showed complete consumption of the starting material. The reaction mixture was concentrated, water (100 mL) was added and the mixture was extracted with EtOAc (3 × 100 mL). The combined organic extracts were evaporated in vacuo and the residue was dissolved in a mixture of MeOH (20 mL) and aqueous 3 M HCl (20 mL). After stirring overnight at rt, the crude product was concentrated and further purified by column chromatography on silica gel to afford the corresponding α -hydroxy ketones.

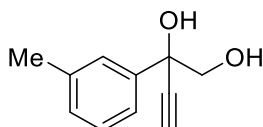
Step2: The alkyne-1,2-diols **2.1d**, **2.1k** and **2.1r** in this section were prepared according to a literature procedure.²⁵ In an oven-dried Schleck flask conditioned under a nitrogen atmosphere was introduced the appropriate α -hydroxy carbonyl compound (5 mmol, 1.0 equiv) in anhydrous THF (40 mL). The solution was cooled down to 0 °C (ice/water) and ethynyl magnesium bromide (0.5 M in THF, 3.0 equiv, 30 mL) was added dropwise via a syringe. The reaction mixture was allowed to warm to room temperature and further stirred for 16 h. Then, the reaction mixture was quenched with saturated aqueous NH₄Cl. The organic phase was extracted with EtOAc (3 × 50 mL). All the organic fractions were combined, dried with anhydrous Na₂SO₄, filtered and concentrated. The crude products were purified by flash chromatography on silica gel to afford the corresponding alkyne-1,2 diols.

²⁵ J. E. Gómez, A. Cristòfol, A. W. Kleij, *Angew. Chem. Int. Ed.* **2019**, 58, 3903–390.

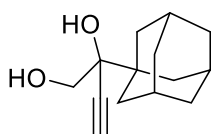
²⁶ Z. Liu, W. Zhang, S. Guo, *J. Org. Chem.* **2019**, 84, 11945–11957.

2-(4-(tert-Butyl)phenyl)but-3-yne-1,2-diol (2.1d)

Yellow solid (794.0 mg, 73% yield). Eluent hexanes/EtOAc = 5/1. ¹H NMR (500 MHz, CDCl₃) δ 7.56 – 7.55 (m, 2H), 7.42 – 7.40 (m, 2H), 3.77 (d, *J* = 11.3 Hz, 1H), 3.68 (d, *J* = 11.3 Hz, 1H), 2.70 (s, 1H), 2.25 (brs, 2H), 1.32 (s, 9H); ¹³C NMR (126 MHz, CDCl₃) δ 151.6, 137.1, 125.6, 125.5, 84.6, 74.8, 73.6, 72.1, 34.7, 31.4. HRMS (ESI/TOF) *m/z* Calcd for C₁₄H₁₈NaO₂ [M + Na]⁺ 241.1199; Found 241.1203.

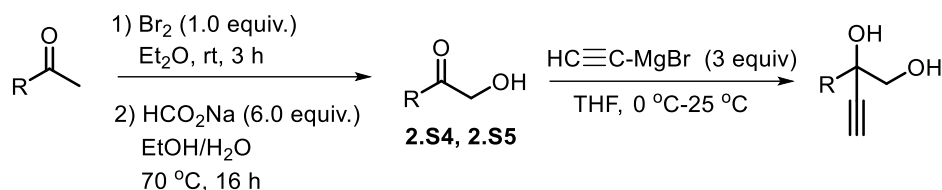
2-(*m*-Tolyl)but-3-yne-1,2-diol (2.1k)

Yellow solid (537.0 mg, 61% yield). Eluent hexanes/EtOAc = 3/1. ¹H NMR (400 MHz, CDCl₃) δ 7.44 – 7.42 (m, 2H), 7.30 – 7.26 (m, 1H), 7.16 – 7.14 (m, 1H), 3.77 (d, *J* = 11.2 Hz, 1H), 3.66 (d, *J* = 11.2 Hz, 1H), 2.70 (s, 1H), 2.38 (s, 3H), 2.17 (s, 1H); ¹³C NMR (101 MHz, CDCl₃) δ 140.1, 138.3, 129.3, 128.5, 126.5, 123.0, 84.6, 74.9, 73.7, 72.1, 21.7. HRMS (ESI/TOF) *m/z* Calcd for C₁₁H₁₂NaO₂ [M + Na]⁺ 199.0730; Found 199.0735.

2-(Adamantan-1-yl)-but-3-yne-1,2-diol (2.1r)

White solid (511.0 mg, 50% yield). Eluent hexanes/EtOAc = 3/1. ¹H NMR (400 MHz, CDCl₃) δ 3.75 (d, *J* = 10.9 Hz, 1H), 3.67 (d, *J* = 10.9, 1H), 2.49 (s, 1H), 2.04 – 2.01 (m, 4H), 1.77 – 1.65 (m, 13H); ¹³C NMR (101 MHz, CDCl₃) δ 84.4, 77.8, 74.7, 65.6, 38.5, 37.1, 36.8, 28.5. HRMS (ESI/TOF) *m/z* Calcd for C₁₄H₂₀NaO₂ [M + Na]⁺ 243.1356; Found 243.1352.

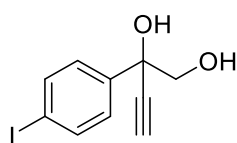
General Procedure B for alkyne-1,2-diol synthesis:



2.S4 and **2.S5** were synthesized according to the literature procedure.²⁷ Bromine (1.0 mL, 1.0 equiv) was added dropwise to a solution of the respective ketone derivative (20.0 mmol, 1.0 equiv) in Et₂O (30 mL) at 0 °C in a round-bottomed flask. Then the mixture was allowed to warm to room temperature and stirred for 3 h. When the starting material had disappeared (followed by TLC), the reaction mixture was quenched with ice water (20 mL) and extracted with Et₂O (3 × 20 mL). The combined organic layers were washed with saturated aqueous NaHCO₃ solution (40 mL), and dried over Na₂SO₄. After being filtered and concentrated, the residue was dissolved in a mixture of EtOH (80 mL) and H₂O (40 mL), and sodium formate (120.0 mmol, 6.0 equiv) was added. This mixture was stirred for 16 h at 70 °C, then concentrated under vacuum, diluted with H₂O (20 mL) and extracted with EtOAc (3 × 20 mL). The combined layers were dried over anhydrous Na₂SO₄, filtered, and concentrated in *vacuo*. The crude product was purified by flash chromatography on silica gel to obtain the respective α -hydroxy ketone.

Note: The alkyne-1,2-diols **2.1h** and **2.1s** were obtained according to the final one step from **General Procedure A**.

²⁷ K. Guo, A. W. Kleij, *Angew. Chem. Int. Ed.* **2021**, *60*, 4901–4906.

2-(4-Iodophenyl)but-3-yne-1,2-diol (2.1h)

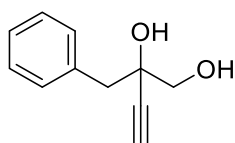
Brown solid (743.8 mg, 51% yield). Eluent hexanes/EtOAc = 3/1. ¹H

NMR (500 MHz, CDCl₃) δ 7.72 – 7.70 (m, 2H), 7.38 – 7.35 (m, 2H), 3.73

(d, *J* = 11.3 Hz, 1H), 3.60 (d, *J* = 11.3 Hz, 1H), 2.71 (s, 1H); ¹³C **NMR**

(126 MHz, CDCl₃) δ 140.0, 137.6, 127.9, 94.4, 83.9, 75.3, 73.4, 71.9. **HRMS** (ESI/TOF) *m/z*

Calcd for C₁₀H₉INaO₂ [M + Na]⁺ 310.9539; Found 310.9533.

2-Benzyl-but-3-yne-1,2-diol (2.1s)

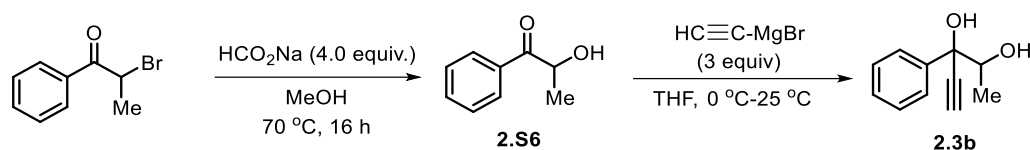
Yellow solid (474.1 mg, 52% yield). Eluent hexanes/EtOAc = 3/1. ¹H

NMR (400 MHz, CDCl₃) δ 7.36 – 7.28 (m, 5H), 3.72 (d, *J* = 11.2 Hz,

1H), 3.60 (d, *J* = 11.2 Hz, 1H), 3.01 (dd, *J* = 16.3, 13.4 Hz, 2H), 2.52 (s,

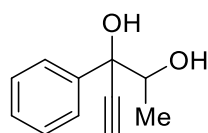
1H), 2.22 (brs, 2H); ¹³C **NMR** (101 MHz, CDCl₃) δ 135.3, 130.9, 128.4, 127.3, 84.3, 75.0, 71.6, 69.2,

43.8. **HRMS** (ESI/TOF) *m/z* Calcd for C₁₁H₁₂NaO₂ [M + Na]⁺ 199.0730; Found 199.0723.

Procedure C for the synthesis of alkyne-1,2-diol 2.3b:

2.S6 was synthesized according to the literature procedure.²⁸ To a solution of 2-bromopropiophenone (16.4 mmol, 1.0 equiv) in MeOH (17 mL) was added sodium formate (64.8 mmol, 4.0 equiv), and the reaction mixture was stirred for 16 h at 70 °C. Then, it was concentrated under vacuum, diluted with H₂O (20 mL) and extracted with EtOAc (3 × 20 mL). The combined layers were dried over anhydrous Na₂SO₄, filtered, and concentrated in *vacuo*. The crude product was purified by flash chromatography on silica gel to obtain the corresponding α -hydroxy ketone **2.S6**.

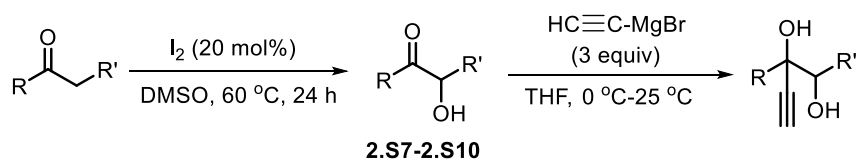
Note: Alkyne-1,2-diol **2.3b** was obtained according to the final step **General Procedure A**.

3-Phenyl-pent-4-yne-2,3-diol (2.3b)

Yellow oil (485.6 mg, 55% yield). Eluent hexanes/EtOAc = 3/1. **¹H NMR** (400 MHz, CDCl₃) δ 7.62-7.59 (m, 2H), 7.40-7.30 (m, 3H), 4.04 (q, J = 6.3 Hz, 1H), 2.68 (s, 1H), 1.06 (d, J = 6.3 Hz, 3H); **¹³C NMR** (101 MHz, CDCl₃) δ 140.0, 128.29, 128.27, 126.3, 85.5, 75.9, 74.9, 74.7, 16.2. **HRMS** (ESI/TOF) m/z . Calcd for C₁₁H₁₂NaO₂ [M + Na]⁺ 199.0730; Found 199.0733.

²⁸ S. Kang, J. Han, E. S. Lee, *Org. Lett.* **2010**, *12*, 4184–4187.

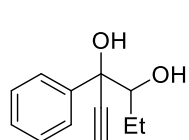
General procedure D for alkyne-1,2-diol synthesis:



2.S7-2.S10 were synthesized according to the literature procedure.²⁹ To a solution of the respective ketone (10.0 mmol, 1.0 equiv) in DMSO (10 mL) was added I₂ (2.0 mmol, 20 mol %) under air, and the reaction mixture was stirred for 24 h at 60 °C while followed by TLC. When complete consumption of the starting material was observed, the mixture was allowed to cool down to room temperature, and the solution was diluted with ethyl acetate (200 mL), washed with 0.1 M Na₂S₂O₃ (100 mL) aqueous solution and extracted with EtOAc (3 × 100 mL). The combined organic layers were dried over anhydrous Na₂SO₄, filtered and concentrated in *vacuo*. The crude product was purified by flash chromatography on silica gel to obtain the respective α -hydroxy ketone.

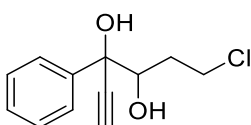
Note: Alkyne-1,2-diols **2.3c**, **2.3d**, **2.3e** and **2.3g** were obtained according to the final of **General Procedure A**.

3-Phenylhex-1-yne-3,4-diol (2.3c)



Yellow oil (855.7 mg, 90% yield). Eluent hexanes/EtOAc = 3/1. **¹H NMR** (500 MHz, CDCl₃) δ 7.62 – 7.60 (m, 2H), 7.40 – 7.36 (m, 2H), 7.34 – 7.31 (m, 1H), 3.75 (dd, J = 10.3, 2.3 Hz, 1H), 2.93 (brs, 1H), 2.68 (s, 1H), 1.53 – 1.45 (m, 1H), 1.31 – 1.22 (m, 1H), 0.93 (t, J = 7.5 Hz, 3H); **¹³C NMR** (126 MHz, CDCl₃) δ 140.2, 128.30, 128.26, 126.3, 85.7, 80.3, 75.9, 74.6, 23.4, 10.9. **HRMS** (ESI/TOF) m/z Calcd for C₁₂H₁₄NaO₂ [M + Na]⁺ 213.0886; Found 213.0887.

6-Chloro-3-phenyl-hex-1-yne-3,4-diol (2.3d)



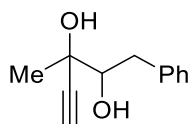
Brown oil (940.1 mg, 84% yield). Eluent hexanes/EtOAc = 3/1.

¹H NMR (400 MHz, CDCl₃) δ 7.62 – 7.59 (m, 2H), 7.43 – 7.32 (m, 3H), 4.09 (dd, J = 9.4, 3.2 Hz, 1H), 3.68 – 3.58 (m, 2H), 2.94 (brs, 1H), 2.71

²⁹ Y. F. Liang, K. Wu, S. Song, *Org. Lett.* **2015**, *17*, 876–879.

(s, 1H), 2.40 (brs, 1H), 1.90 – 1.76 (m, 2H); ¹³C NMR (101 MHz, CDCl₃) δ 139.7, 128.6, 128.5, 126.2, 85.1, 75.54, 75.50, 75.1, 42.0, 33.1. HRMS (ESI/TOF) *m/z* Calcd for C₁₂H₁₃ClNaO₂ [M + Na]⁺ 247.0496; Found 247.0498.

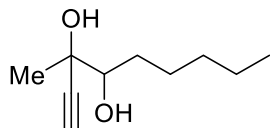
3-Methyl-1-phenyl-pent-4-yne-2,3-diol (2.3e)



Yellow solid (287.1 mg, 30% yield, 77:23 *dr*). Eluent hexanes/EtOAc = 3/1.

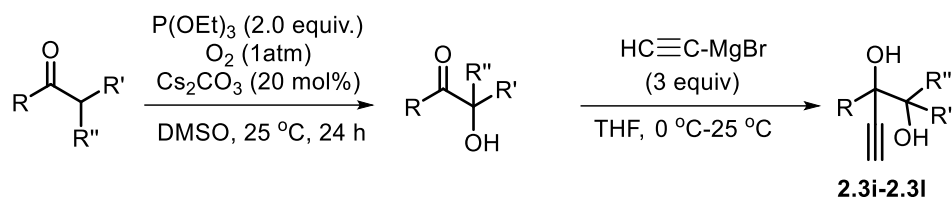
¹H NMR (400 MHz, CDCl₃) (major) δ 7.36 – 7.31 (m, 2H), 7.29 – 7.23 (m, 3H), 3.84 (dd, *J* = 10.5, 2.3 Hz, 1H), 3.09 (dd, *J* = 14.0, 2.3 Hz, 1H), 2.65 (dd, *J* = 14.0, 10.5 Hz, 1H), 2.54 (s, 1H), 2.34 (brs, 2H), 1.55 (s, 3H); ¹H NMR (400 MHz, CDCl₃) (minor) δ 7.36 – 7.31 (m, 2H), 7.29 – 7.23 (m, 3H), 3.70 (dd, *J* = 10.3, 2.7 Hz, 1H), 3.07 (dd, *J* = 14.0, 2.7 Hz, 1H), 2.80 (dd, *J* = 14.0, 10.3 Hz, 1H), 2.56 (s, 1H), 2.34 (brs, 2H), 1.55 (s, 3H); ¹³C NMR (101 MHz, CDCl₃) (major) δ 138.7, 129.4, 128.7, 126.7, 86.0, 78.5, 73.2, 70.8, 37.7, 24.1; ¹³C NMR (101 MHz, CDCl₃) (minor) δ 138.2, 129.5, 128.8, 126.8, 85.0, 78.8, 73.6, 71.0, 38.9, 26.0. HRMS (ESI/TOF) *m/z* Calcd for C₁₂H₁₄NaO₂ [M + Na]⁺ 213.0886; Found 213.0889.

3-Methyl-non-1-yne-3,4-diol (2.3g)



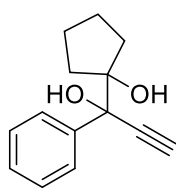
Yellow oil (299.5 mg, 35% yield, 4:1 *dr*). Eluent hexanes/EtOAc = 3/1.

¹H NMR (400 MHz, CDCl₃) (major) δ 3.60 – 3.58 (m, 1H), 2.48 (s, 1H), 2.41 (brs, 1H), 2.23 (brs, 1H), 1.69 – 1.49 (m, 3H), 1.44 (s, 3H), 1.38 – 1.30 (m, 5H), 0.90 (t, *J* = 6.8 Hz, 3H); ¹H NMR (400 MHz, CDCl₃) (minor) δ 3.41 – 3.38 (m, 1H), 2.96 (brs, 1H), 2.47 (s, 1H), 1.87 (brs, 1H), 1.69 – 1.49 (m, 3H), 1.45 (s, 3H), 1.38 – 1.30 (m, 5H), 0.90 (t, *J* = 6.8 Hz, 3H); ¹³C NMR (101 MHz, CDCl₃) (major) δ 86.4, 77.6, 72.9, 71.1, 31.90, 30.8, 26.3, 23.6, 22.7, 14.2; ¹³C NMR (101 MHz, CDCl₃) (minor) δ 85.1, 78.5, 73.4, 71.6, 32.3, 31.87, 26.0, 25.6, 22.7, 14.2. HRMS (ESI/TOF) *m/z* Calcd for C₁₀H₁₈NaO₂ [M + Na]⁺ 193.1199; Found 193.1198.

General Procedure E for alkyne-1,2-diol synthesis:

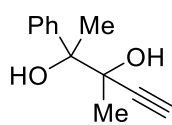
The α -hydroxy ketones of this section were synthesized according to the literature procedure.³⁰ Cs₂CO₃ (2.0 mmol, 20 mol %), P(OEt)₃ (20.0 mmol, 2.0 equiv), the respective ketone (10.0 mmol, 1.0 equiv.) were added to a 100 mL Schlenk tube under air. DMSO (40 mL) was added, the reaction mixture was stirred for 24-72 h at room temperature under air (1 atm). When complete consumption of the starting material had been observed (TLC), the solution was diluted with ethyl acetate (200 mL), washed with brine (50 mL), and extracted with EtOAc (3 × 100 mL). The combined organic layers were dried over anhydrous Na₂SO₄, filtered and concentrated in *vacuo*. The crude product was purified by flash chromatography on silica gel to obtain the respective α -hydroxy ketone.

Note: Alkyne-1,2-diols (**2.3i–2.3l**) were obtained according to the final one step of **General Procedure A**.

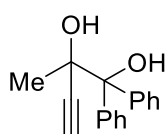
1-(1-Hydroxy-1-phenyl-prop-2-yn-1-yl)cyclopentan-1-ol (2.3i)

Brown solid (872.0 mg, 80% yield). Eluent hexanes/EtOAc = 3/1. **¹H NMR** (400 MHz, CDCl₃) δ 7.70 – 7.67 (m, 2H), 7.38 – 7.29 (m, 3H), 2.67 (s, 1H), 2.17 – 2.10 (m, 1H), 1.92 – 1.85 (m, 1H), 1.84 – 1.72 (m, 2H), 1.65 – 1.47 (m, 3H), 1.45 – 1.37 (m, 1H); **¹³C NMR** (101 MHz, CDCl₃) δ 140.4, 128.2, 127.8, 127.3, 87.8, 85.9, 77.8, 74.3, 36.2, 34.9, 24.13, 24.07. **HRMS** (ESI/TOF) *m/z*. Calcd for C₁₄H₁₆NaO₂ [M + Na]⁺ 239.1043; Found 239.1051.

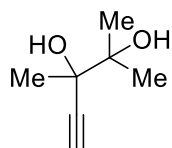
³⁰ Y. F. Liang, N. Jiao, *Angew. Chem. Int. Ed.* **2014**, *53*, 548-552.

3-Methyl-2-phenyl-pent-4-yne-2,3-diol (2.3k)

Yellow solid (446.7 mg, 47% yield). Eluent hexanes/EtOAc = 3/1. **¹H NMR** (400 MHz, CDCl₃) δ 7.62 – 7.59 (m, 2H), 7.36 – 7.28 (m, 3H), 4.98 (brs, 1H), 2.71 (brs, 1H), 2.56 (s, 1H), 1.80 (s, 3H), 1.31 (s, 3H); **¹³C NMR** (101 MHz, CDCl₃) δ 142.5, 127.8, 127.4, 126.8, 86.3, 77.9, 74.0, 73.9, 25.5, 25.0; **HRMS** (ESI/TOF) *m/z* Calcd for C₁₂H₁₄NaO₂ [M + Na]⁺ 213.0886; Found 213.0885.

2-Methyl-1,1-diphenylbut-3-yne-1,2-diol (2.3l)

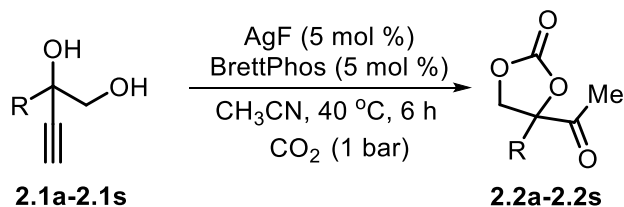
Yellow oil (516.9 mg, 41% yield). Eluent hexanes/EtOAc = 3/1. **¹H NMR** (400 MHz, CDCl₃) δ 7.74 – 7.70 (m, 4H), 7.33 – 7.26 (m, 6H), 3.15 (brs, 1H), 2.67 (s, 1H), 2.53 (brs, 1H), 1.55 (s, 3H); **¹³C NMR** (101 MHz, CDCl₃) δ 128.5, 128.1, 127.8, 127.64, 127.56, 127.4, 86.5, 26.8. **HRMS** (ESI/TOF) *m/z* Calcd for C₁₇H₁₆NaO₂ [M + Na]⁺ 275.1043; Found 275.1046.

2,3-Dimethylpent-4-yne-2,3-diol (2.3m)

Yellow oil (448.9 mg, 70% yield). Eluent hexanes/EtOAc = 3/1. **¹H NMR** (500 MHz, CDCl₃) δ 2.48 (s, 1H), 2.21 (brs, 2H), 1.47 (s, 3H), 1.40 (s, 3H), 1.28 (s, 3H); **¹³C NMR** (126 MHz, CDCl₃) δ 86.3, 75.3, 74.0, 73.0, 25.7, 24.3, 22.8. **HRMS** (ESI/TOF) *m/z* Calcd for C₇H₁₂NaO₂ [M + Na]⁺ 151.0730; Found 151.0729.

2.6.4 Procedures and characterization data for the carbonate products

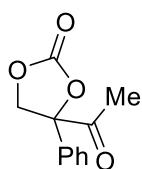
General Procedure F for the synthesis of the cyclic carbonates 2.2a-2.2s:



The respective 1,2-diol (0.3 mmol, 1.0 equiv), AgF (0.015 mmol, 5 mol %), BrettPhos (0.015 mmol, 5 mol%) were added to a 25 mL reaction tube. The tube was purged three times with CO₂ and then charged with a CO₂ balloon (1 bar). Hereafter, MeCN (0.6 mL) was added using a syringe. The reaction mixture was stirred at 40 °C for 6 h. When complete consumption of the starting material had been observed by TLC, the mixture was transferred to a round-bottom flask, concentrated and purified by flash column chromatography on silica to afford the corresponding cyclic carbonate product. **Note:** only the characteristic *carbonyl/carbonate* IR frequencies are provided in the analytical data descriptions.

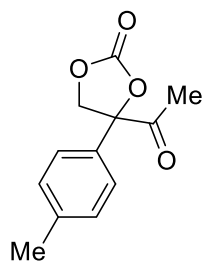
Gram-scale reaction: The 1,2-diol **2.1a** (6.5 mmol, 1.0 equiv), AgF (0.325 mmol, 5 mol%), BrettPhos (0.325 mmol, 5 mol%) were added to an oven-dried Schleck flask. The tube was purged three times with CO₂ and then charged with a CO₂ balloon (1 bar). Hereafter, MeCN (13.0 mL) was added using a syringe. The reaction mixture was stirred at 40 °C for 6 h. When complete consumption of the starting material had been observed by TLC, the mixture was transferred to a round-bottom flask, concentrated and purified by flash column chromatography on silica to afford the corresponding cyclic carbonate product **2.2a** with a 85% isolated yield.

4-Acetyl-4-phenyl-1,3-dioxolan-2-one (2.2a)



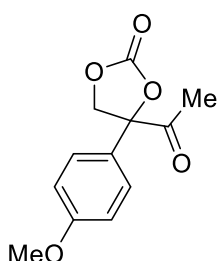
Colorless solid (54.5 mg, 88% yield). Eluent hexanes/EtOAc = 4/1. **¹H NMR** (400 MHz, CDCl₃) δ 7.47 – 7.42 (m, 3H), 7.40 – 7.36 (m, 2H), 5.26 (d, *J* = 8.6 Hz, 1H), 4.38 (d, *J* = 8.6 Hz, 1H), 2.26 (s, 3H); **¹³C NMR** (101 MHz, CDCl₃) δ 202.9, 153.1, 135.0, 129.8, 129.6, 124.1, 88.6, 72.5, 24.9; **IR (neat):** ν = 1803, 1729 cm⁻¹; **HRMS** (ESI/TOF) *m/z* Calcd for C₁₁H₁₀NaO₄ [M + Na]⁺ 229.0471; Found 229.0474. This compound was further characterized by X-ray crystallography.

4-Acetyl-4-(*p*-tolyl)-1,3-dioxolan-2-one (2.2b)



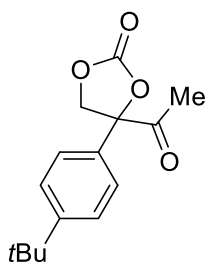
Colorless oil (58.6 mg, 88% yield). Eluent hexanes/EtOAc = 4/1. **¹H NMR** (400 MHz, CDCl₃) δ 7.26 – 7.24 (m, 4H), 5.23 (d, *J* = 8.6 Hz, 1H), 4.36 (d, *J* = 8.6 Hz, 1H), 2.37 (s, 3H), 2.26 (s, 3H); **¹³C NMR** (101 MHz, CDCl₃) δ 203.0, 153.2, 140.0, 132.0, 130.3, 124.0, 88.7, 72.5, 24.8, 21.3; **IR (neat):** *ν* = 1806, 1724 cm⁻¹; **HRMS (ESI/TOF)** *m/z* Calcd for C₁₂H₁₂NaO₄ [M + Na]⁺ 243.0628; Found 243.0626.

4-Acetyl-4-(4-methoxyphenyl)-1,3-dioxolan-2-one (2.2c)



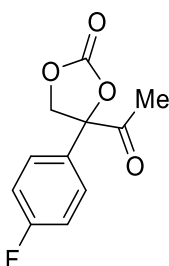
White solid (64.0 mg, 91% yield). Eluent hexanes/EtOAc = 4/1. **¹H NMR** (400 MHz, CDCl₃) δ 7.31 – 7.27 (m, 2H), 6.97 – 6.93 (m, 2H), 5.22 (d, *J* = 8.6 Hz, 1H), 4.36 (d, *J* = 8.6 Hz, 1H), 3.82 (s, 3H), 2.26 (s, 3H); **¹³C NMR** (101 MHz, CDCl₃) δ 203.1, 160.7, 153.2, 126.7, 125.6, 115.0, 88.6, 72.6, 55.6, 24.8; **IR (neat):** *ν* = 1796, 1721 cm⁻¹; **HRMS (ESI/TOF)** *m/z* Calcd for C₁₂H₁₂NaO₅ [M + Na]⁺ 259.0577; Found 259.0575.

4-Acetyl-4-(4-(*tert*-butyl)phenyl)-1,3-dioxolan-2-one (2.2d)



Yellow solid (56.3 mg, 71% yield). Eluent hexanes/EtOAc = 4/1. **¹H NMR** (400 MHz, CDCl₃) δ 7.47 – 7.44 (m, 2H), 7.31 – 7.29 (m, 2H), 5.23 (d, *J* = 8.6 Hz, 1H), 4.38 (d, *J* = 8.6 Hz, 1H), 2.27 (s, 3H), 1.32 (s, 9H); **¹³C NMR** (101 MHz, CDCl₃) δ 203.1, 153.2, 153.1, 131.9, 126.6, 123.9, 88.8, 72.5, 34.9, 31.3, 24.9; **IR (neat):** *ν* = 1809, 1725 cm⁻¹; **HRMS (ESI/TOF)** *m/z* Calcd for C₁₅H₁₈NaO₄ [M + Na]⁺ 285.1097; Found 285.1085.

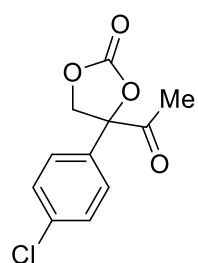
4-Acetyl-4-(4-fluorophenyl)-1,3-dioxolan-2-one (2.2e)



White solid (59.1 mg, 87% yield). Eluent hexanes/EtOAc = 4/1. **¹H NMR** (400 MHz, CDCl₃) δ 7.40 – 7.36 (m, 2H), 7.17 – 7.13 (m, 2H), 5.23 (d, *J* = 8.6 Hz, 1H), 4.36 (d, *J* = 8.6 Hz, 1H), 2.27 (s, 3H); **¹³C NMR** (101 MHz, CDCl₃) δ 203.0, 163.5 (d, *J* = 250.2 Hz), 152.9, 130.8 (d, *J* = 3.1 Hz), 126.2 (d, *J* = 8.3 Hz), 116.8 (d, *J* = 22.1 Hz), 88.2, 72.6, 24.9; **¹⁹F NMR** (376 MHz, CDCl₃) δ

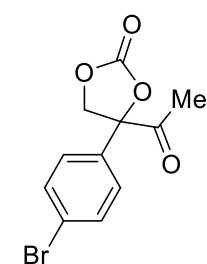
-110.96; **IR (neat)**: $\nu = 1809, 1736 \text{ cm}^{-1}$; **HRMS (ESI/TOF)** m/z Calcd for C₁₁H₉FNaO₄ [M + Na]⁺ 247.0377; Found 247.0383.

4-Acetyl-4-(4-chlorophenyl)-1,3-dioxolan-2-one (2.2f)



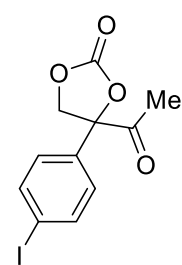
White solid (62.2 mg, 86% yield). Eluent hexanes/EtOAc = 4/1. **¹H NMR** (400 MHz, CDCl₃) δ 7.44 – 7.42 (m, 2H), 7.35 – 7.32 (m, 2H), 5.22 (d, $J = 8.6 \text{ Hz}$, 1H), 4.35 (d, $J = 8.6 \text{ Hz}$, 1H), 2.27 (s, 3H); **¹³C NMR** (101 MHz, CDCl₃) δ 202.8, 152.8, 136.2, 133.4, 129.9, 125.6, 88.2, 72.5, 24.9; **IR (neat)**: $\nu = 1810, 1727 \text{ cm}^{-1}$; **HRMS (ESI/TOF)** m/z Calcd for C₁₁H₉ClNaO₄ [M + Na]⁺ 263.0082; Found 263.0084.

4-Acetyl-4-(4-bromophenyl)-1,3-dioxolan-2-one (2.2g)



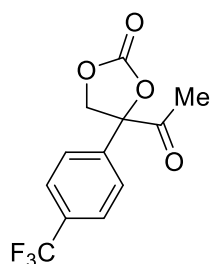
White solid (71.2 mg, 83% yield). Eluent hexanes/EtOAc = 4/1. **¹H NMR** (400 MHz, CDCl₃) δ 7.54 – 7.50 (m, 2H), 7.22 – 7.19 (m, 2H), 5.15 (d, $J = 8.6 \text{ Hz}$, 1H), 4.28 (d, $J = 8.6 \text{ Hz}$, 1H), 2.20 (s, 3H); **¹³C NMR** (101 MHz, CDCl₃) δ 202.7, 152.7, 134.0, 132.9, 125.8, 124.3, 88.2, 72.4, 24.9; **IR (neat)**: $\nu = 1809, 1725 \text{ cm}^{-1}$; **HRMS (ESI/TOF)** m/z Calcd for C₁₁H₉BrNaO₄ [M + Na]⁺ 306.9576; Found 306.9581.

4-Acetyl-4-(4-iodophenyl)-1,3-dioxolan-2-one (2.2h)



White solid (89.2 mg, 80% yield). Eluent hexanes/EtOAc = 4/1. **¹H NMR** (400 MHz, CDCl₃) δ 7.81 – 7.77 (m, 2H), 7.15 – 7.11 (m, 2H), 5.21 (d, $J = 8.7 \text{ Hz}$, 1H), 4.34 (d, $J = 8.7 \text{ Hz}$, 1H), 2.26 (s, 3H); **¹³C NMR** (101 MHz, CDCl₃) δ 202.6, 152.8, 138.8, 134.7, 125.9, 96.0, 88.2, 72.3, 24.9; **IR (neat)**: $\nu = 1805, 1725 \text{ cm}^{-1}$; **HRMS (ESI/TOF)** m/z Calcd for C₁₁H₉INaO₄ [M + Na]⁺ 354.9438; Found 354.9433.

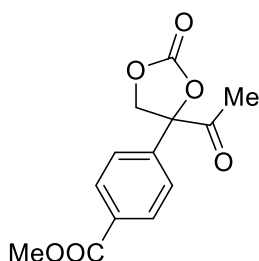
4-Acetyl-4-(4-(trifluoromethyl)phenyl)-1,3-dioxolan-2-one (2.2i)



White solid (48.6 mg, 59% yield). Eluent hexanes/EtOAc = 4/1. **¹H NMR** (400 MHz, CDCl₃) δ 7.74 – 7.72 (m, 2H), 7.57 – 7.54 (m, 2H), 5.26 (d, *J* = 8.7 Hz, 1H), 4.38 (d, *J* = 8.7 Hz, 1H), 2.29 (s, 3H); **¹³C NMR** (101 MHz, CDCl₃) δ 202.5, 152.6, 138.8, 132.3 (d, *J* = 32.9 Hz), 126.7 (d, *J* = 3.7 Hz), 124.8, 123.6 (d, *J* = 272.5 Hz), 88.2, 72.4, 25.1; **¹⁹F NMR** (376 MHz, CDCl₃) δ -63.10; **IR (neat):** ν = 1813, 1727 cm⁻¹; **HRMS (ESI/TOF) *m/z***

Calcd for C₁₂H₉F₃NaO₄ [M + Na]⁺ 297.0345; Found 297.0351.

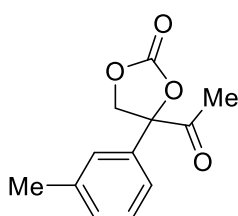
Methyl 4-(4-acetyl-2-oxo-1,3-dioxolan-4-yl)benzoate (2.2j)



White solid (61.6 mg, 84% yield). Eluent hexanes/EtOAc = 4/1. **¹H NMR** (400 MHz, CDCl₃) δ 8.10 – 8.08 (m, 2H), 7.48 – 7.45 (m, 2H), 5.25 (d, *J* = 8.7 Hz, 1H), 4.37 (d, *J* = 8.7 Hz, 1H), 3.91 (s, 3H), 2.25 (s, 3H); **¹³C NMR** (101 MHz, CDCl₃) δ 202.4, 166.1, 152.7, 139.4, 131.7, 130.9, 124.3, 88.4, 72.3, 52.6, 25.0; **IR (neat):** ν = 1811, 1714 cm⁻¹;

HRMS (ESI/TOF) *m/z* Calcd for C₁₃H₁₂NaO₆ [M + Na]⁺ 287.0526; Found 287.0531.

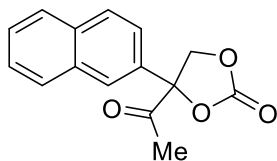
4-Acetyl-4-(*m*-tolyl)-1,3-dioxolan-2-one (2.2k)



Yellow solid (62.1 mg, 95% yield). Eluent hexanes/EtOAc = 4/1. **¹H NMR** (400 MHz, CDCl₃) δ 7.34 – 7.30 (m, 1H), 7.24 – 7.20 (m, 1H), 7.18 – 7.15 (m, 2H), 5.24 (d, *J* = 8.5 Hz, 1H), 4.36 (d, *J* = 8.5 Hz, 1H), 2.38 (s, 3H), 2.26 (s, 3H); **¹³C NMR** (101 MHz, CDCl₃) δ 202.9, 153.2, 139.7, 134.9, 130.5, 129.5, 124.5, 121.1, 88.7, 72.5, 24.9, 21.6; **IR (neat):**

ν = 1805, 1726 cm⁻¹; **HRMS (ESI/TOF) *m/z*** Calcd for C₁₂H₁₂NaO₄ [M + Na]⁺ 243.0628; Found 243.0623.

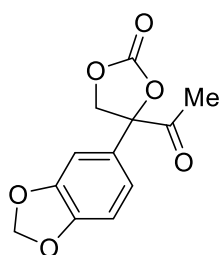
4-Acetyl-4-(naphthalen-2-yl)-1,3-dioxolan-2-one (2.2l)



Obtained at 60 °C, white solid (42.9 mg, 57% yield). Eluent hexanes/EtOAc = 4/1. **¹H NMR** (400 MHz, CDCl₃) δ 7.95 – 7.86 (m, 4H), 7.59 – 7.56 (m, 2H), 7.38 – 7.35 (m, 1H), 5.34 (d, *J* = 8.6 Hz, 1H), 4.47 (d, *J* = 8.6 Hz, 1H), 2.30 (s, 3H); **¹³C NMR** (101 MHz,

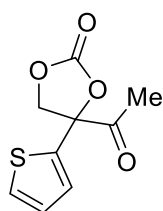
CDCl₃) δ 202.9, 153.1, 133.6, 133.1, 132.1, 130.0, 128.4, 128.0, 127.6, 127.5, 123.8, 120.8, 88.8, 72.4, 24.9; **IR (neat)**: ν = 1820, 1720 cm⁻¹; **HRMS (ESI/TOF)** m/z Calcd for C₁₅H₁₂NaO₄ [M + Na]⁺ 279.0628; Found 279.0633.

4-Acetyl-4-(benzo[d][1,3]dioxol-5-yl)-1,3-dioxolan-2-one (2.2m)



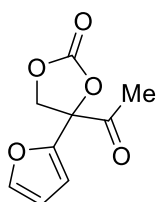
Yellow solid (67.9 mg, 90% yield). Eluent hexanes/EtOAc = 4/1. **¹H NMR** (400 MHz, CDCl₃) δ 6.83 – 6.82 (m, 3H), 6.00 – 5.99 (m, 2H), 5.18 (d, J = 8.6 Hz, 1H), 4.33 (d, J = 8.6 Hz, 1H), 2.25 (s, 3H); **¹³C NMR** (101 MHz, CDCl₃) δ 202.8, 153.0, 148.95, 148.93, 128.5, 118.0, 109.2, 104.7, 101.9, 88.4, 72.5, 24.7; **IR (neat)**: ν = 1796, 1721 cm⁻¹; **HRMS (ESI/TOF)** m/z Calcd for C₁₂H₁₀NaO₆ [M + Na]⁺ 273.0370; Found 273.0374.

4-Acetyl-4-(thiophen-2-yl)-1,3-dioxolan-2-one (2.2n)

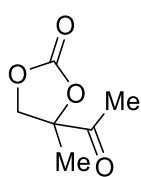


Brown solid (52.1 mg, 81% yield). Eluent hexanes/EtOAc = 4/1. **¹H NMR** (400 MHz, CDCl₃) δ 7.42 – 7.41 (m, 1H), 7.08 – 7.04 (m, 2H), 5.11 (d, J = 8.8 Hz, 1H), 4.49 (d, J = 8.8 Hz, 1H), 2.38 (s, 3H); **¹³C NMR** (101 MHz, CDCl₃) δ 202.2, 152.7, 137.4, 128.0, 127.7, 125.8, 87.0, 73.0, 25.1; **IR (neat)**: ν = 1791, 1719 cm⁻¹; **HRMS (ESI/TOF)** m/z Calcd for C₉H₈SNaO₄ [M + Na]⁺ 235.0036; Found 235.0039.

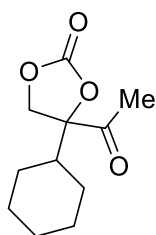
4-Acetyl-4-(furan-2-yl)-1,3-dioxolan-2-one (2.2o)



Yellow solid (45.5 mg, 77% yield). Eluent hexanes/EtOAc = 4/1. **¹H NMR** (400 MHz, CDCl₃) δ 7.52 – 7.51 (m, 1H), 6.54 – 6.53 (m, 1H), 6.46 – 6.45 (m, 1H), 4.91 (d, J = 9.1 Hz, 1H), 4.71 (d, J = 9.1 Hz, 1H), 2.48 (s, 3H); **¹³C NMR** (101 MHz, CDCl₃) δ 201.4, 152.9, 146.6, 145.2, 111.2, 110.9, 84.0, 69.9, 26.3; **IR (neat)**: ν = 1784, 1726 cm⁻¹; **HRMS (ESI/TOF)** m/z Calcd for C₉H₈NaO₅ [M + Na]⁺ 219.0264; Found 219.0260.

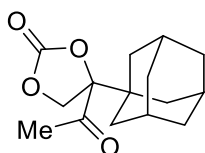
4-Acetyl-4-methyl-1,3-dioxolan-2-one (2.2p)

Colorless oil (34.8 mg, 78% yield). Eluent hexanes/EtOAc = 4/1. **¹H NMR** (400 MHz, CDCl₃) δ 4.65 (d, *J* = 8.9 Hz, 1H), 4.17 (d, *J* = 8.9 Hz, 1H), 2.36 (s, 3H), 1.61 (s, 3H); **¹³C NMR** (101 MHz, CDCl₃) δ 206.2, 153.5, 85.9, 72.0, 25.2, 22.3; **IR (neat):** ν = 1776, 1720 cm⁻¹; **HRMS** (ESI/TOF) *m/z* Calcd for C₆H₉O₄ [M + H]⁺ 145.0495; Found 145.0494.

4-acetyl-4-cyclohexyl-1,3-dioxolan-2-one (2.2q)

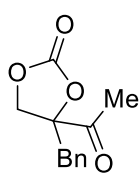
Colorless oil (55.3 mg, 86% yield). Eluent hexanes/EtOAc = 4/1. **¹H NMR** (400 MHz, CDCl₃) δ 4.48 (d, *J* = 9.1 Hz, 1H), 4.32 (d, *J* = 9.1 Hz, 1H), 2.34 (s, 3H), 1.91 – 1.81 (m, 3H), 1.73 – 1.64 (m, 3H), 1.28 – 1.15 (m, 4H), 1.04 – 0.98 (m, 1H); **¹³C NMR** (101 MHz, CDCl₃) δ 207.6, 153.8, 90.7, 69.0, 43.4, 27.4, 26.2, 25.83, 25.77, 25.6; **IR (neat):** ν = 1802, 1718 cm⁻¹; **HRMS** (ESI/TOF) *m/z*

Calcd for C₁₁H₁₆NaO₄ [M + Na]⁺ 235.0941; Found 235.0941.

4-Acetyl-4-(adamantan-1-yl)-1,3-dioxolan-2-one (2.2r)

White solid (45.3 mg, 57% yield). Eluent hexanes/EtOAc = 4/1. **¹H NMR** (400 MHz, CDCl₃) δ 4.47 (d, *J* = 9.3 Hz, 1H), 4.35 (d, *J* = 9.3 Hz, 1H), 2.34 (s, 3H), 2.07 – 2.05 (m, 3H), 1.75 – 1.71 (m, 6H), 1.65 – 1.61 (m, 3H), 1.54 – 1.49 (m, 3H); **¹³C NMR** (101 MHz, CDCl₃) δ 208.9, 153.9, 92.7, 68.1,

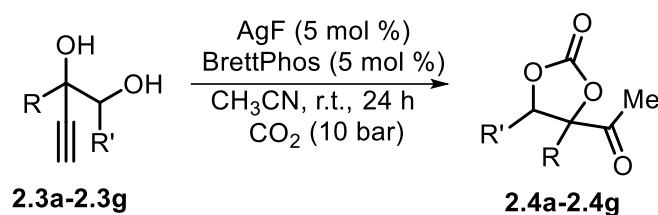
38.7, 36.4, 35.5, 29.5, 27.8; **IR (neat):** ν = 1789, 1717 cm⁻¹; **HRMS** (ESI/TOF) *m/z* Calcd for C₁₅H₂₀NaO₄ [M + Na]⁺ 287.1254; Found 287.1259.

4-Acetyl-4-benzyl-1,3-dioxolan-2-one (2.2s)

White solid (63.0 mg, 95% yield). Eluent hexanes/EtOAc = 4/1. **¹H NMR** (400 MHz, CDCl₃) δ 7.36 – 7.32 (m, 3H), 7.23 – 7.21 (m, 2H), 4.54 (d, *J* = 9.0 Hz, 1H), 4.29 (d, *J* = 9.0 Hz, 1H), 3.24 (d, *J* = 14.3 Hz, 1H), 3.04 (d, *J* = 14.3 Hz, 1H), 2.15 (s, 3H); **¹³C NMR** (101 MHz, CDCl₃) δ 207.5, 153.4, 132.0, 130.4,

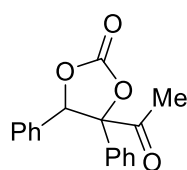
129.1, 128.3, 88.2, 70.4, 41.8, 26.9; **IR (neat):** ν = 1807, 1719 cm⁻¹; **HRMS** (ESI/TOF) *m/z* Calcd for C₁₂H₁₂NaO₄ [M + Na]⁺ 243.0628; Found 243.0631.

General Procedure G for synthesis of cyclic carbonates 2.4a-2.4g:



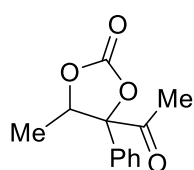
In a stainless-steel HEL-multireactor, the respective 1,2-diol (0.3 mmol, 1.0 equiv), AgF (0.015 mmol, 5 mol%), BrettPhos (0.015 mol%) were dissolved in CH₃CN (0.2 mL). The reactor was purged three times with CO₂ (10 bar) and then charged with CO₂ (10 bar). The reaction mixture was stirred at room temperature for 24 h. The mixture was then transferred to a round-bottom flask, concentrated and purified by flash column chromatography on silica to afford the corresponding carbonate product.

4-Acetyl-4,5-diphenyl-1,3-dioxolan-2-one (2.4a)



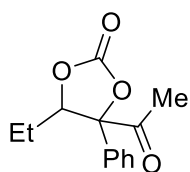
White solid (77.5 mg, 90% yield). Eluent hexanes/EtOAc = 4/1. ¹H NMR (400 MHz, CDCl₃) δ 7.17 – 7.10 (m, 6H), 7.04 – 6.98 (m, 4H), 6.33 (s, 1H), 2.28 (s, 3H); ¹³C NMR (101 MHz, CDCl₃) δ 203.2, 153.0, 133.0, 131.3, 129.2, 129.1, 128.6, 128.3, 127.3, 125.2, 92.4, 83.3, 25.6; **IR (neat):** ν = 1798, 1719 cm⁻¹; **HRMS** (ESI/TOF) *m/z* Calcd for C₁₇H₁₄NaO₄ [M + Na]⁺ 305.0784; Found 305.0790. This compound was further characterized by X-ray crystallography.

4-Acetyl-5-methyl-4-phenyl-1,3-dioxolan-2-one (2.4b)



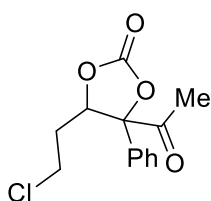
Colorless oil (56.0 mg, 85% yield). Eluent hexanes/EtOAc = 4/1. ¹H NMR (400 MHz, CDCl₃) δ 7.46 – 7.41 (m, 3H), 7.34 – 7.31 (m, 2H), 5.47 (q, *J* = 6.6 Hz, 1H), 2.23 (s, 3H), 1.02 (d, *J* = 6.6 Hz, 3H); ¹³C NMR (101 MHz, CDCl₃) δ 203.7, 152.8, 131.2, 129.7, 129.3, 125.1, 91.5, 78.3, 25.4, 17.4; **IR (neat):** ν = 1807, 1722 cm⁻¹; **HRMS** (ESI/TOF) *m/z* Calcd for C₁₂H₁₂NaO₄ [M + Na]⁺ 243.0628; Found 243.0626.

4-Acetyl-5-ethyl-4-phenyl-1,3-dioxolan-2-one (2.4c)



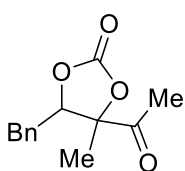
Yellow oil (53.8 mg, 76% yield). Eluent hexanes/EtOAc = 4/1. **¹H NMR** (400 MHz, CDCl₃) δ 7.45 – 7.41 (m, 3H), 7.34 – 7.29 (m, 2H), 5.22 (dd, *J* = 10.5, 3.1 Hz, 1H), 2.23 (s, 3H), 1.32 – 1.22 (m, 1H), 1.16 – 1.04 (m, 1H), 0.93 (t, *J* = 7.3 Hz, 3H); **¹³C NMR** (101 MHz, CDCl₃) δ 203.8, 152.9, 131.3, 129.7, 129.3, 125.1, 91.4, 83.1, 25.4, 25.3, 9.8; **IR (neat)**: ν = 1807, 1722 cm⁻¹; **HRMS (ESI/TOF)** *m/z* Calcd for C₁₃H₁₄NaO₄ [M + Na]⁺ 257.0784; Found 257.0790.

4-Acetyl-5-(2-chloroethyl)-4-phenyl-1,3-dioxolan-2-one (2.4d)

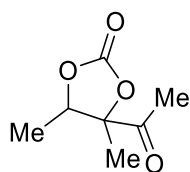


White solid (64.4 mg, 77% yield). Eluent hexanes/EtOAc = 4/1. **¹H NMR** (400 MHz, CDCl₃) δ 7.48 – 7.44 (m, 3H), 7.34 – 7.30 (m, 2H), 5.58 (dd, *J* = 10.9, 3.0 Hz, 1H), 3.60 – 3.52 (m, 2H), 2.24 (s, 3H), 1.63 – 1.48 (m, 2H); **¹³C NMR** (101 MHz, CDCl₃) δ 203.0, 152.3, 130.8, 130.1, 129.6, 125.0, 91.0, 78.4, 39.8, 34.8, 25.4; **IR (neat)**: ν = 1811, 1726 cm⁻¹; **HRMS (ESI/TOF)** *m/z* Calcd for C₁₃H₁₃ClNaO₄ [M + Na]⁺ 291.0395; Found 291.0394.

4-Acetyl-5-benzyl-4-methyl-1,3-dioxolan-2-one (2.4e)



Yellow oil (54.4 mg, 77% yield, 76:24 *dr*). Eluent hexanes/EtOAc = 4/1. **¹H NMR** (400 MHz, CDCl₃) (major) δ 7.35 – 7.24 (m, 5H), 4.85 – 4.77 (m, 1H), 3.03 – 2.99 (m, 2H), 2.37 (s, 3H), 1.57 (s, 3H); **¹H NMR** (400 MHz, CDCl₃) (minor) δ 7.35 – 7.24 (m, 3H), 7.21 – 7.19 (m, 2H), 4.62 (dd, *J* = 9.5, 3.0 Hz, 1H), 3.03 – 2.99 (m, 1H), 2.73 (dd, *J* = 14.8, 9.5 Hz, 1H), 2.29 (s, 3H), 1.61 (s, 3H); **¹³C NMR** (101 MHz, CDCl₃) (major) δ 206.68, 152.7, 135.4, 129.2, 128.9, 127.5, 88.1, 81.8, 36.2, 25.4, 17.8; **¹³C NMR** (101 MHz, CDCl₃) (minor) δ 206.72, 153.1, 134.9, 129.6, 128.9, 127.6, 88.5, 85.9, 36.3, 28.1, 23.1; **IR (neat)**: ν = 1802, 1720 cm⁻¹; **HRMS (ESI/TOF)** *m/z* Calcd for C₁₃H₁₄NaO₄ [M + Na]⁺ 257.0784; Found 257.0784.

4-Acetyl-4,5-dimethyl-1,3-dioxolan-2-one (2.4f)

Colorless oil (35.7 mg, 73% yield, 68:32 *dr*). Eluent hexanes/EtOAc = 4/1.

¹H NMR (400 MHz, CDCl₃) (major) δ 4.79 (q, *J* = 6.6 Hz, 1H), 2.35 (s, 3H),

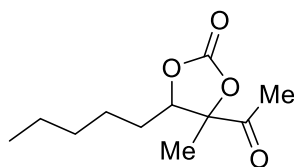
1.45 (s, 3H), 1.43 (d, *J* = 6.6 Hz, 3H); **¹H NMR** (400 MHz, CDCl₃) (minor)

δ 4.54 (q, *J* = 6.6 Hz, 1H), 2.33 (s, 3H), 1.57 (s, 3H), 1.29 (d, *J* = 6.6 Hz, 3H);

¹³C NMR (101 MHz, CDCl₃) (major) δ 206.9, 152.9, 88.2, 77.5, 25.4, 17.4, 15.3; **¹³C NMR**

(101 MHz, CDCl₃) (minor) δ 206.5, 153.3, 88.9, 81.6, 28.0, 22.5, 16.0; **IR (neat)**: ν = 1800,

1721 cm⁻¹; **HRMS** (ESI/TOF) *m/z* Calcd for C₇H₁₀NaO₄ [M + Na]⁺ 181.0471; Found 181.0471.

4-Acetyl-4-methyl-5-pentyl-1,3-dioxolan-2-one (2.4g)

Colorless oil (40.8 mg, 62% yield, 76:24 *dr*). Eluent hexanes/EtOAc

= 4/1. **¹H NMR** (400 MHz, CDCl₃) (major) δ 4.57 (dd, *J* = 10.1, 3.1

Hz, 1H), 2.35 (s, 3H), 1.74 – 1.53 (m, 3H), 1.45 (s, 3H), 1.34 – 1.25

(m, 5H), 0.89 (t, *J* = 6.9 Hz, 3H); **¹H NMR** (400 MHz, CDCl₃) (minor)

δ 4.35 (dd, *J* = 10.1, 3.1 Hz, 1H), 2.33 (s, 3H), 1.74 – 1.53 (m, 3H), 1.57 (s, 3H), 1.34 – 1.25

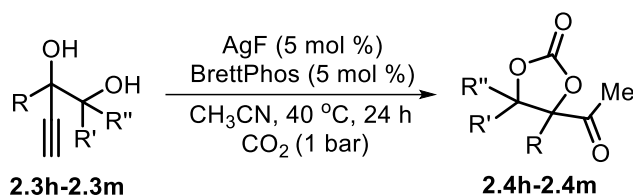
(m, 5H), 0.89 (t, *J* = 6.9 Hz, 3H); **¹³C NMR** (101 MHz, CDCl₃) (major) δ 207.0, 153.0, 88.2,

81.4, 31.4, 29.9, 25.53, 25.4, 22.5, 17.6, 14.0; **¹³C NMR** (101 MHz, CDCl₃) (minor) δ 206.4,

153.5, 88.7, 85.7, 31.3, 30.3, 28.0, 25.51, 22.7, 22.4, 13.97; **IR (neat)**: ν = 1805, 1722 cm⁻¹;

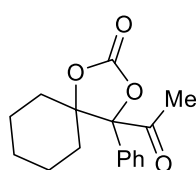
HRMS (ESI/TOF) *m/z* Calcd for C₁₁H₁₈NaO₄ [M + Na]⁺ 237.1097; Found 237.1092.

General Procedure H for synthesis of cyclic carbonates 2.4h-2.4m:



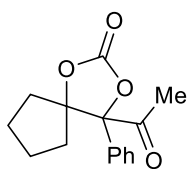
The respective 1,2-diol (0.3 mmol, 1.0 equiv), AgF (0.015 mmol, 5 mol%), BrettPhos (0.015 mmol, 5 mol%) were added to a 25 mL reaction tube. The tube was purged three times with CO₂ and then charged with a CO₂ balloon (1 bar). Hereafter, MeCN (0.6 mL) was added using a syringe. The reaction mixture was stirred at 40 °C for 24 h. When complete consumption of the starting material had been observed by TLC, the mixture was transferred to a round-bottom flask, concentrated and purified by flash column chromatography on silica to afford the corresponding carbonate product.

4-Acetyl-4-phenyl-1,3-dioxaspiro[4.5]decan-2-one (2.4h)

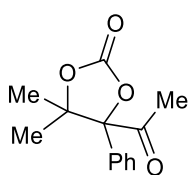


White solid (72.0 mg, 87% yield). Eluent hexanes/EtOAc = 4/1. ¹H NMR (400 MHz, CDCl₃) δ 7.49 – 7.44 (m, 2H), 7.42 – 7.37 (m, 3H), 2.29 (s, 3H), 1.92 – 1.77 (m, 2H), 1.74 – 1.53 (m, 4H), 1.50 – 1.34 (m, 2H), 1.24 – 1.14 (m, 2H); ¹³C NMR (101 MHz, CDCl₃) δ 204.6, 152.8, 132.0, 129.4, 128.8, 126.1, 93.6, 90.1, 33.1, 32.9, 28.7, 24.7, 22.2, 22.0; IR (neat): ν = 1798, 1712 cm⁻¹; HRMS (ESI/TOF) *m/z* Calcd for C₁₆H₁₈NaO₄ [M + Na]⁺ 297.1097; Found 297.1094.

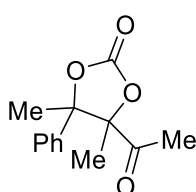
4-Acetyl-4-phenyl-1,3-dioxaspiro[4.4]nonan-2-one (2.4i)



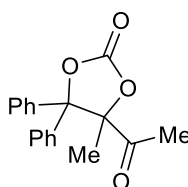
Yellow oil (69.5 mg, 89% yield). Eluent hexanes/EtOAc = 4/1. ¹H NMR (400 MHz, CDCl₃) δ 7.52 – 7.48 (m, 2H), 7.44 – 7.38 (m, 3H), 2.32 (s, 3H), 2.29 – 2.21 (m, 1H), 1.98 – 1.74 (m, 3H), 1.72 – 1.52 (m, 3H), 1.46 – 1.40 (m, 1H); ¹³C NMR (101 MHz, CDCl₃) δ 204.7, 152.9, 132.8, 129.4, 129.0, 125.3, 99.3, 91.3, 35.6, 34.0, 28.0, 23.2, 22.1; IR (neat): ν = 1805, 1720 cm⁻¹; HRMS (ESI/TOF) *m/z* Calcd for C₁₅H₁₆NaO₄ [M + Na]⁺ 283.0941; Found 283.0932.

4-Acetyl-5,5-dimethyl-4-phenyl-1,3-dioxolan-2-one (2.4j)

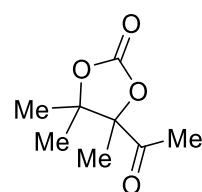
Colorless oil (59.5 mg, 85% yield). Eluent hexanes/EtOAc = 4/1. **¹H NMR** (400 MHz, CDCl₃) δ 7.48 – 7.45 (m, 2H), 7.43 – 7.40 (m, 3H), 2.32 (s, 3H), 1.58 (s, 3H), 1.18 (s, 3H); **¹³C NMR** (101 MHz, CDCl₃) δ 204.3, 152.8, 132.3, 129.6, 129.0, 125.8, 93.2, 88.4, 28.2, 24.9, 24.7; **IR (neat)**: ν = 1803, 1720 cm⁻¹; **HRMS** (ESI/TOF) *m/z* Calcd for C₁₃H₁₄NaO₄ [M + Na]⁺ 257.0784; Found 257.0779.

4-Acetyl-4,5-dimethyl-5-phenyl-1,3-dioxolan-2-one (2.4k)

White solid (58.4 mg, 83% yield, *dr* >95:5). Eluent hexanes/EtOAc = 4/1. **¹H NMR** (400 MHz, CDCl₃) δ 7.54 – 7.51 (m, 2H), 7.43 – 7.34 (m, 3H), 2.48 (s, 3H), 1.69 (s, 3H), 1.10 (s, 3H); **¹³C NMR** (101 MHz, CDCl₃) δ 207.2, 152.2, 137.5, 128.8, 128.7, 125.4, 91.7, 88.8, 28.3, 25.3, 22.3; **IR (neat)**: ν = 1803, 1723 cm⁻¹; **HRMS** (ESI/TOF) *m/z* Calcd for C₁₃H₁₄NaO₄ [M + Na]⁺ 257.0784; Found 257.0778.

4-Acetyl-4-methyl-5,5-diphenyl-1,3-dioxolan-2-one (2.4l)

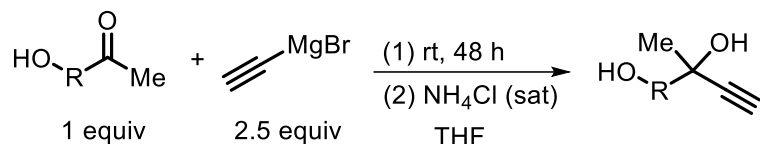
White solid (84.3 mg, 95% yield). Eluent hexanes/EtOAc = 4/1. **¹H NMR** (400 MHz, CDCl₃) δ 7.75 – 7.72 (m, 2H), 7.46 – 7.36 (m, 3H), 7.34 – 7.30 (m, 5H), 1.87 (s, 3H), 1.48 (s, 3H); **¹³C NMR** (101 MHz, CDCl₃) δ 206.2, 152.7, 137.6, 136.2, 129.1, 129.0, 128.8, 128.6, 127.0, 126.4, 93.8, 91.3, 27.5, 22.8; **IR (neat)**: ν = 1809, 1720 cm⁻¹; **HRMS** (ESI/TOF) *m/z* Calcd for C₁₈H₁₆NaO₄ [M + Na]⁺ 319.0941; Found 319.0934.

4-Acetyl-4,5,5-trimethyl-1,3-dioxolan-2-one (2.4m)

48 h reaction time, white solid (46.0 mg, 91% yield). Eluent hexanes/EtOAc = 4/1. **¹H NMR** (400 MHz, CDCl₃) δ 2.37 (s, 3H), 1.52 (s, 3H), 1.49 (s, 3H), 1.35 (s, 3H); **¹³C NMR** (101 MHz, CDCl₃) δ 207.1, 152.7, 91.0, 85.8, 27.8, 23.8, 22.4, 19.7; **IR (neat)**: ν = 1783, 1715 cm⁻¹; **HRMS** (ESI/TOF) *m/z* Calcd for C₈H₁₂NaO₄ [M + Na]⁺ 195.0628; Found 195.0629.

2.6.5 Catalytic screening towards larger ring cyclic carbonates

General procedure for the synthesis of 1,3- and 1,4-diols 2.5a and 2.5b



For 2.5a: In a clean dry double-neck 2L round bottom flask conditioned under an inert atmosphere was introduced ethynyl magnesium bromide (800 mL, 0.5 M in THF, 0.4 mole). Then, 4-hydroxy-2-butanone (13.8 mL, 0.16 mole) was added dropwise using a syringe. The reaction mixture was stirred at room temperature for 48 h, during which the conversion of the ketone was monitored by ATR-IR. Then, a saturated solution of NH₄Cl was added and the mixture was transferred into a separating funnel to recover the organic phase. The aqueous phase was extracted with diethyl ether (200 + 150 mL). The combined organic fractions were dried with anhydrous MgSO₄ and filtered. Then the organic phase was evaporated in vacuo and the residue purified by fractional distillation. A transparent to light yellow oil was recovered in a yield of around 60% at 55°C with a vacuum of 1 mbar.

Note: A similar procedure was applied for the synthesis of **2.5b** using the appropriate hydroxy ketone precursor giving a similar isolated yield.

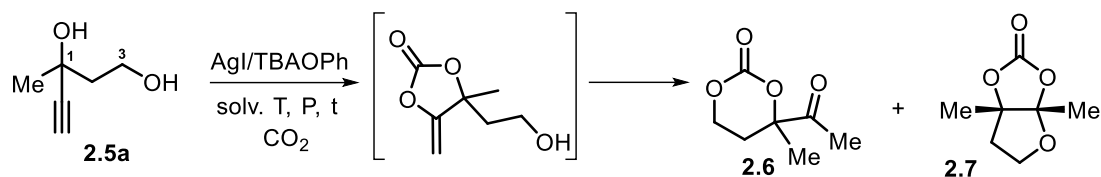
3-Methylpent-4-yne-1,3-diol (2.5a)

Light yellow oil. ¹H NMR (400 MHz, DMSO-d₆) δ 5.29 (s, 1H), 4.44 (s, 1H), 3.59 (s, 2H), 3.23 (s, 1H), 1.74 (s, 2H), 1.34 (s, 3H); ¹³C NMR (101 MHz, DMSO-d₆) δ 73.10, 65.62, 58.21, 46.12, 39.56, 30.71.

4-Methylhex-5-yne-1,4-diol (2.5b)

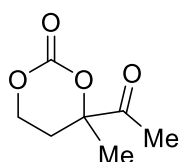
Light orange oil. ¹H NMR (400 MHz, DMSO-d₆) δ 5.23 (s, 1H), 4.42 (t, J = 5.2 Hz, 1H), 3.40 (t, J = 5.7 Hz, 2H), 3.16 (s, 1H), 1.70 – 1.46 (m, 4H), 1.33 (s, 3H); ¹³C NMR (101 MHz, DMSO-d₆) δ 89.69, 72.83, 66.44, 61.47, 40.60, 30.33, 28.43.

Screening of reaction parameters for the carboxylative coupling of CO₂ to 3-methylpent-4-yne-1,3-diol (2.5a)



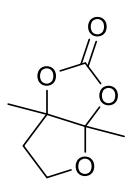
In a clean dry reactor, equipped with a magnetic rod, a manometer and a gas inlet/outlet were introduced 3-methylpent-4-yne-1,3-diol (1 g, 8.76 mmol), tetrabutylammonium phenolate TBAOPh (0.147 g, 0.438 mmol), silver iodide (AgI) (0.102 g, 0.438 mmol) and dried DMSO (2-4 mL). The reactor was closed and placed in a silicon oil bath set heated at the desired temperature. After 30 minutes, CO₂ gas was added at a constant pressure. The reaction ran for 24-72 h after which the reactor was depressurized and placed in a water bath to cool it down to room temperature. The crude reaction mixture was characterized by ¹H NMR spectroscopy in DMSO-*d*₆. Isolation of products was achieved by extraction of the crude mixture with 80 mL of salted water and 80 mL of CH₂Cl₂, followed by a silica gel chromatography (5-50% ethyl acetate/petroleum ether 40/60 v/v).

4-Methyl-4-(prop-1-en-2-yl)-1,3-dioxan-2-one (2.6)



White solid, 51%. Eluent petroleum ether /EtOAc = 1/1 ¹H NMR (400 MHz, DMSO-*d*₆) δ 4.37 (dt, *J* = 11.3, 4.7 Hz, 1H), 4.10 (ddd, *J* = 11.3, 10.2, 4.1 Hz, 1H), 2.41 (dt, *J* = 14.7, 4.1 Hz, 1H), 2.28 (s, 3H), 2.12 (ddd, *J* = 14.7, 10.2, 5.0 Hz, 1H), 1.53 (s, 3H); ¹³C NMR (101 MHz, DMSO-*d*₆) δ 206.91, 147.83, 87.28, 65.52, 39.57, 28.20, 25.15, 23.35; IR (neat) ν = 1750, 1720 cm⁻¹; HRMS (QTOF) *m/z* Calcd for C₇H₁₀NaO₄ [M + Na]⁺ 181.0477; Found 181.0472.

3a,6a-Dimethyltetrahydrofuro[2,3-*d*][1,3]dioxol-2-one (2.7)



White solid, 70% Eluent hexanes/EtOAc = 5/1. ¹H NMR (400 MHz, DMSO-*d*₆) δ 4.05 (dd, *J* = 9.3, 7.9 Hz, 1H), 3.77 (ddd, *J* = 11.9, 9.4, 4.7 Hz, 1H), 2.29 (dd, *J* = 13.9, 4.6 Hz, 1H), 2.05 (ddd, *J* = 13.9, 11.9, 7.9 Hz, 1H), 1.57 (d, *J* = 4.7 Hz, 6H); ¹³C NMR (101 MHz, DMSO-*d*₆) δ 152.7, 114.8, 91.8, 65.6, 38.2, 20.3, 20.0; IR (neat): ν = 1802 cm⁻¹; HRMS (ESI/TOF) *m/z* Calcd for C₇H₁₀NaO₄ [M + Na]⁺ 181.0471; Found 181.0472. This compound was further characterized by X-ray crystallography.

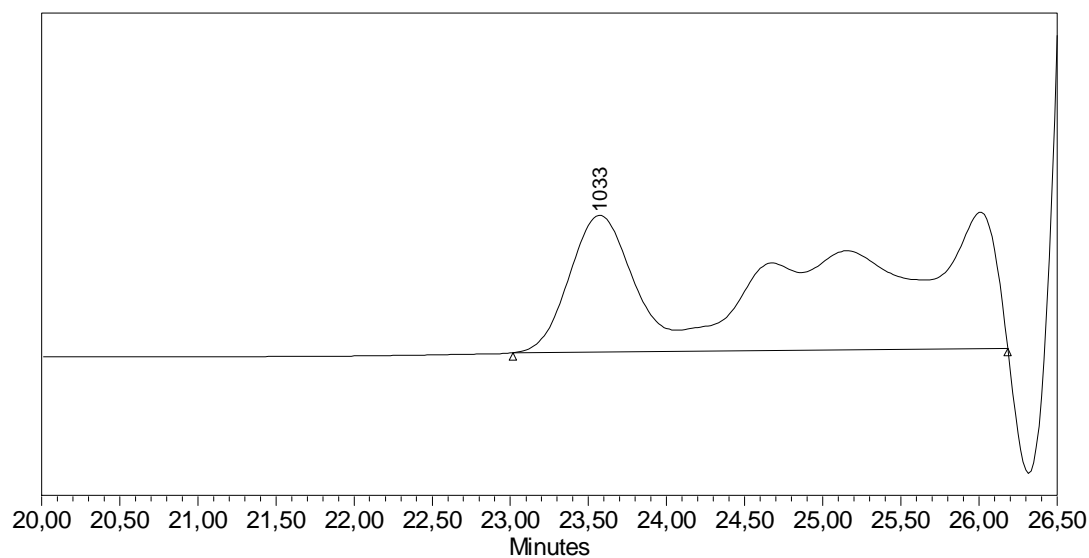
Table 2.6: Screening of the carboxylative coupling of 1,3-diol 2.5a with CO₂ to give 2.6 and 2.7.^[a]

Entry	Solvent	Conc. [mol/L]	T [°C]	Conv. of 2.5a [%] ^[b]	Sel. for 2.6 [%] ^[b]	Sel. for 2.7 [%] ^[b]
1^[c]	DMSO	2.2	25	100	98 (51)^[d]	–
2	DMSO	2.2	25	100	85	–
3	DMSO	4.4	25	34	84	–
4	ACN	2.2	25	0	–	–
5	–	–	25	0	–	–
6 ^[e]	DMSO	2.2	60	100	98	–
7	DMSO	4.4	60	100	85	6
8 ^[f]	DMSO	4.4	60	100	44	49
9	ACN	4.4	60	100	57	21
10	–	–	60	100	13	42
11	DMSO	2.2	80	100	32	35
12	DMSO	4.4	80	100	13	69
13	DMF	4.4	80	100	5	86
14	ACN	4.4	80	100	0	90 (70)^[d]
15	–	–	80	70	0	67
16 ^[f]	–	–	80	100	0	90

[a] Conditions: 1,3-diol **2.5a** (1 g, 8.76 mmol), TBAOPh (0.147 g, 0.438 mmol), AgI (0.102 g, 0.438 mmol), P(CO₂) = 15 bar and t = 24 h. [b] Determined by ¹H NMR spectroscopy with 1,3,5-trimethoxybenzene as internal standard. [c] Reaction time was 16 h. [d] Yields in brackets refer to isolated yield after purification by silica gel column chromatography. [e] Reaction time was 3.5 h. [f] Reaction time was 72 h.

Description of the procedure for the SEC analysis: Number-average molecular weight (M_n) and dispersity (D) of the different polymers were determined by size exclusion chromatography (SEC) in dimethyl formamide (DMF) containing LiBr (0.025 M) at 55 °C (flow rate: 1 mL/min) with a Waters chromatograph equipped with two columns dedicated to the analysis of low molar mass polymers (PSS gram analytical 100 Å, separation range 300-60000 Da) and a pre-column (100 Å), a dual λ absorbance detector (Waters 2487) and a refractive index detector (Waters 2414). The system was calibrated by polystyrene (PS) standards.

The crude sample of Table 2.6 (entry 12) was injected into the SEC equipment and the corresponding SEC chromatogram is shown in Figure 2.2. It reveals that the crude product contains a small amount of oligomers of very low molar mass (apparent $M_n = 440$ g/mol). It is important to note that the tailing at very low molar mass is out of calibration and contains products **2.6** and **2.7**, as well as dimers/trimers.



	SampleName	RT	Mn (Daltons)	Mw (Daltons)	MP (Daltons)	Polydispersity
1	chng f40a	15,212				
2	chng f40a	19,750				
3	chng f40a	23,571	443	591	1033	1,332618

Figure 2.2. SEC trace and data for the crude mixture of Table 2.6, entry 12.

Monitoring of the carboxylative coupling of CO₂ to 3-methylpent-4-yne-1,3-diol **2.5a** by FT-IR spectroscopy

In a clean and dry reactor of 40 mL equipped with a manometer, a heating mantle, gas inlet/outlets, a mechanical stirrer and a high-pressure FT-IR probe were introduced 3-methylpent-4-yne-1,3-diol **2.5a** (3 g, 26.28 mmol), tetrabutylammonium phenolate TBAOPh (0.4410 g, 1.3141 mmol), AgI (0.3085 g, 1.3141 mmol) and dry DMSO (12 mL). The reactor was closed and heated to the desired temperature after which the FT-IR acquisition was initiated. Then, CO₂ gas was added and the pressure maintained at 15 bar. Spectra were recorded every 1-5 min. Once the reaction was complete, the reactor was cooled down to room temperature and depressurized. The crude reaction mixture was recovered and analyzed by ¹H NMR spectroscopy.

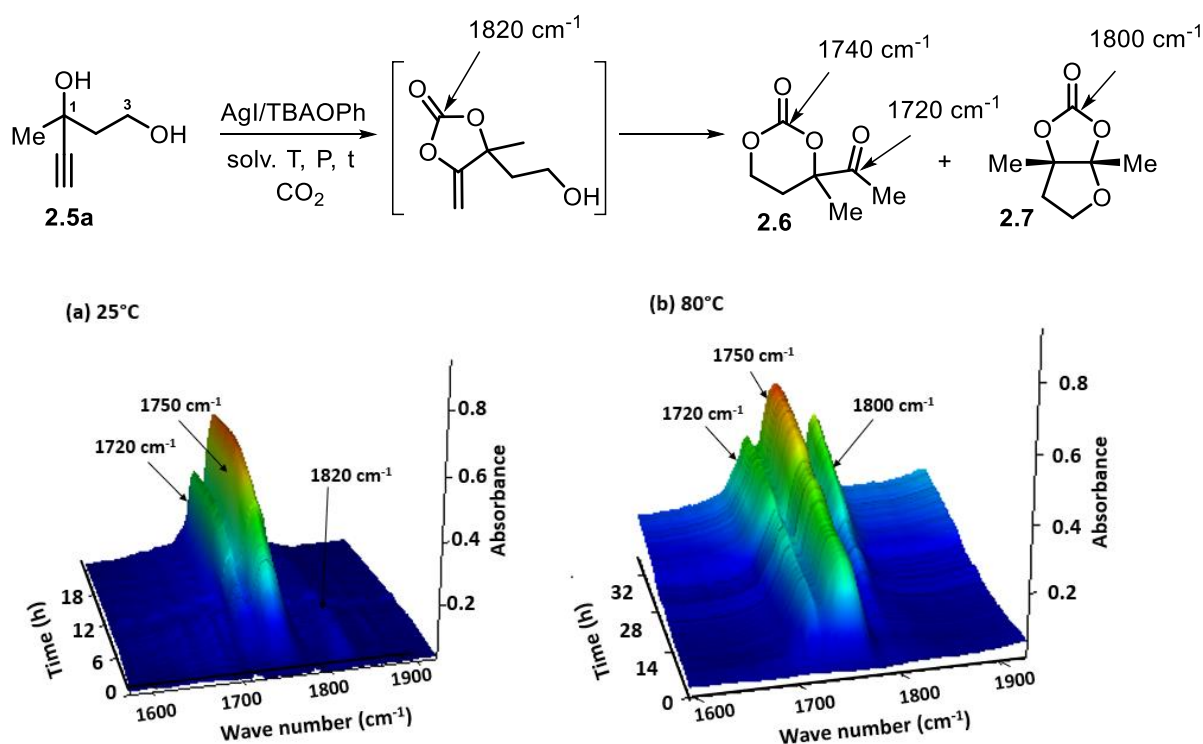


Figure 2.3. Online monitoring via operando FT-ATR spectroscopy at 25 °C (a) and 80 °C (b) of the carboxylative coupling of 3-methylpent-4-yne-1,3-diol **2.5a** with CO₂ to afford carbonates **2.6** and **2.7**.

At 25 °C, we briefly observed the formation of the alkylidene cyclic carbonate as attested by the presence of the band at 1820 cm⁻¹, which disappeared after few hours in favour of the six-membered keto-carbonate **2.6** with the characteristic bands at 1750 cm⁻¹ (carbonate) and 1720 cm⁻¹ (ketone). At 80 °C, a new bicyclic tetrasubstituted five-membered cyclic carbonate **2.7**,

with a characteristic band at 1802 cm⁻¹, was formed together with the 6-membered keto-carbonate **2.6** (Figure 2.3) The formation of both products, **2.6** and **2.7**, was also confirmed by ¹H NMR spectroscopy (Figure 2.4).

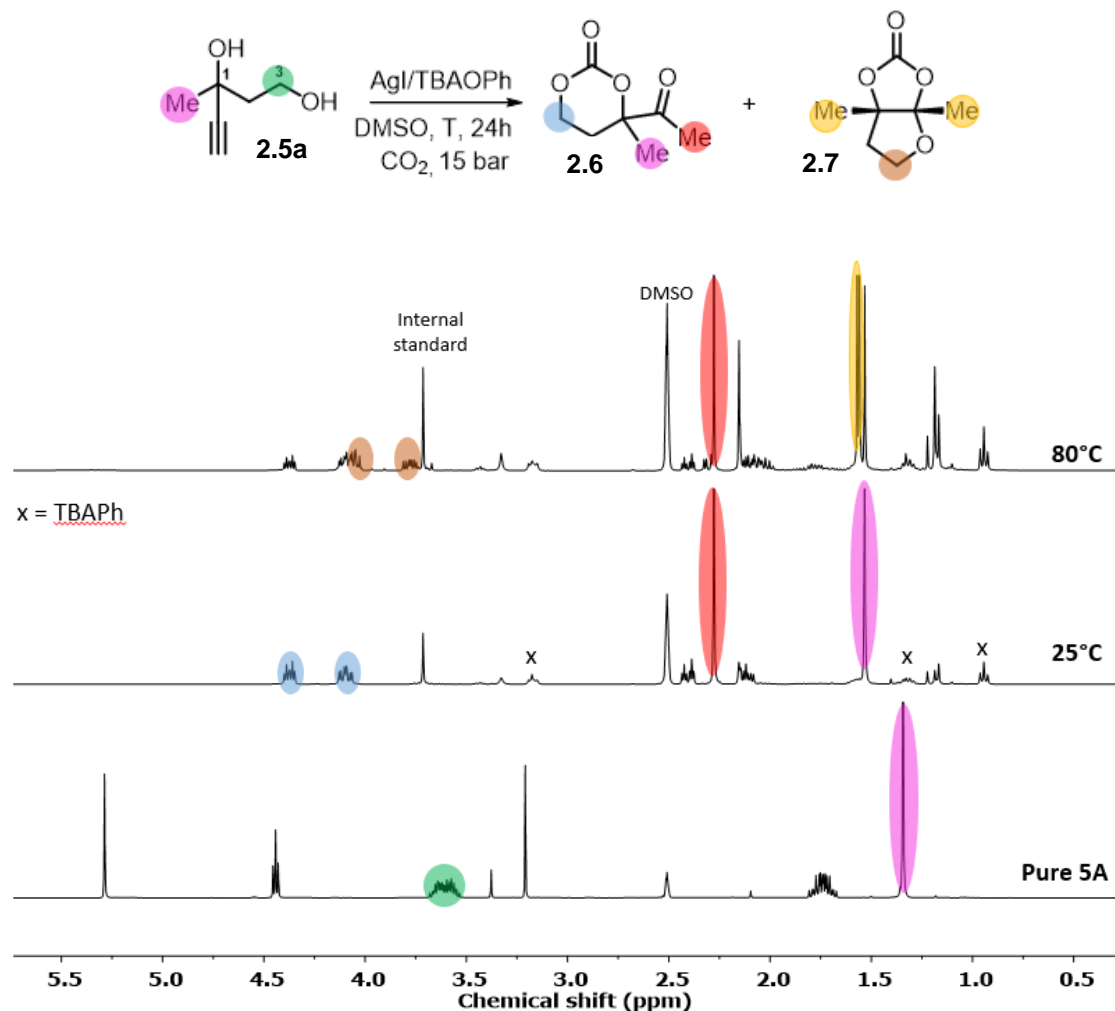
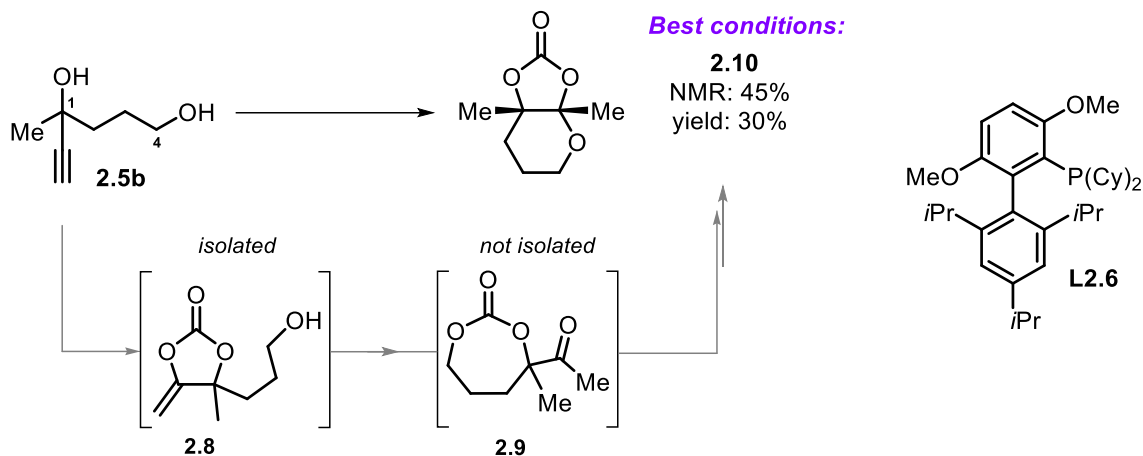


Figure 2.4. ¹H NMR overlay of pure alcohol **2.5a** (bottom), the crude reaction mixtures obtained at 25 °C (middle) and 80 °C (top) for the carboxylative coupling of CO₂ to 3-methylpent-4-yne-2,3-diol **2.5a**.

Screening of reaction parameters for the carboxylative coupling of CO₂ to 4-methylhex-5-yne-1,4-diol (**2.5b**)

Table 2.7:^[a] Screening of parameters for the carboxylative coupling of 1,4-diol **2.5b** with CO₂ to give **2.8**, **2.9** and **2.10**.



Entry	[Ag] [mol%]	Ligand [mol%]	T/pressure [°C]/[bar]	Conv. 2.5b [%] ^[b]	2.8 [%] ^[b]	2.9 [%] ^[b]	2.10 [%] ^[b]
1	AgF, 10	L2.6 , 5	rt, 30	>99	66	30	–
2	AgF, 10	L2.6 , 5	50, 30	>99	–	–	–
3	AgF, 5	L2.1 , 5	rt, 30	>99	31	16	27
4	AgF, 5	L2.2 , 5	rt, 30	>99	–	trace	41
5	AgF, 5	L2.3 , 5	rt, 30	>99	25	32	14
6	AgF, 5	L2.4 , 5	rt, 30	>99	–	10	28
7 ^[c]	AgI, 5	TBAOPh, 5	rt, 15	>99	75, 50 ^[d]	21	–
8 ^[c]	AgI, 5	TBAOPh, 5	80, 15	>99	7	1	24
9	AgI, 5	TBAOPh, 5	80, 15	>99	7	3	16
10	AgI, 5	DBU, 5	80, 15	>99	3	5	25
11	–	DBU, 10	80, 15	>99	–	–	24 ^[d]
12	AgI, 5	DBU, 10	80, 15	>99	–	12	45, 33 ^[d]
13	–	DBU, 10	80, 15	>99	–	–	9

[a] Reaction conditions: **2.5b** (0.3 mmol), ACN (0.2 mL), CO₂ (pressure indicated), 24 h.
 [b] Determined by ¹H NMR using mesitylene as internal standard. [c] DMSO as solvent.
 [d] Isolated yield.

Description of the procedure for the SEC analysis: Number-average molecular weight (M_n) and dispersity (\mathcal{D}) of the polymers were determined by size exclusion chromatography (SEC) in dimethyl formamide (DMF) containing LiBr (0.025 M) at 55 °C (flow rate: 1 mL/min) with a SECcurity GPC1260 chromatograph from PSS equipped with three columns (PSS gram 1000 Å (x2), 30 Å) and a pre-column, a SECcurity refractive index detector, a SECcurity variable wavelength UV-Vis detector and a MALLS detector SLD7000. The system was calibrated by polystyrene (PS) standards.

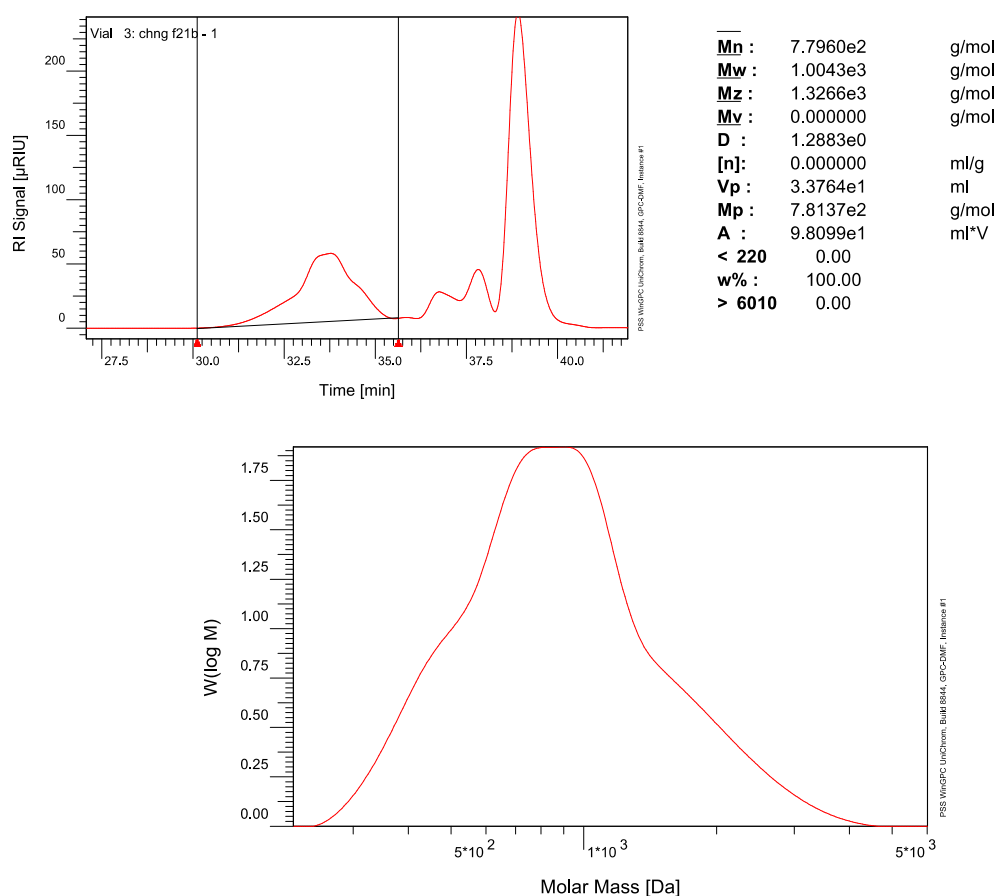
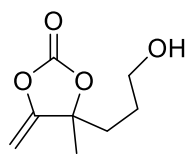
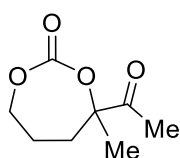


Figure 2.5. SEC chromatogram and data of the crude mixture (Table 2.7, entry 9).

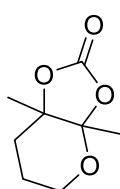
The reaction of alkyne-1,4 diol (**2.5b**) provides the tetrasubstituted carbonate **2.10** at lower yield and favors the formation of some oligomeric compounds (Figure 2.5). The oligomers have an apparent M_n of 780 g/mol and a dispersity of 1.29. All attempts to push the polymerization further to reach higher molar masses were unsuccessful as the formation of product **2.10** could not be avoided. Products appearing at elution volumes higher than 36 min are out of calibration and correspond to a mixture of products **2.8**, **2.9** and **2.10**. The intense sharp peak at around 39 min corresponds to DMSO, which was used as the solvent for the reaction.

4-(3-Hydroxypropyl)-4-methyl-5-methylene-1,3-dioxolan-2-one (2.8)

Yellow oil, NMR yield 75%, isolated: 50%. Eluent petroleum ether/EtOAc 1:1 **¹H NMR** (400 MHz, DMSO-*d*₆) δ 4.85 (d, *J* = 3.9 Hz, 1H), 4.63 (d, *J* = 3.9 Hz, 1H), 4.53 (t, *J* = 5.2 Hz, 1H), 3.41 (td, *J* = 6.3, 5.1 Hz, 2H), 1.89 (qdd, *J* = 14.4, 9.8, 6.0, 2H), 1.60 (s, 3H), 1.43 (m, 2H); **¹³C NMR** (101 MHz, DMSO-*d*₆) δ 157.43, 151.46, 87.99, 86.46, 60.56, 36.68, 26.72, 25.94; **IR** (neat) ν = 1686, 1818 cm⁻¹; **HRMS** (QTOF) *m/z* Calcd for C₈H₁₂NaO₄ [M + Na]⁺ 195.1698; Found 195.0633.

4-Acetyl-4-methyl-1,3-dioxepan-2-one (2.9)

Note: This compound was isolated as a mixture with **2.8**. The data are here provided for completion. Selected features: **¹H NMR** (400 MHz, DMSO-*d*₆) δ 4.07 (m, 2H), 2.39 (m, 2H), 2.25 (s, 3H, C(O)Me), 1.80 (m, 2H), 1.49 (s, 3H, Me); **¹³C NMR** (75 MHz, DMSO-*d*₆) δ 206.51, 153.07, 90.31, 70.04, 36.88; **IR** (neat) ν = 1720, 1752 cm⁻¹.

3a,7a-Dimethyltetrahydro-5H-[1,3]dioxolo[4,5-b]pyran-2-one (2.10)

White solid, NMR yield 45%, isolated 30%. Eluent hexanes/EtOAc = 5/1. **¹H NMR** (400 MHz, DMSO-*d*₆) δ 3.72 (td, *J* = 6.4, 1.9 Hz, 2H), 1.97 (ddd, *J* = 14.8, 5.5, 4.1 Hz, 1H), 1.85 (ddd, *J* = 14.7, 10.6, 6.4 Hz, 1H), 1.76 – 1.60 (m, 2H), 1.54 (s, 3H), 1.40 (s, 3H); **¹³C NMR** (101 MHz, DMSO-*d*₆) δ 153.1, 107.3, 83.6, 60.7, 28.6, 22.9, 19.8, 18.6; **IR** (neat): ν = 1803 cm⁻¹; **HRMS** (ESI/TOF) *m/z* Calcd for C₈H₁₂NaO₄ [M + Na]⁺ 195.0628; Found 195.0628.

Monitoring of the carboxylative coupling of CO₂ to 4-methylhex-5-yne-1,4-diol (**2.5b**) by FT-IR spectroscopy

At 25 °C, we observed the formation of the alkylidene cyclic carbonate **2.8** (1818 cm⁻¹ and 1685 cm⁻¹) which could be isolated at 50% yield. The seven-membered carbonate **2.9**, with its characteristic carbonyl vibration at 1752 cm⁻¹, was also formed at the two investigated temperatures, 25 °C and 80 °C. Note that the progressive broadening of the band at 1818 cm⁻¹ with time (for the reaction carried out at 80 °C) results from the appearance of a band at 1807 cm⁻¹, the signature of the tetrasubstituted carbonate **2.10**.

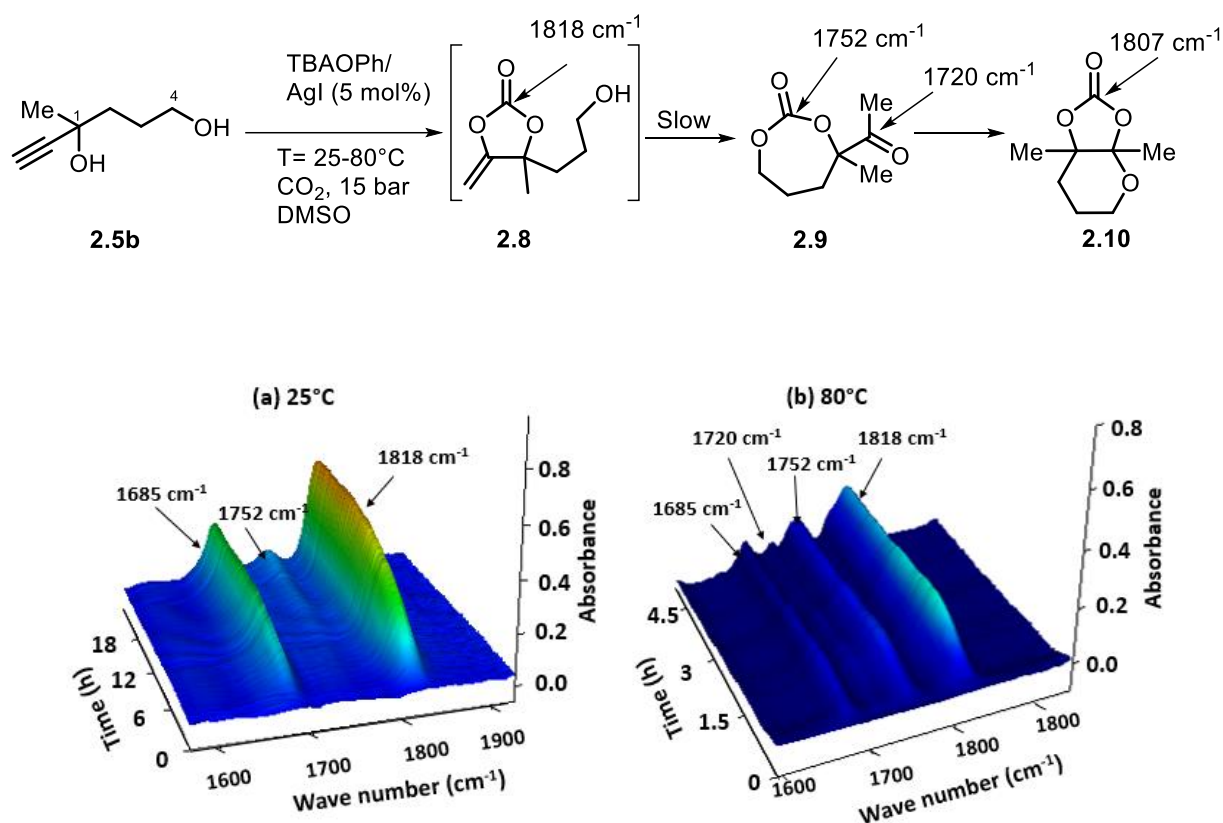
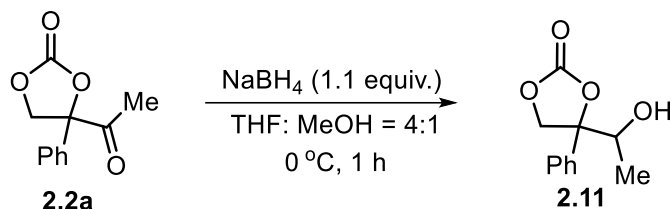


Figure 2.6. Online monitoring of the carboxylative coupling of 4-methylhex-5-yne-1,4-diol **2.5b** with CO₂ via operando FT-ATR spectroscopy at (a) 25 °C and (b) 80 °C showing the seven-membered carbonate **2.9** with absorptions at 1752 and 1720 cm⁻¹.

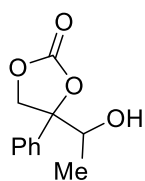
2.6.6 Synthetic and analytical details for compound 2.11 and 2.12

Procedures for the synthesis of the cyclic carbonates 2.11 and 2.12:

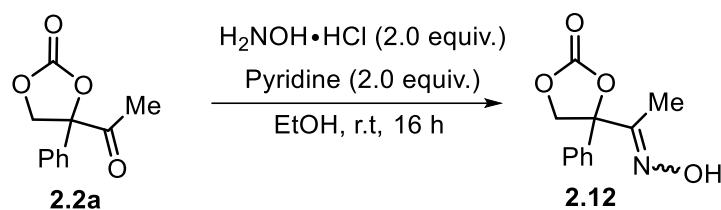


To a solution of 1,3-dioxolan-2-one product **2.2a** (0.3 mmol, 1.0 equiv) in a 4:1 mixture of tetrahydrofuran and methanol (1.5 mL) was added NaBH₄ (0.33 mmol, 1.1 equiv) under an argon atmosphere at 0 °C. Then, the reaction mixture was stirred for 1 h. When the starting material had disappeared (as followed by TLC), the solvent was removed by evaporation and the residue was quenched by addition of a saturated ammonium chloride (5 mL) solution. Ethyl acetate (5 mL) was added to it and the aqueous layer was separated. Further extraction was carried out of the aqueous layer with ethyl acetate (3 × 5 mL). The combined organic layers were dried over anhydrous Na₂SO₄, filtered, and concentrated in *vacuo*. The crude product was purified by flash chromatography on silica gel to obtain the corresponding product.

4-(1-Hydroxyethyl)-4-phenyl-1,3-dioxolan-2-one (2.11)



Colorless oil (42.8 mg, 67% yield, 2:1 *dr*). Eluent hexanes/EtOAc = 4/1. ¹H NMR (400 MHz, CDCl₃) δ 7.44 – 7.33 (m, 7.6H), 4.95 (d, *J* = 8.4 Hz, 0.5H), 4.81 (q, *J* = 6.6 Hz, 1H), 4.64 (d, *J* = 8.4 Hz, 0.5H), 4.16 – 4.07 (m, 1.5H), 3.95 (d, *J* = 12.8 Hz, 1H), 2.55 (brs, 1.6 H), 1.78 (d, *J* = 6.6 Hz, 3H), 1.06 (d, *J* = 6.6 Hz, 1.6H); ¹³C NMR (101 MHz, CDCl₃) δ 154.5, 154.3, 137.6, 137.0, 129.2, 129.12, 129.07, 128.8, 125.7, 124.2, 88.1, 88.0, 82.0, 71.5, 71.0, 65.4, 17.1, 14.8; IR (neat): ν = 1770 cm⁻¹; HRMS (ESI/TOF) *m/z* Calcd for C₁₁H₁₂NaO₄ [M + Na]⁺ 231.0628; Found 231.0620.



To a stirred solution of hydroxylamine hydrochloride (0.6 mmol, 2.0 equiv), pyridine (0.6 mmol, 2.0 equiv) in ethanol (3 mL) maintained at room temperature was added the 1,3-dioxolan-2-one **2.2a** (0.3 mmol, 1.0 equiv) dissolved in ethanol (3 mL). After the reaction was complete (followed by TLC), the solvent was removed under reduced pressure. To the residue was added water and the product was extracted twice with methylene chloride (2×5 mL) and washed with a 0.1 M HCl solution. The organic layer was dried over anhydrous Na_2SO_4 , filtered and concentrated in *vacuo*. The crude product was purified by flash chromatography on silica gel to obtain the final product.

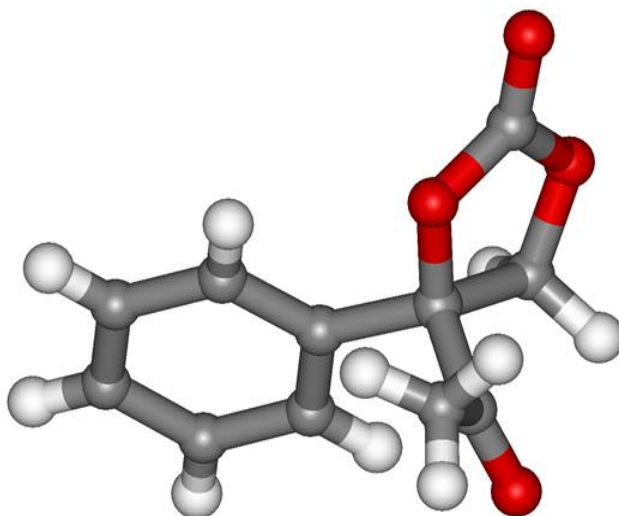
4-(1-(Hydroxyimino)ethyl)-4-phenyl-1,3-dioxolan-2-one (2.12)

White solid (55.3 mg, 85% yield, *Z/E* = 3:1). Eluent hexanes/EtOAc = 5/1. **¹H NMR** (400 MHz, CDCl_3) δ 7.45 – 7.34 (m, 6.9H), 5.45 (d, *J* = 8.5 Hz, 1H), 4.49 (d, *J* = 10.3 Hz, 0.3H), 4.40 (d, *J* = 10.3 Hz, 0.3H), 4.28 (d, *J* = 8.5 Hz, 1H), 1.85 (s, 1H), 1.82 (s, 3H); **¹³C NMR** (101 MHz, CDCl_3) δ 159.7, 155.0, 154.1, 139.1, 137.8, 129.4, 129.3, 128.9, 128.4, 125.1, 124.4, 89.5, 86.9, 82.6, 72.6, 10.6, 8.7; **IR** (neat): ν = 1804 cm^{-1} ; **HRMS** (ESI/TOF) *m/z*. Calcd for $\text{C}_{11}\text{H}_{11}\text{NNaO}_4$ [*M* + Na]⁺ 244.0580; Found 244.0578.

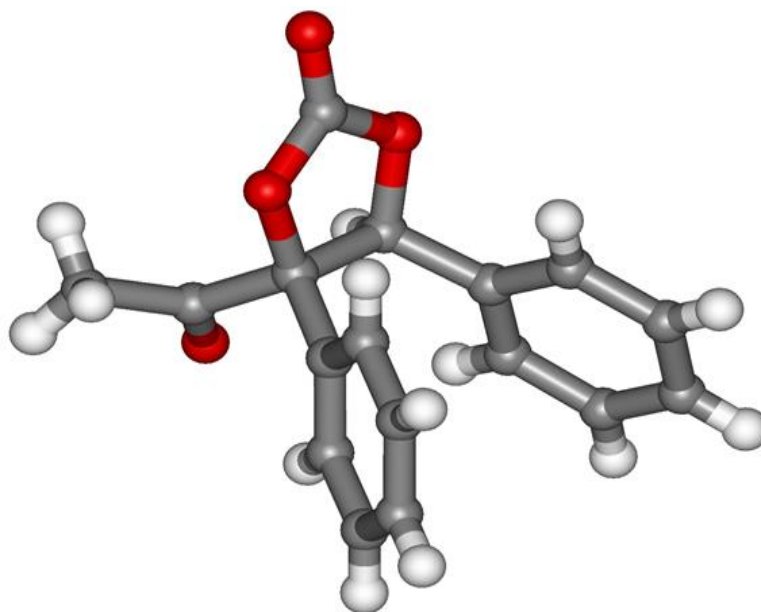
2.6.7 X-ray details

General experimental procedure for X-ray analysis: single crystals of each compound suitable for X-ray diffraction were stable under atmospheric conditions; nevertheless, they were treated under inert conditions immersed in perfluoro-polyether as protecting oil for manipulation. Data Collection: measurements were made on a Bruker-Nonius diffractometer equipped with an APPEX II 4K CCD area detector, a FR591 rotating anode with MoK α radiation, Montel mirrors and a Kryoflex low temperature device ($T = -173$ °C). Full-sphere data collection was used with ω and ϕ scans. Programs used: Data collection Apex2 V2011.3 (Bruker-Nonius 2008), data reduction Saint+Version 7.60A (Bruker AXS 2008) and absorption correction SADABS V. 2008-1 (2008). Structure Solution: SHELXTL Version 6.10 (Sheldrick, 2000) was used (Sheldrick, G. M. SHELXTL Crystallographic System, version 6.10; Bruker AXS, Inc.: Madison, WI, 2000). Structure Refinement: SHELXTL-97-UNIX VERSION.

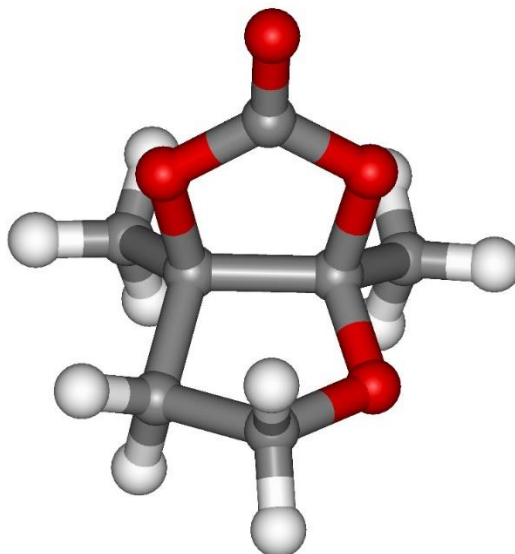
Disubstituted keto-carbonate 2.2a (CCDC-2088491):



Crystallographic data for 2.2a: C₁₁H₁₀O₄, $M_r = 206.19$, monoclinic, $P2_1/c$, $a = 7.4832(7)$ Å, $b = 16.3724(16)$ Å, $c = 8.0317(8)$ Å, $\alpha = 90^\circ$, $\beta = 109.335(2)^\circ$, $\gamma = 90^\circ$, $V = 928.53(16)$ Å³, $Z = 4$, $\rho = 1.475$ mg·M⁻³, $\mu = 0.113$ mm⁻¹, $\lambda = 0.71073$ Å, $T = 100(2)$ K, $F(000) = 432$, $\theta(\text{min}) = 2.488^\circ$, $\theta(\text{max}) = 30.127^\circ$, 14506 reflections collected, 2573 reflections unique ($R_{\text{int}} = 0.0236$), $\text{GoF} = 1.137$, $R_1 = 0.0359$, $wR_2 = 0.0964$ [$I > 2\sigma(I)$], $R_1 = 0.0415$, $wR_2 = 0.1004$ (all indices), min/max residual density = $-0.204/0.441$ [e·Å⁻³], Completeness to $\theta(30.127^\circ) = 93.5\%$.

Trisubstituted keto-carbonate **2.4a** (CCDC-2088492):

Crystallographic data for 2.4a: C₁₇H₁₄O₄, *M_r* = 282.28, orthorhombic, *P*2₁2₁2₁, *a* = 6.37486(13) Å, *b* = 13.7162(3) Å, *c* = 15.6002(4) Å, $\alpha = 90^\circ$, $\beta = 90^\circ$, $\gamma = 90^\circ$, *V* = 1364.06(5) Å³, *Z* = 4, $\rho = 1.375 \text{ mg}\cdot\text{M}^{-3}$, $\mu = 0.098 \text{ mm}^{-1}$, $\lambda = 0.71073 \text{ \AA}$, *T* = 100(2) K, *F*(000) = 592, $\theta(\text{min}) = 2.611^\circ$, $\theta(\text{max}) = 32.152^\circ$, 21982 reflections collected, 4536 reflections unique (*R*_{int} = 0.0248), GoF = 1.053, *R*₁ = 0.0299, *wR*₂ = 0.0758 [*I* > 2σ(*I*)], *R*₁ = 0.0316, *wR*₂ = 0.0767 (all indices), min/max residual density = -0.181/0.311 [e·Å⁻³], Completeness to $\theta(32.152^\circ) = 96.4 \%$.

Bicyclic carbonate 2.7 (CCDC-2112335):

Crystallographic data for 2.7: C₇H₁₀O₄, *M*_r = 158.13, monoclinic, *P*2₁/*c*, *a* = 6.8234(12) Å, *b* = 9.9156(18) Å, *c* = 10.9182(18) Å, α = 90°, β = 93.902(4)°, γ = 90°, *V* = 737.0(2) Å³, *Z* = 4, ρ = 1.425 mg·M⁻³, μ = 0.118 mm⁻¹, λ = 0.71073 Å, *T* = 100(2) K, *F*(000) = 336, θ (min) = 2.778°, θ (max) = 32.129°, 8943 reflections collected, 2530 reflections unique (*R*_{int} = 0.0469), *GoF* = 1.053, *R*₁ = 0.0468, *wR*₂ = 0.1242 [*I* > 2σ(*I*)], *R*₁ = 0.0579, *wR*₂ = 0.1332 (all indices), min/max residual density = -0.304/0.430 [e·Å⁻³], Completeness to θ (32.129°) = 98.1 %.

2.6.8 DFT details

As indicated in footnote 18 of the main text, the Gaussian 16^[S1] program was used with the implemented functional and basis set PBE0-D3(BJ)/SDD/def2tzv being chosen using dispersion correction with Becke-Johnson damping. All calculations were carried out at 298 K using an acetonitrile implicit solvent model SMD.

Full access to the computational data set is provided through:

<http://dx.doi.org/10.19061/iochem-bd-1-214>.

Please find below (**Figure 2.7**, next page) a full description of all energies involved in the conversion of both (*R*)- and (*S*)-**2.1a** using the selected chiral conformation of **L2.1** in the Ag(**L2.1**)OAc (pre)-catalyst. Obviously, upon using the other catalyst enantiomer, the energies for the conversion of (*R*)- and (*S*)-**2.1a** should be **reversed**.

[S1] Gaussian 16, Revision A.03, M. J. Frisch, G. W. Trucks, H. B. Schlegel, G. E. Scuseria, M. A. Robb, J. R. Cheeseman, G. Scalmani, V. Barone, G. A. Petersson, H. Nakatsuji, X. Li, M. Caricato, A. V. Marenich, J. Bloino, B. G. Janesko, R. Gomperts, B. Mennucci, H. P. Hratchian, J. V. Ortiz, A. F. Izmaylov, J. L. Sonnenberg, D. Williams-Young, F. Ding, F. Lipparini, F. Egidi, J. Goings, B. Peng, A. Petrone, T. Henderson, D. Ranasinghe, V. G. Zakrzewski, J. Gao, N. Rega, G. Zheng, W. Liang, M. Hada, M. Ehara, K. Toyota, R. Fukuda, J. Hasegawa, M. Ishida, T. Nakajima, Y. Honda, O. Kitao, H. Nakai, T. Vreven, K. Throssell, J. A. Montgomery, Jr., J. E. Peralta, F. Ogliaro, M. J. Bearpark, J. J. Heyd, E. N. Brothers, K. N. Kudin, V. N. Staroverov, T. A. Keith, R. Kobayashi, J. Normand, K. Raghavachari, A. P. Rendell, J. C. Burant, S. S. Iyengar, J. Tomasi,; Cossi, J. M. Millam, M. Klene, C. Adamo, R. Cammi, J. W. Ochterski, R. L. Martin, K. Morokuma, O. Farkas, J. B. Foresman, D. J. Fox, Gaussian, Inc., Wallingford CT, **2016**.

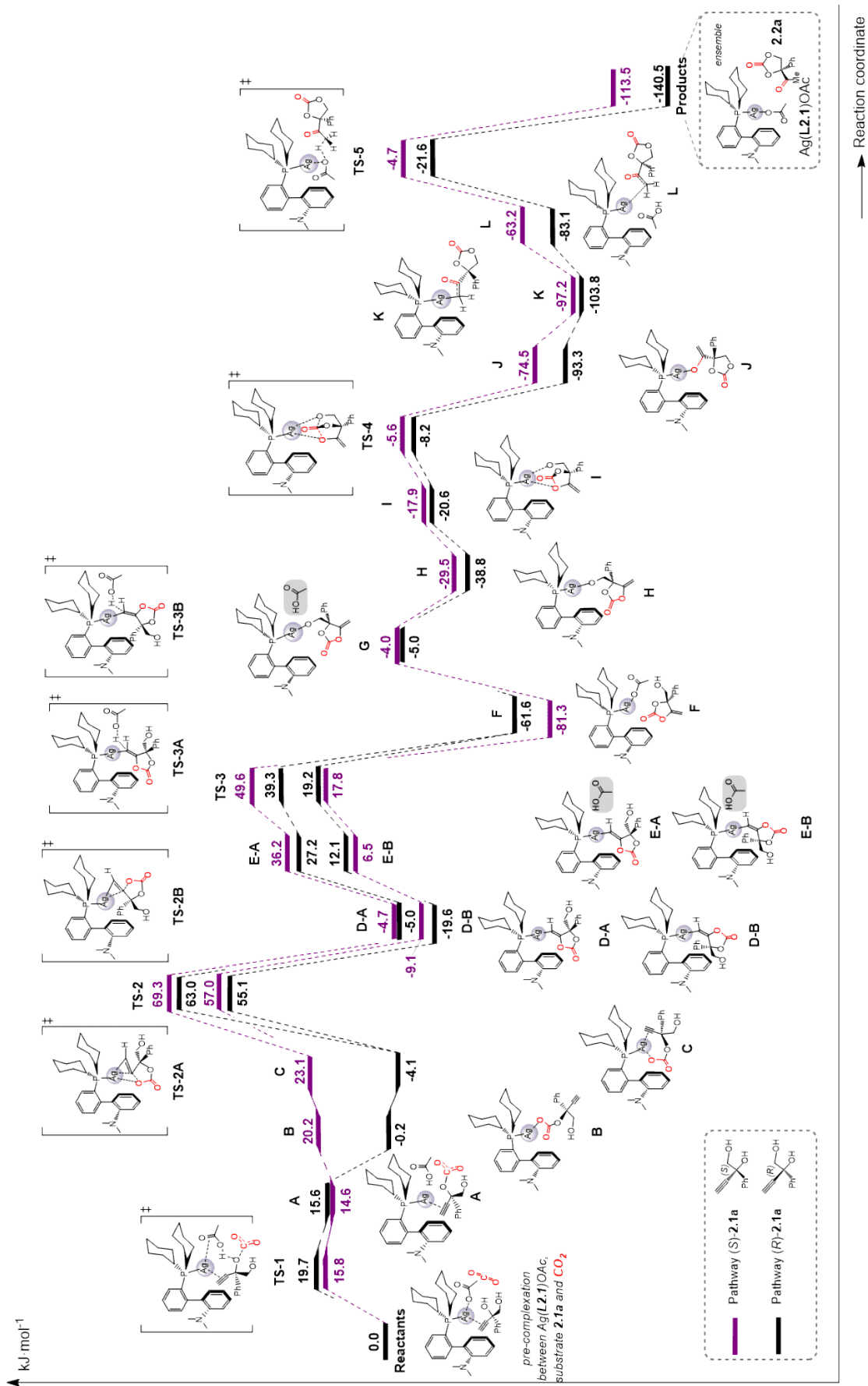


Figure 2.7 DFT-calculated pathway for the conversion of (R)-2.1a and (S)-2.1a into keto-carbonate 2.2a by catalyst Ag(L2.1)OAc in the presence of carbon dioxide.

UNIVERSITAT ROVIRA I VIRGILI
SILVER-CATALYZED CASCADE CONVERSIONS OF CO₂ INTO HETEROCYCLES
Xuetong Li

Chapter 3.

Silver-Mediated Cascade Synthesis of Functionalized 1,4-Dihydro-2H-benzo-1,3-oxazin-2-ones from Carbon Dioxide

The results described in this chapter have been published in:

X. Li, J. Benet-Buchholz, E. C. Escudero-Adán, and A. W. Kleij, *Angew. Chem. Int. Ed.* **2023**, *62*, e202217803.

UNIVERSITAT ROVIRA I VIRGILI
SILVER-CATALYZED CASCADE CONVERSIONS OF CO₂ INTO HETEROCYCLES
Xuetong Li

3.1 Introduction

The synthesis of heterocyclic compounds from carbon dioxide represents a vibrant area of research allowing to valorize a low-value carbon reagent into synthetically valuable intermediates and targets.¹ Cyclic carbamates are a class of substances that are particularly attractive as intermediates in the context of pharmaceutical development aimed at assembling scaffolds with biological activity.² In addition, the potential of five-membered cyclic carbamates serving as monomers for polyurethane synthesis through ring-opening polymerization was also recently discovered.³ Benzoxazine-2-one derivatives (i.e., six-membered cyclic carbamates with a fused aryl group) are a specific class of cyclic carbamates with high pharmaceutical relevance as these cores are frequently found in drug molecules such as Efavirenz and Droxicam, and form an essential part of various biologically potent 4-alkyl-substituted 1,4-dihydro-2*H*-1,3-benzoxazine-2-ones (Scheme 3.1a).⁴

The design and development of straightforward catalytic methods towards a diversity-oriented library of benzoxazine-2-ones remains a challenge, despite notable progress reported for the structurally more basic 1,3-oxazinan-2-one analogues.⁵ Apart from stoichiometric

¹ a) S. Wang, C. Xi, *Chem. Soc. Rev.* **2019**, *48*, 382–404; b) B. Yu, L.-N. He, *ChemSusChem* **2015**, *8*, 52–62; c) B. Limburg, À. Cristòfol, F. Della Monica, A. W. Kleij, *ChemSusChem* **2020**, *13*, 6056–6065; d) H. Long Ngo, D. K. Mishra, V. Mishra, C. C. Truong, *Chem. Eng. Sci.* **2021**, *229*, 116142; e) W. Guo, J. E. Gómez, À. Cristòfol, J. Xie, A. W. Kleij, *Angew. Chem. Int. Ed.* **2018**, *57*, 13735–13747; *Angew. Chem.* **2018**, *130*, 13928–13941; f) C. N. Tounzoua, B. Grignard, C. Detrembleur, *Angew. Chem. Int. Ed.* **2022**, *61*, e202116066; *Angew. Chem.* **2022**, *134*, e202116066; g) R. Rajjak Shaikh, S. Pornpraprom, V. D’Elia, *ACS Catal.* **2018**, *8*, 419–450; h) Q. Liu, L. Wu, R. Jackstell, M. Beller, *Nat. Commun.* **2015**, *6*, 5933.

² a) L. Aurelio, R. T. C. Brownlee, A. B. Hughes, *Chem. Rev.* **2004**, *104*, 5823–5846; b) T. A. Mukhtar, G. D. Wright, *Chem. Rev.* **2005**, *105*, 529–542; c) A. K. Ghosh, M. Brindisi, *J. Med. Chem.* **2015**, *58*, 2895–2940; d) F. Vacondio, C. Silva, M. Mor, B. Testa, *Drug Metab. Rev.* **2010**, *42*, 551–589; e) A. R. Renslo, G. W. Luehr, M. F. Gordeev, *Bioorg. Med. Chem.* **2006**, *14*, 4227–4240; f) M. R. Barbachyn, C. W. Ford, *Angew. Chem. Int. Ed.* **2003**, *42*, 2010–2023; *Angew. Chem.* **2003**, *115*, 2056–2070.

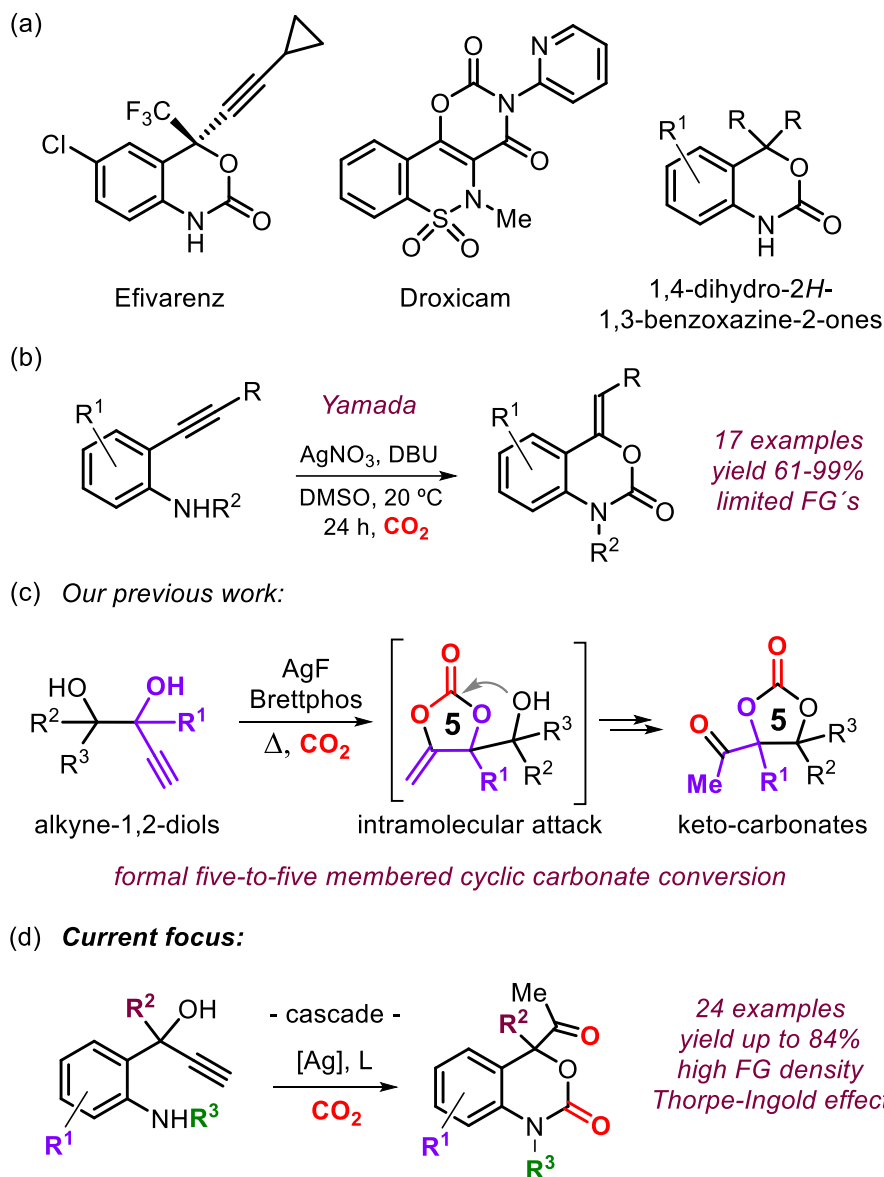
³ D. Zhang, Y. Zhang, Y. Fan, M.-N. Rager, V. Guérineau, L. Bouteiller, M.-H. Li, C. M. Thomas, *Macromolecules* **2019**, *52*, 2719–2724.

⁴ a) P. Chang, E. A. Terefenko, J. Wrobel, Z. Zhang, Y. Zhu, J. Cohen, K. B. Marschke, D. Mais, *Bioorg. Med. Chem. Lett.* **2001**, *11*, 2747–2750; b) J. C. Kern, E. A. Terefenko, A. Fensome, R. Unwalla, J. Wrobel, Y. Zhu, J. Cohen, R. Winneker, Z. Zhang, P. Zhang, *Bioorg. Med. Chem. Lett.* **2007**, *17*, 189–192; c) M. Patel, S. S. Ko, R. J. McHugh, J. A. Markwalder, A. S. Srivasta, B. C. Cordova, R. M. Klabe, S. Erickson-Viitanen, G. L. Trainor, S. P. Seitz, *Bioorg. Med. Chem. Lett.* **1999**, *9*, 2805–2810; d) S. R. Rabel, S. Sun, M. B. Maurin, M. Patel, *AAPS PharmSci* **2001**, *3*, 26–29.

⁵ X. Zhao, S. Yang, S. Ebrahimiasl, S. Arshadie, A. Hosseinian, *J. CO₂ Util.* **2019**, *33*, 37–45.

conversion of 1,3-aminoalcohols,⁶ 1,3-dihaloalkanes and related precursors,⁷ and 1-amino-3-chloropropan-2-ol derivatives,⁸ CeO₂-promoted formation of these compounds is feasible at high pressure (50 bar) using a sacrificial nitrile as a water scavenger.⁹ Enantioselective preparation of six-membered cyclic carbamates is viable using *N*-iodo-succinimide (NIS) based activation of homoallylic amines in the presence of CO₂.^{10a} Notably, Yamada and co-workers reported an efficient synthesis of benzoxazine-2-ones from 2-alkynylanilines and CO₂ under Ag catalysis,¹¹ which to date stands as a rare example of a catalytic process^{9, 10a, 12} delivering six-membered cyclic carbamates featuring a (*Z*)-configured *exo*-cyclic double bond (Scheme 3.1b). We recently disclosed the use of 1,2-alkyne-diols that upon combining with CO₂ could be conveniently converted into *keto* cyclic carbonates by first forming an α -alkylidene carbonate followed by intramolecular alcohol-induced isomerization.¹³ This process is hence a cascade process with a formal interconversion between two distinct 5-membered cyclic carbonates (Scheme 3.1c).¹⁴

-
- ⁶ a) J. Paz, C. Pérez-Balado, B. Iglesias, L. Muñoz, *J. Org. Chem.* **2010**, *75*, 3037–3046; b) R. Juárez, P. Concepción, A. Corma, H. García, *Chem. Commun.* **2010**, *46*, 4181–4183; c) T. Niemi, I. Fernández, B. Steadman, J. K. Mannisto, T. Repo, *Chem. Commun.* **2018**, *54*, 3166–3169.
- ⁷ a) T. Niemi, J. E. Perea-Buceta, I. Fernández, S. Alakurtti, E. Rantala, T. Repo, *Chem. Eur. J.* **2014**, *20*, 8867–8871; b) T. Niemi, J. E. Perea-Buceta, I. Fernández, O. M. Hiltunen, V. Salo, S. Rautiainen, M. T. Räisänen, T. Repo, *Chem. Eur. J.* **2016**, *22*, 10355–10359; c) C. Mei, Y. Zhao, Q. Chen, C. Cao, G. Pang, Y. Shi, *ChemCatChem* **2018**, *10*, 3057–3068.
- ⁸ Y. Toda, M. Shishido, T. Aoki, K. Sukegawa, H. Suga, *Chem. Commun.* **2021**, *57*, 6672–6675.
- ⁹ M. Tamura, M. Honda, K. Noro, Y. Nakagawa, K. Tomishige, *J. Catal.* **2013**, *305*, 191–203.
- ¹⁰ a) R. Yousefi, T. J. Struble, J. L. Payne, M. Vishe, N. D. Schley, J. N. Johnston, *J. Am. Chem. Soc.* **2019**, *141*, 618–625; For earlier contributions using similar substrate activation strategies see: b) T. Toda, Y. Kitagawa, *Angew. Chem. Int. Ed.* **1987**, *26*, 334–335; *Angew. Chem.* **1987**, *99*, 366–367; c) Y. Takeda, S. Okumura, S. Tone, I. Sasaki, S. Minakata, *Org. Lett.* **2012**, *14*, 4874–4877.
- ¹¹ a) T. Ishida, S. Kikuchi, T. Tsubo, T. Yamada, *Org. Lett.* **2013**, *15*, 848–851; b) S. Kikuchi, T. Yamada, *Chem. Rec.* **2014**, *14*, 62–69.
- ¹² For some other examples see: a) P. Brunel, J. Monot, C. E. Kefalidis, L. Maron, B. Martin-Vaca, D. Bourissou, *ACS Catal.* **2017**, *7*, 2652–2660; b) J. Rintjema, W. Guo, E. Martin, E. C. Escudero-Adán, A. W. Kleij, *Chem. Eur. J.* **2015**, *21*, 10754–10762.
- ¹³ X. Li, A. Villar-Yanez, C. Ngassam Tounzoua, J. Benet Buchholz, B. Grignard, C. Bo, C. Detrembleur, A. W. Kleij, *ACS Catal.* **2022**, *12*, 2854–2860.
- ¹⁴ S. Sopeña, M. Cozzolino, C. Maquilón, E. C. Escudero-Adán, M. Martínez Belmonte, A. W. Kleij, *Angew. Chem. Int. Ed.* **2018**, *57*, 11203–11207; *Angew. Chem.* **2018**, *130*, 11373–11377.



Scheme 3.1 (a) Representative drug molecules comprising of a 1,3-benzoxazine-2-one or related core. (b) Yamada's work using 2-alkynylanilines as precursors. (c) Previous approach to *keto*-carbonates via a cascade approach. (d) Current focus involving a unique domino synthesis of elusive 1,4-dihydro-2H-1,3-benzoxazine-2-one compounds.

3.2 Aims and objectives

Inspired by the design in Scheme 3.1c and a lack of suitable methodologies for the construction of small-molecule therapeutics based on benzoxazine-2-ones, we set out to explore the potential of a new and conceptually different cascade approach that first allows the formation of a five-membered α -alkylidene cyclic carbonate, which then is intercepted by a properly positioned *N*-nucleophile thereby forming the desired six-membered cyclic carbamate (Scheme 3.1d).¹⁵ This approach is different from our previous work on the formation of six-membered cyclic carbonates.¹⁶ Here we report the development of a catalytic domino process allowing to significantly expand the chemical space of functional benzoxazine-2-ones, their synthetic utility and the isolation of the initially postulated cyclic carbonate intermediate. Access to a wider diversity of these CO₂-based heterobicycles should further boost the design of new biologically active compounds from a simple, cheap and readily available carbon reagent.¹⁷

¹⁵ Cascade approaches are of our ongoing interest, see: a) W. Guo, R. Kuniyil, J. E. Gómez, F. Maseras, A. W. Kleij, *J. Am. Chem. Soc.* **2018**, *140*, 3981–3987; b) J. Xie, S. Xue, E. C. Escudero-Adán, A. W. Kleij, *Angew. Chem. Int. Ed.* **2018**, *57*, 16727–16731; *Angew. Chem.* **2018**, *130*, 16969–16973.

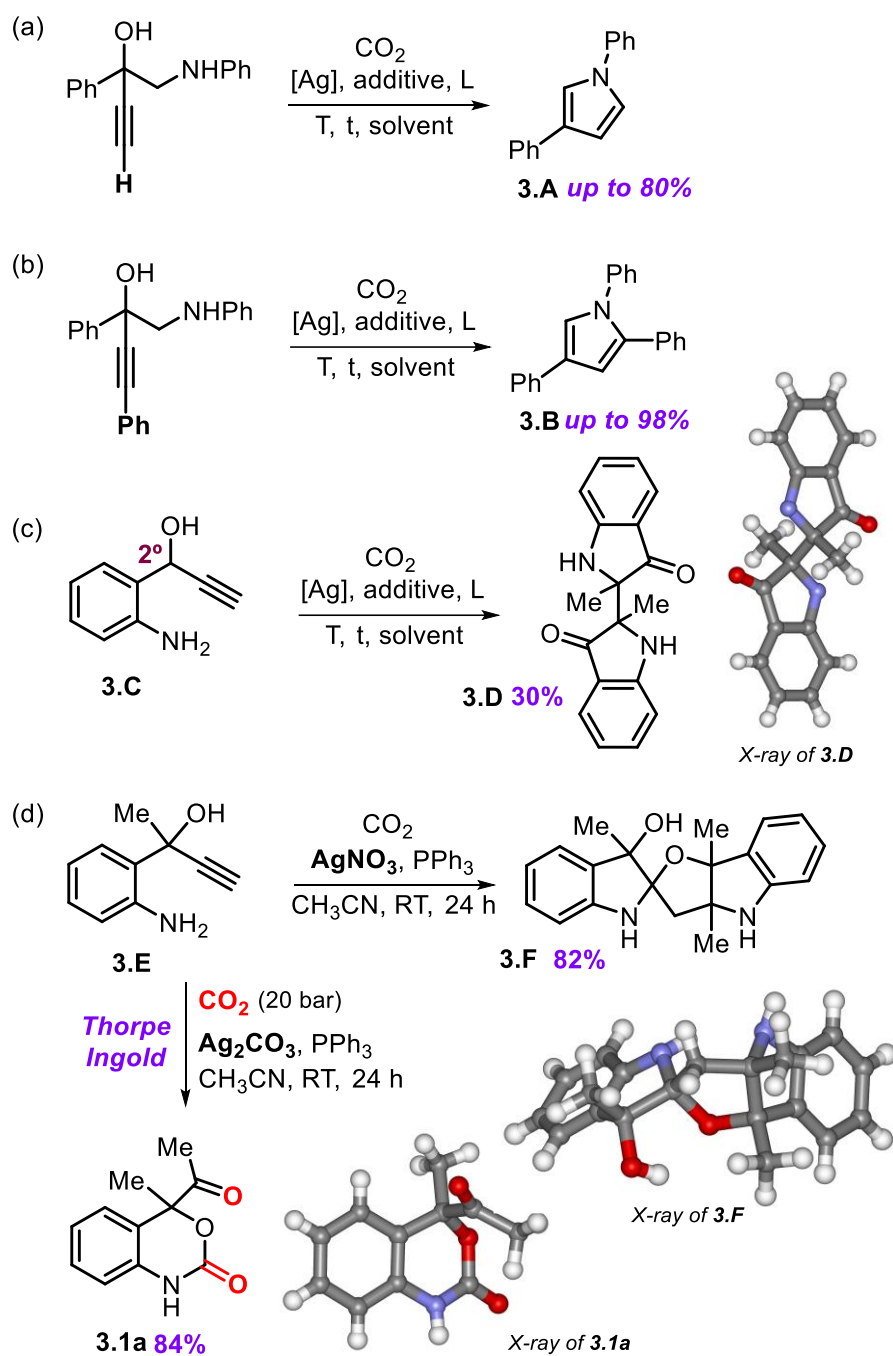
¹⁶ Previous work from our laboratory is based on the use of epoxy alcohol substrates that under Al-catalysis could be coupled with CO₂ to afford six-membered cyclic carbonates either via a sequential and partially stoichiometric *O*-protection, or through stereochemically defined cyclic β -epoxy alcohol precursors thereby yielding bicyclic carbonates in a single step, see: a) C. Qiao, A. Villar-Yanez, J. Sprachmann, B. Limburg, C. Bo, A. W. Kleij, *Angew. Chem. Int. Ed.* **2020**, *59*, 18446–18451; *Angew. Chem.* **2020**, *132*, 18604–18609; b) C. Qiao, W. Shi, A. Brandolese, J. Benet-Buchholz, E. C. Escudero-Adán, A. W. Kleij, *Angew. Chem. Int. Ed.* **2022**, *61*, e202205053; *Angew. Chem.* **2022**, *134*, e202205053. Both of these approaches are further different as they do not represent cascade processes. The current focus of the present work is on biologically relevant benzoxazine-2-ones, which possess much higher chemical stability than their carbonate congeners. They are derived from α -alkylidene carbonates that feature higher reactivities towards ring-opening when compared to saturated carbonates reported in our previous communications.

¹⁷ a) J. Vaitla, Y. Guttormsen, J. K. Mannisto, A. Nova, T. Repo, A. Bayer, K. H. Hopmann, *ACS Catal.* **2017**, *7*, 7231–7244; b) N. Kielland, C. J. Whiteoak, A. W. Kleij, *Adv. Synth. Catal.* **2013**, *355*, 2115–2138; c) W. Guo, V. Laserna, J. Rintjema, A. W. Kleij, *Adv. Synth. Catal.* **2016**, *358*, 1602–1607; d) J. Davies, J. R. Lyonnet, D. P. Zimin, R. Martin, *Chem* **2021**, *7*, 2927–2942.

Based on the successful conversion of alkyne-1,2-diols towards cyclic carbonates (Scheme 3.1c),¹³ we believed that by replacing one of the alcohol groups by an amine would favor the in situ formation of a hemi-carbamate species upon addition of CO₂. We anticipated that this activated intermediate could then collapse onto the alkyne unit favoring (direct) five- or six-membered cyclic carbamate formation (Scheme 3.2a). However, extensive screening of suitable catalytic conditions (i.e., Ag precursors, ligands, temperature, solvents; see the Experimental Section, Table 3.2) did not provide any evidence for any significant cyclic carbamate formation, and instead pyrrole **3.A** was preferentially formed in high yields of up to 80%. This outcome shows that the activation of CO₂ by the amine cannot compete with the thermodynamically favored 5-membered ring formation. In addition, an alkyne end-capped substrate (Scheme 3.2b) also undergoes easy cyclization to give the pyrrole product **3.B** (Experimental Section, Table 3.3). We subsequently turned to a different and more rigid substrate design (**3.C**) akin of Yamada's previous work (Scheme 3.2c).¹¹

Screening of various reaction conditions and catalysts (Experimental Section, Table 3.4) did not provoke the formation of a six-membered cyclic carbamate product, but unexpectedly provided 2,2'-biindoline-3,3'-dione **3.D** (confirmed by X-ray analysis)¹⁸ in a maximum yield of 30% as a major reaction component. We then selected a slightly modified substrate design (**3.E**) changing the secondary for a tertiary alcohol (Scheme 3.2d) to improve the probability for ring-closure by Thorpe–Ingold effects upon activating of CO₂ by the OH group. The influence of the reaction conditions and nature of the catalysts on the reaction outcome will be discussed here in more detail (Table 3.1; see Table 3.2–3.7 in the Experimental Section for a more extensive overview).

¹⁸ CCDC numbers 2208330, 2208331, 2208332, and 2208333 contain the supplementary crystallographic data for the structures reported in this chapter. These data are provided free of charge by the joint Cambridge Crystallographic Data Centre and Fachinformationszentrum Karlsruhe Access Structures service.



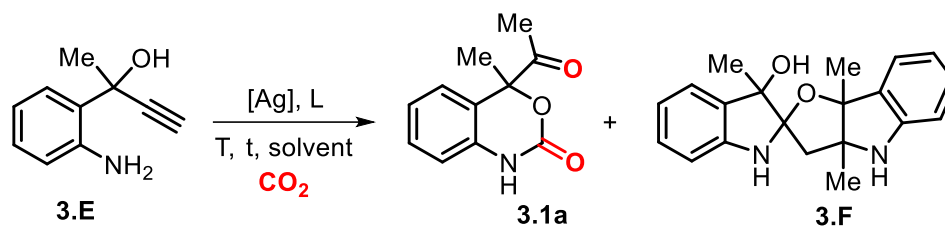
Scheme 3.2. Use of various types of substrates in the screening phase.

3.3 Results and discussion

While many (mostly) phosphine ligands were tested (see Table 3.5–3.7), we found that simple and cheap PPh₃ provided productive catalysis. The nature of the Ag-precursor has a pronounced effect on the reaction selectivity (entries 1–5) in the presence of PPh₃. The use of AgOAc, Ag₂O and AgF resulted in high conversion of substrate **3.E** though with low to moderate selectivity for either **3.1a** or **3.F**. The utilization of AgNO₃ (entry 4; 6 mol%), however, provided the unusual pentacyclic, spiro byproduct **3.F** in 82% yield.^{18,19} The chemo-selectivity could be switched to the desired cyclic carbamate **3.1a** (45%) by changing the anion to carbonate (entry 5; Ag₂CO₃). By adjusting the scale of the reaction and the concentration of the substrates (entries 6 and 7) we could improve the yield of **3.1a** to 77%. Replacing monodentate PPh₃ for a bidentate phosphine (3 mol% dppe, entry 8; 47%) caused the transformation to be more sluggish. The presence of other solvents such as CH₂Cl₂, MeOH or toluene (entries 9–11) did not improve the process efficiency, but increasing the CO₂ pressure from 10 to 20 bar further improved the yield of **3.1a** to 84% (entry 12). The presence of both the Ag salt and PPh₃ are indispensable as in the absence of either component no conversion of **3.E** was noted (entries 13 and 14). Finally, we doubled the amount of each catalyst component but the desired product **3.1a** was delivered in virtually the same yield (entry 15 versus 12).

¹⁹ The formation mechanism of **3.F** is unknown but appears to involve the Ag-catalyst mediating a cross-coupling of two molecules of **3.E** after initial cyclization to an indolinol derivative.

Table 3.1 Selected screening data for the catalytic conversion of substrate **3.E** into products **3.1a** and **3.F**.^[a]



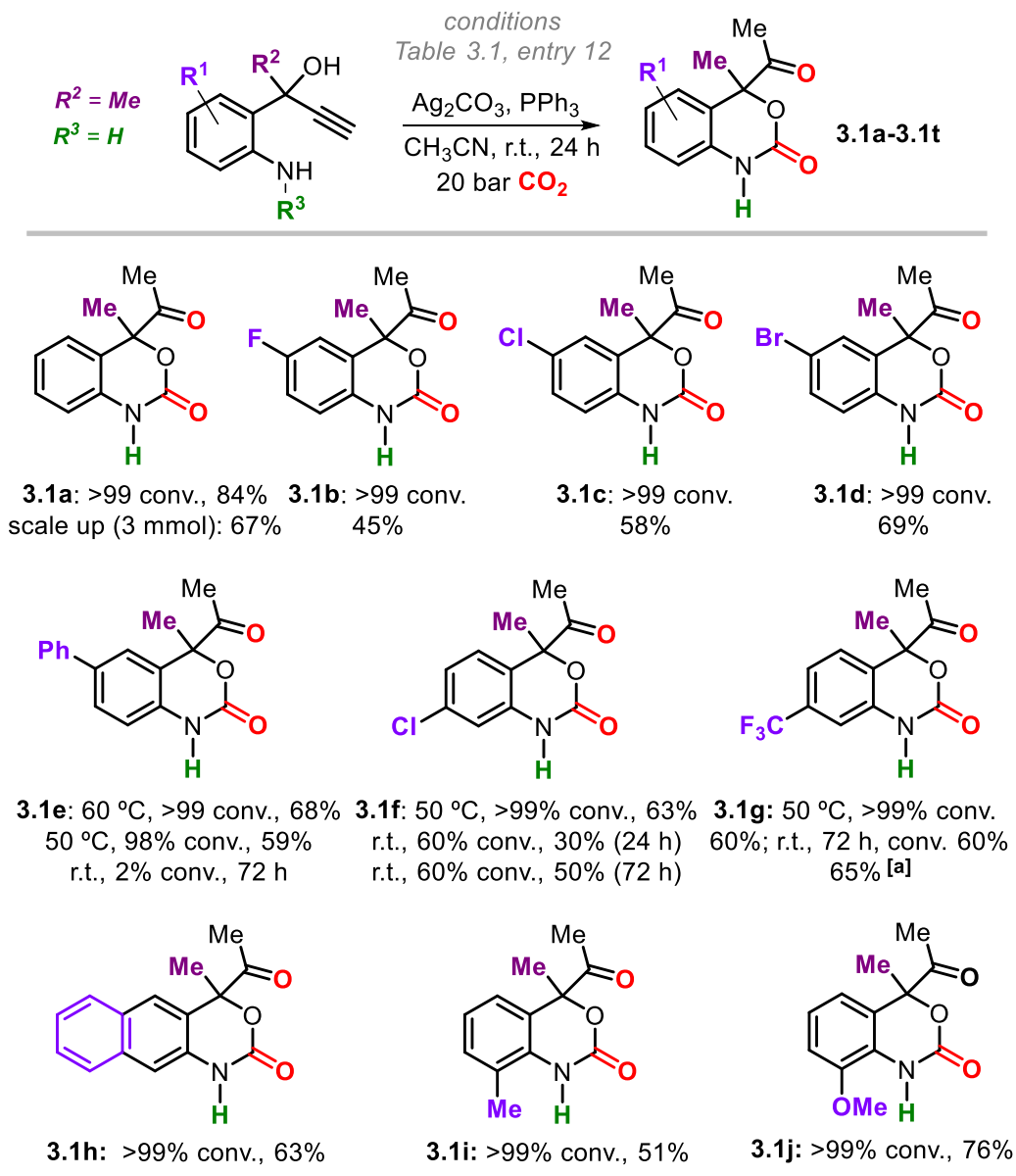
Entry	[Ag] [mol%]	[L] [mol%]	T/t [°C, h]	Conv [%] ^[b]	3.F ^[b] [%]	3.1a [%] ^[b]
1	AgOAc/6	PPh ₃ /12	r.t., 24	>99	24	21
2	Ag ₂ O/3	PPh ₃ /12	r.t., 24	80	0	<10
3	AgF/6	PPh ₃ /12	r.t., 24	>99	55	30
4	AgNO₃/6	PPh₃/12	r.t., 24	>99	82	0
5	Ag ₂ CO ₃ /3	PPh ₃ /12	r.t., 24	69	0	45
6 ^[c]	Ag ₂ CO ₃ /3	PPh ₃ /12	r.t., 24	>99	0	77
7 ^[c]	Ag ₂ CO ₃ /1.5	PPh ₃ /6	r.t., 24	>99	0	75
8 ^[c]	Ag ₂ CO ₃ /1.5	dppe/3	r.t., 24	63	0	47
9 ^[c,d]	Ag ₂ CO ₃ /1.5	PPh ₃ /6	r.t., 24	>99	0	70
10 ^[c,e]	Ag ₂ CO ₃ /1.5	PPh ₃ /6	r.t., 24	>99 ^[g]	<1	0
11 ^[c,f]	Ag ₂ CO ₃ /1.5	PPh ₃ /6	r.t., 24	>99	0	24
12^[c,h]	Ag₂CO₃/1.5	PPh₃/6	r.t., 24	>99	0	84
13 ^[c]	Ag ₂ CO ₃ /1.5	-	r.t., 24	0	0	0
14 ^[c]	-	PPh ₃ /6	r.t., 24	0	0	0
15 ^[c,g]	Ag ₂ CO ₃ /3	PPh ₃ /12	r.t., 24	>99	0	83

[a] Conditions: **3.E** (0.30 mmol), CH₃CN (0.60 mL), *p*(CO₂)=1 (entries 1–5) or 10 bar (entries 6–11, 13–14), temperature (°C) and time (h) indicated. [b] Determined by ¹H NMR (CDCl₃) using mesitylene as internal standard. [c] Using CH₃CN (0.40 mL) and **3.E** (0.20 mmol). [d] CH₂Cl₂ (0.40 mL) was used as solvent. [e] MeOH (0.40 mL) was used as solvent. [f] Toluene (0.40 mL) was used as solvent. [g] An unidentified byproduct was formed. [h] *p*(CO₂)=20 bar. [L] for the ligand used and [Ag] for the silver precursor.

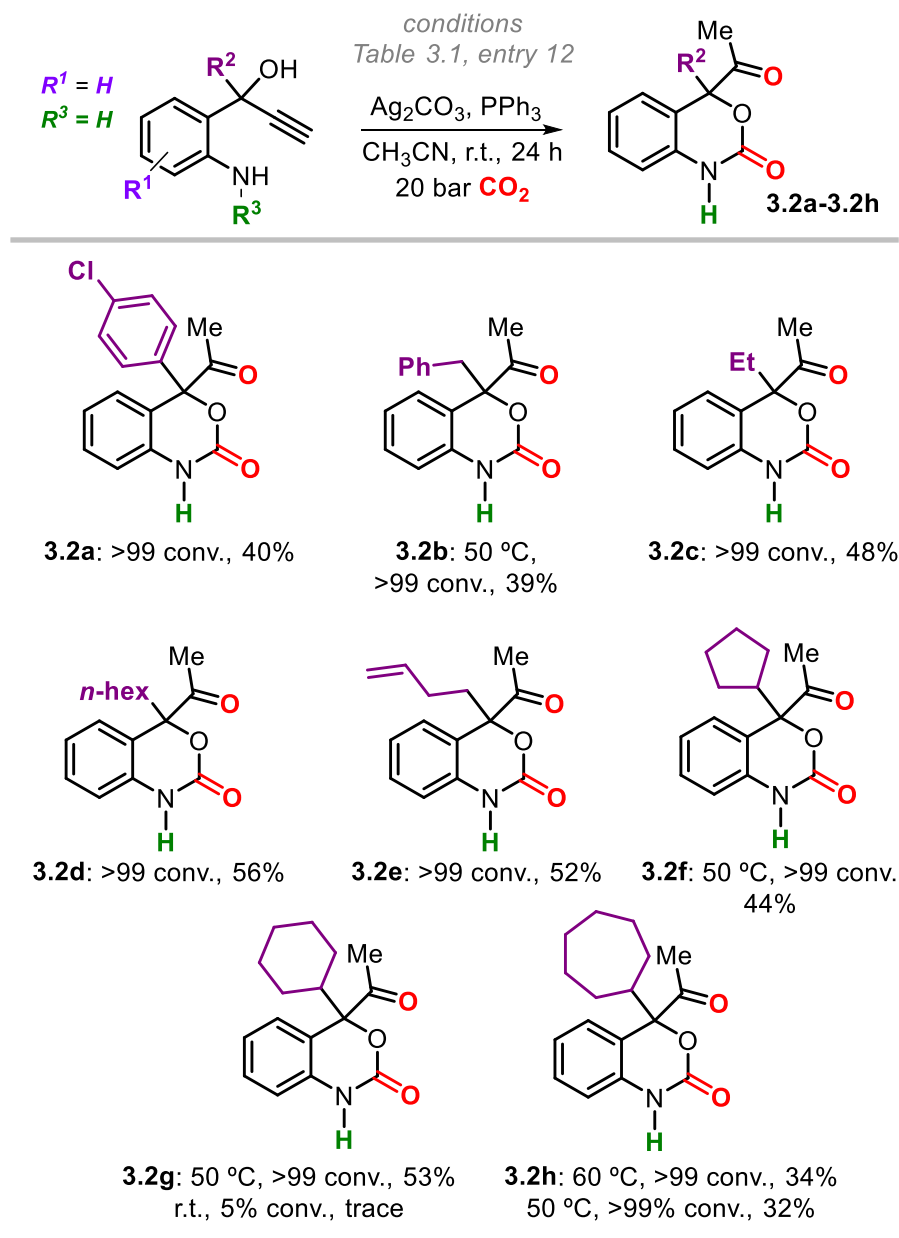
With productive conditions for 1,4-dihydro-2*H*-1,3-benzoxazine-2-one formation established (Table 3.1, entry 12), we then investigated the scope of this transformation (Scheme 3.3) by first varying the R¹-substituent in the propargylic precursors. Apart from the benchmark conversion leading to the simplest product **3.1a** in 84% yield (67%, 412 mg, scaled up 15-fold),²⁰ variation of the position and nature of R¹ in the substrate allowed to produce halide-appended benzoxazine-2-ones (**3.1b**, **3.1c**, **3.1d**, **3.1f** and **3.1g**) in up to 65% yield. In some cases, longer reaction times and/or the use of slightly elevated reaction temperatures were needed to improve the yields obtained under the optimized conditions (Table 3.1, entry 12). The phenyl-substituted (**3.1e**, 68%) and benzannulated product **3.1h** (63%) could also be isolated in appreciable yields. *Ortho*-substitution in the arene (**3.1i** and **3.1j**; cf., the NH₂ group in the substrate) was feasible leading to high substrate conversion and good product yields (51–76%).

Next we investigated how the variation of R² influenced benzoxazine-2-one formation (Scheme 3.4). The aryl-functionalized product **3.2a** was generated in a moderate yield of 40%, whereas products with more elaborate alkyl-substituents (**3.2b–3.2h**) gave similar or slightly improved yields within a reasonably narrow range of 34–56%. These results can be expected when at the onset of these transformations the steric requirements of R² plays a key role, in particular when the first step of the overall manifold involves a carboxylative cyclization featuring the propargylic alcohol unit of the substrate. This may explain that the yields for **3.2a** (40%) and **3.2h** (32%) are relatively low compared to the other cases. Notwithstanding, the catalytic procedure does allow to widen the scope of benzoxazine-2-ones to more complex examples including those comprising a potentially useful terminal alkene (**3.2e**) and sterically challenging cycloheptyl (**3.2h**) groups. When the propargylic alcohol unit in the substrate contained heterocycles such as a NH₂-substituted pyridine or pyrimidine (R²), no observable conversion was noted. This can be explained by catalyst deactivation through coordination of the *N*-donor atoms to the Ag complex preventing the key alkyne activation step (see Experimental Section for full details).

²⁰ The somewhat lower yield for **3.1a** when scaled up is attributed to the competitive formation of higher amounts of byproducts. For the synthesis of **3.1b** and **3.2h** we have further detailed the analysis of their crudes in the Experimental Section.



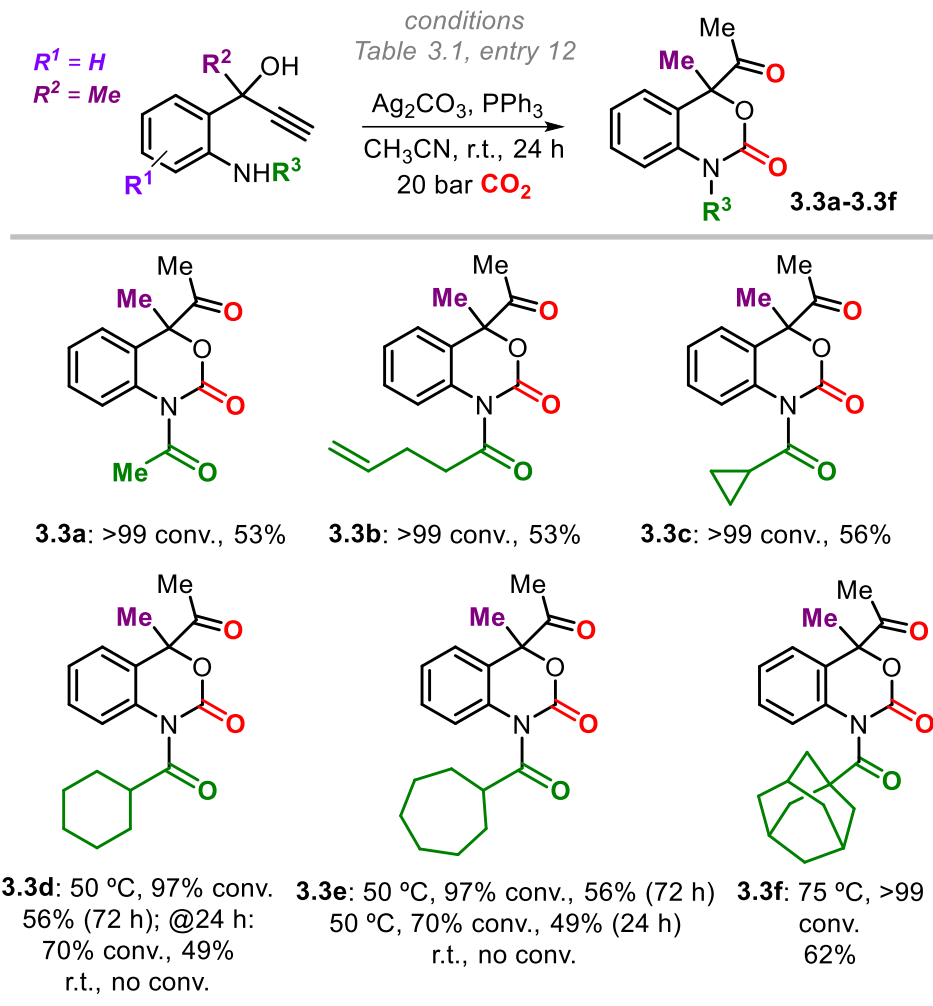
Scheme 3.3. Variation of R^1 in the precursors leading to cyclic carbamates **3.1a–3.1j**. General: All conversions were measured from the crude reaction mixtures using mesitylene as internal standard. Reported yields are of the isolated, purified products. [a] In this case, the conversion was based on the isolated, unreacted starting material by column purification.



Scheme 3.4 Variation of R² in the precursors leading to cyclic carbamates **3.2a-3.2h**. See the general comments in the caption to Scheme 3.3.

Lastly, we decided to alter the *N*-groups in the substrate by introducing various acyl substituent (Scheme 3.5). The *N*-acetyl based product **3.3a** was isolated in 53% yield, whereas the presence of more complex acyl groups (**3.3b** and **3.3c**) did not substantially alter the outcome giving the respective products in 53% and 56% yield. However, increasing the size of the *N*-acyl group did require the process to be adjusted to the use of higher reaction temperatures/pressures and reaction times as exemplified by the isolation of **3.3d** (56%, 72 h,

50 °C) and **3.3 e** (84%, 50 bar, 75°C). The adamantyl-based product **3.3f** (62%) also required a significantly higher reaction temperature (75°C) suggesting an important role for the *N*-based pronucleophile during the product formation process.



Scheme 3.5. Variation of R³ in the precursors leading to cyclic carbamates **3.3a–3.3f**. See the general comments in the caption to Scheme 3.3.

With these observations and the ones for the synthesis of **3.3a–3.3f** in mind, we scrutinized the conversion of the adamantyl-based substrate **3.G** in more detail (Scheme 3.6a). When the optimized conditions (Table 3.1, entry 12; r.t.) are used, no observable substrate conversion is noted after 24 h. When the reaction temperature is raised to 50°C, a new product (**3.H**) can be isolated in 79%. Analysis by ¹H NMR and IR spectroscopy strongly suggested the formation of an α -alkylidene carbonate,^{13,21} which could be corroborated by an X-ray crystallographic

²¹ For a few selected, recent examples of catalytic α -alkylidene carbonate formation processes see: a) A. Cervantes-Reyes, K. Farshadfar, M. Rudolph, F. Rominger, T. Schaub, A. Ariafard, A. S. K. Hashmi,

analysis of this product.¹⁸ Since the desired six-membered cyclic carbamate **3.3f** was produced at 75 °C (Scheme 3.5), we wondered whether **3.H** could be converted to **3.3f** by the Ag catalyst. Treatment of **3.H** at 82 °C in the presence of Ag₂CO₃/PPh₃ slowly converted **3.H** into **3.3f** (35% yield). However, repeating the same synthesis in the absence of catalyst provided a rather similar substrate conversion and yield for **3.3f** (41%). This may suggest that the Ag-catalyst is not involved in the second step, but some caution is needed with this hypothesis. The pre-isolated sample of **3.H** entails a rather different starting point for the Ag catalyst departing from a different reaction mixture speciation. The in situ reaction of the propargylic alcohol into the α -alkylidene carbonate typically results into an intermediate Ag-alkylidene species²¹ that is likely much more reactive than **3.H** towards the formation of **3.3f**.

The envisioned path leading to the benzoxazine-2-one products follows a cascade that first involves five-membered ring carbonate formation and then proceeds towards the final six-membered cyclic carbamate through in situ attack of the *N*-based pronucleophile on the Ag-activated cyclic carbonate, with the size of the *N*-substitution being important for the kinetics involved in this second step (cf., formation of **3.3f**). Notably, the intermolecular ring-opening of an α -alkylidene carbonate by either primary or secondary *N*-based nucleophiles such as amines typically results into different cyclic or acyclic products, while in the present case the intramolecular process only allows the formation of a six-membered (cyclic) keto-carbamate.²²

The privileged nature of the used catalyst system (Ag₂CO₃/PPh₃) in the formation of α -alkylidene intermediates was recently described by He and co-workers,²³ with a bifunctional role disclosed for this catalyst activating both the propargylic alcohol and CO₂ simultaneously. The presence of a relatively electron-poor phosphine (PPh₃) is believed to maximize the alkyne activation potential of the Ag cation. While the second step can be slowed down by increasing the size of the *N*-substituent, the first step should also be susceptible for steric modulation (Scheme 3.6b). As may be expected, when the Me in **3.1Ea** is replaced by a much bulkier *t*Bu group (**3.I**), no reaction was observed even when raising the temperature up to 60 °C. This

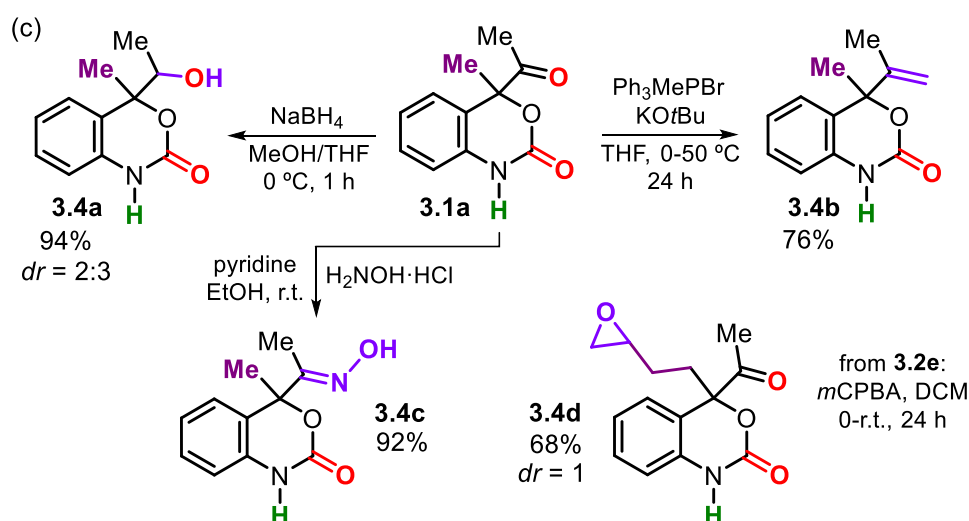
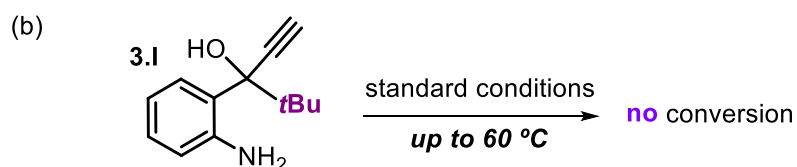
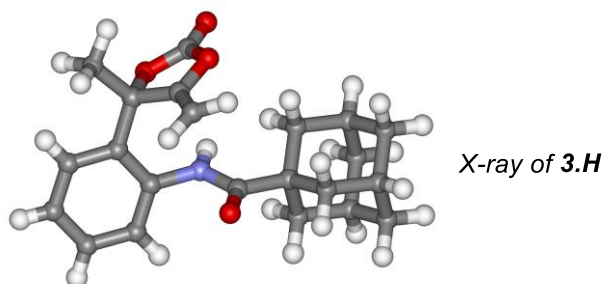
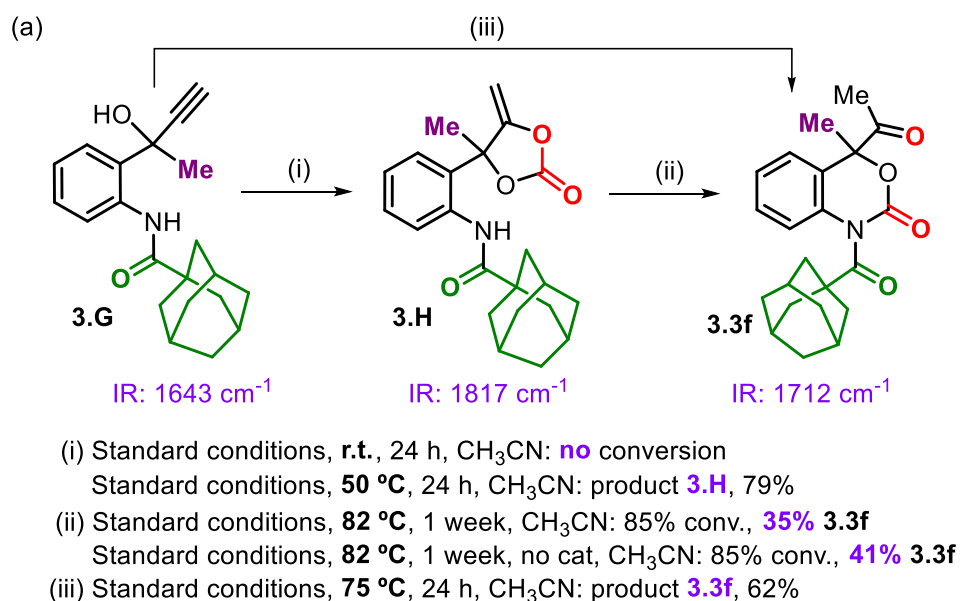
Green Chem. **2021**, *23*, 889–897; b) Y. Hu, J. Song, C. Xie, H. Wu, T. Jiang, G. Yang, B. Han, *ACS Sustainable Chem. Eng.* **2019**, *7*, 5614–5619; c) S. Dabral, B. Bayarmagnai, M. Hermsen, J. Schießl, V. Mormul, A. S. K. Hashmi, T. Schaub, *Org. Lett.* **2019**, *21*, 1422–1425.

²² See: a) C.-R. Qi, H.-F. Jiang, *Green Chem.* **2007**, *9*, 1284–1286; b) B. Jiang, X. Yan, Y. Xu, N. Likhanova, H. Díaz Velázquez, Y. Gong, Y. Yuan, F. Verpoort, *Catalysts* **2022**, *12*, 73.

²³ Q.-W. Song, W.-Q. Chen, R. Ma, A. Yu, Q.-Y. Li, Y. Chang, L.-N. He, *ChemSusChem* **2015**, *8*, 821–827.

aligns well with our mechanistic hypothesis of a cascade process that provides a unique 5-to-6 atom ring expansion thereby providing new pharmacores.

The stability of two selected benzoxazine-2-ones (**3.1a** and **3.2e**, Scheme 3.6c) was probed to examine their suitability as synthons in post-modifications. When **3.1a** is treated with NaBH₄, the resultant alcohol derivative **3.4a** was isolated as a mixture of diastereoisomers ($dr = 2:3$) in excellent yield (94%) without affecting the carbamate group. A Wittig olefination of **3.1a** provided **3.4b** in 76% yield, and the ketone group in **3.1a** is also easily converted into the hydroxyl-imine product **3.4c** (92%) under mild conditions. Lastly, epoxidation of **3.2e** using *m*CPBA (*meta*-chloro-perbenzoic acid) afforded **3.4d** ($dr = 1$) in 68% yield, allowing to further extend the molecular complexity of these carbamate scaffolds.



Scheme 3.6. Control experiments (a-b) and synthetic utility of benzoxazine-2-ones **3.1a** and **3.2e** (c). For more details, see the Experimental Section.

3.4 Conclusions

In this chapter, we present a conceptually new cascade route towards the synthesis of functional 1,4-dihydro-2*H*-1,3-benzoxazine-2-one products with an unparalleled scope. The approach takes advantage of a unique Ag-promoted sequence with intermediate formation of an α -alkylidene carbonate, which is intramolecularly intercepted by an *N*-based nucleophile affording the six-membered carbamate targets. This new process allows to rapidly expand the repertoire of pharma-relevant compounds thereby creating new incentives for drug discovery programs. It may also inspire other types of cascade approaches with reactive cyclic carbonates acting as synthetic intermediates to rapidly build up molecular complexity.

3.5 Experimental section

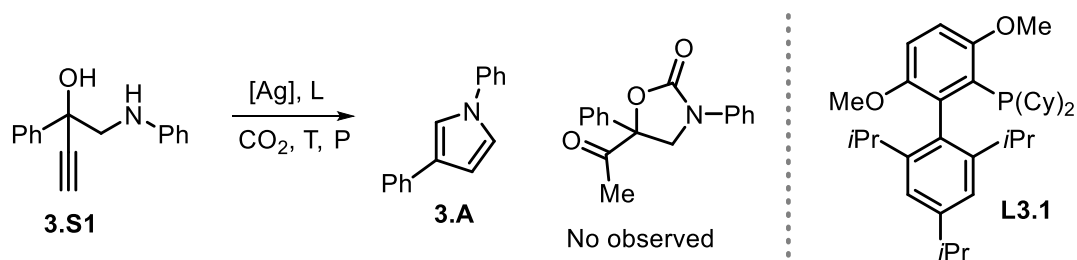
3.5.1 General comments

Unless otherwise noted, all commercially available reagents and solvents were purchased from Sigma-Aldrich, TCI, Strem Chemicals, ABCR GmbH, Acros Organics or Alfa Aesar and were used without further purification. Solvents were dried using an Innovative Technology PURE SOLV solvent purification system. Carbon dioxide was purchased from PRAXAIR and used without further purification. Reactions were performed in a stainless-steel HEL-multireactor or a 30 mL stainless steel reactor under a CO₂ atmosphere. Products were purified by flash chromatography or by preparative thin-layer chromatography on silica gel. NMR spectra were recorded on Bruker 400 MHz and Bruker 500 MHz at room temperature (25 °C). The residual solvent signals were used as references for ¹H and ¹³C spectra [CDCl₃: δ_H = 7.26 ppm, δ_C = 77.16 ppm, (CD₃)₂CO: δ_H = 2.05 ppm, δ_C = 29.84 ppm, CD₃OD: δ_H = 3.31 ppm, δ_C = 49.00 ppm]. ¹⁹F NMR spectra were obtained with ¹H decoupling unless stated otherwise. FT-IR measurements were carried out on a Bruker Optics FTIR-ATR TR0 spectrometer. Exact mass analyses and X-ray diffraction studies were performed by the Research Support Area (RSA) at ICIQ. Elemental analyses were performed by the Unitat Anàlisi Química i Estructural (departament de Serveis Tècnica de Recerca) from the University of Girona (Spain).

3.5.2 Preliminary results with various types of substrates

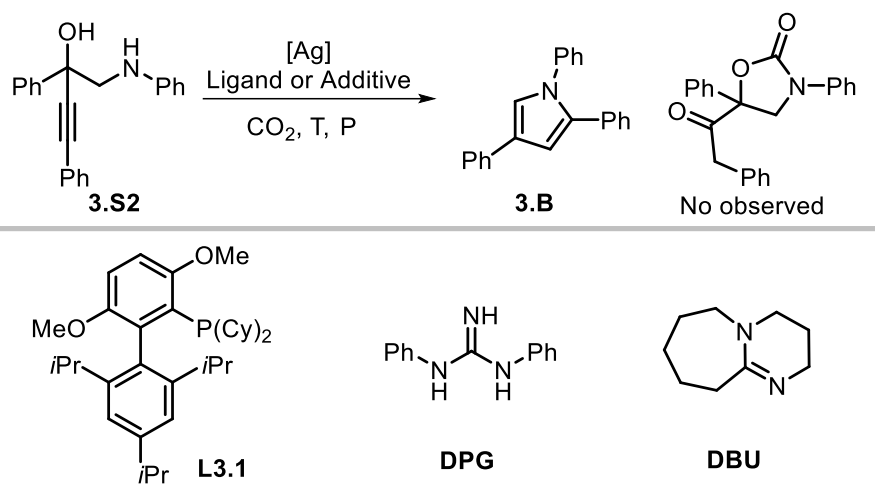
By designing various kinds of substrates, we intended to establish five-, six- or seven-membered cyclic carbamates. Four different compounds (from Table 3.2 to Table 3.5) were examined, the experimental and analytical details are provided as below:

Table 3.2:^[a]



Entry	Catalyst	Ligand	P/[bar]	T/[°C]	Conv. /[%] ^[b]	Y _{3.A} /[%] ^[b]
1	AgF (5 mol%)	L3.1 (5 mol%)	10	25	100	50
2	AgF (5 mol%)	L3.1 (5 mol%)	30	40	100	80

[a] Reaction conditions: **3.S1** (0.3 mmol), MeCN (0.6 mL), 24 h. [b] Determined by ¹H NMR, using mesitylene as the internal standard. Y stands for yield.

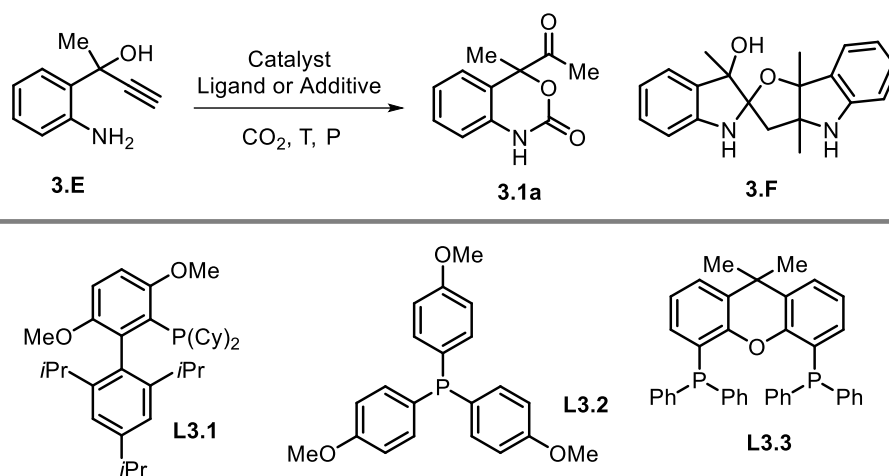
Table 3.3:^[a]

Entry	Catalyst/[mol%]	Ligand/[mol%]	T/[°C]	Conv. [%] ^[b]	Y _{3.B} [%] ^[b]
1	AgF, 5	L3.1 , 5	25	100	95
2	AgI, 5	[TBA][OPh], 5	25	10	trace
3 ^[c]	AgSbF ₆ , 5	DPG, 5	25	100	90
4 ^[c]	AgSbF ₆ , 5	DPG, 50	25	51	87
5	AgNO ₃ , 10	DBU, 100	25	100	89
6	CuI, 10	DBU, 100	40	100	80
7	PdCl ₂ , 10	DBU, 100	40	100	98
8	PtCl ₂ , 10	DBU, 10	40	100	90

[a] Reaction condition: **3.S2** (0.3 mmol), MeCN (0.6 mL), 10 bar CO₂ atmosphere, 24 h. [b] Determined by ¹H NMR, using mesitylene as the internal standard. [c] Using DCE as solvent, under 1 bar CO₂ atmosphere.

Table 3.5:^[a]

Preliminary screening data with substrate **3.E**.

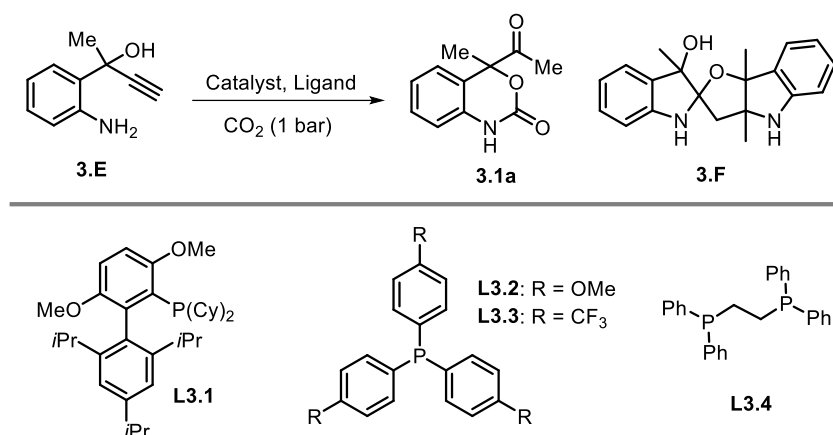


Entry	C. / [mol%]	L / [mol%]	P / [bar]	T / [°C]	Conv. / [%] ^[b]	Y _{3.1a} / [%] ^[b]	Y _{3.F} / [%] ^[b]
1	CuI, 10	DBU, 100	20	25	100	–	–
2	PdCl ₂ , 10	DBU, 100	20	25	100	–	–
3	AgNO ₃ , 10	DBU, 100	20	25	100	–	–
4	AgCl, 5	Et ₄ NCl, 9	1	60	100	–	60
5	AgCl, 5	Et ₄ NCl, 9	20	25	71	–	42
6 ^[c]	AgI, 5	[TBA][OPh], 5	20	25	100	–	–
7	AgF, 5	L3.1 , 5	1	40	100*	–	–
8	AgF, 5	L3.1 , 5	20	25	100**	–	–
9 ^[d]	Ag ₂ CO ₃ , 10	L3.2 , 1	20	25	78	43	–
10 ^[e]	Ag ₂ CO ₃ , 1.5	PPh ₃ , 6	1	25	36	trace	–
11	Ag ₂ CO ₃ , 5	L3.3 , 10	20	60	100	–	–
12 ^[f]	Ag ₂ CO ₃ , 1.5	PPh ₃ , 6	20	25	100	84(82) ^[g]	–

[a] Reaction conditions: **3.E** (0.30 mmol), CH₃CN (0.60 mL), 24 h. [b] Determined by ¹H NMR using mesitylene as an internal standard. [c] Using DMSO as solvent. [d] Using CHCl₃ as solvent. [e] Reaction time was 16 h. [f] 1.0 mmol **3.E** was added. [g] Isolated yield. Y stands for yield, C stands for catalyst, L stands for ligand. * An unidentified byproduct (~50% NMR yield) was formed, which after silica gel purification was converted into product **3.F** (see the main text). ** An unidentified and unstable byproduct (~60% NMR yield) was formed, which after silica gel purification provided a mixture of components.

3.5.3 Optimization of the reaction condition

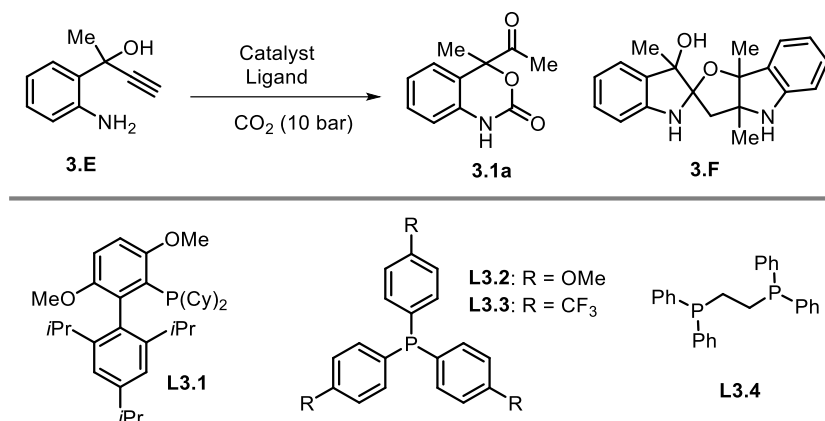
Table 3.6: Screening data with substrate **3.E**, under **1 bar** CO₂ atmosphere.^[a]



Entry	Catalyst/[mol%]	Ligand/[mol%]	Conv. [%] ^[b]	Y _{3.1a} /[%] ^[b]	Y _{3.F} /[%] ^[b]
1	Ag ₂ CO ₃ (1.5 mol%)	–	–	–	–
2	–	PPh ₃ (6 mol%)	–	–	–
3	Ag ₂ CO ₃ (1.5 mol%)	PPh ₃ (6 mol%)	42	33	–
4	Ag ₂ CO ₃ (3 mol%)	PPh ₃ (12 mol%)	69	45	–
5	Ag ₂ CO ₃ (6 mol%)	PPh ₃ (24 mol%)	92	45	–
6	Ag ₂ CO ₃ (1.5 mol%)	PPh ₃ (3 mol%)	27	29	–
7 ^[c]	Ag ₂ CO ₃ (3 mol%)	PPh ₃ (12 mol%)	70	–	–
8	Ag ₂ O (3 mol%)	PPh ₃ (12 mol%)	80	<10	–
9	AgOAc (6 mol%)	PPh ₃ (12 mol%)	100	21	24
10	AgF (6 mol%)	PPh ₃ (12 mol%)	100	30	55
11	AgNO ₃ (6 mol%)	PPh ₃ (12 mol%)	100	–	82
12	AgBF ₄ (6 mol%)	PPh ₃ (12 mol%)	100	–	67
13	AgF ₆ Sb (6 mol%)	PPh ₃ (12 mol%)	100	–	49
14	Ag ₂ CO ₃ (3 mol%)	L3.2 (12 mol%)	100	37	–
15	Ag ₂ CO ₃ (3 mol%)	L3.3 (12 mol%)	100	–	–
16	Ag ₂ CO ₃ (3 mol%)	P(OPh) ₃ (12 mol%)	100	–	73
17	Ag ₂ CO ₃ (3 mol%)	L3.4 (6 mol%)	100	–	–
18	Ag ₂ CO ₃ (3 mol%)	L3.1 (12 mol%)	100*	–	–

[a] Reaction condition: **3.E** (0.3 mmol), CH₃CN (0.6 mL), room temperature, 24 h. [b] Determined by ¹H NMR using mesitylene as an internal standard. [c] At 40 °C. * The same unstable byproduct was formed as discussed for entry 8, Table 3.5 (~70% NMR yield).

Table 3.7: Screening data with substrate **3.E**, under **10 bar** CO₂ atmosphere.



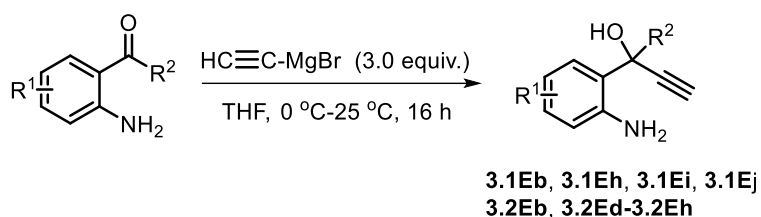
Entry	Catalyst	Ligand	Conv./[%] ^[b]	Y _{3.1a} /[%] ^[b]	Y _{3.F} /[%] ^[b]
1	Ag ₂ CO ₃ (1.5 mol%)	PPh ₃ (6 mol%)	100	75	–
2	Ag ₂ CO ₃ (3 mol%)	PPh ₃ (12 mol%)	100	77	–
3	AgF (3 mol%)	PPh ₃ (6 mol%)	100	33	trace
4	AgOTf (3 mol%)	PPh ₃ (6 mol%)	100	–	64
5	AgNO ₃ (3 mol%)	PPh ₃ (6 mol%)	100	–	73
6	AgBF ₄ (3 mol%)	PPh ₃ (6 mol%)	10	–	–
7	AgF ₆ Sb (3 mol%)	PPh ₃ (6 mol%)	100	–	24
8	Ag ₂ CO ₃ (1.5 mol%)	L3.2 (6 mol%)	100	72	–
9	Ag ₂ CO ₃ (1.5 mol%)	L3.4 (3 mol%)	63	47	–
10	Ag ₂ CO ₃ (1.5 mol%)	L3.1 (6 mol%)	100*	–	–
11	Ag ₂ CO ₃ (1.5 mol%)	L3.3 (6 mol%)	64	47	–
12 ^[c]	Ag ₂ CO ₃ (1.5 mol%)	PPh ₃ (6 mol%)	100	70	–
13 ^[d]	Ag ₂ CO ₃ (1.5 mol%)	PPh ₃ (6 mol%)	100	–	trace
14 ^[e]	Ag ₂ CO ₃ (1.5 mol%)	PPh ₃ (6 mol%)	100	24	–
15 ^[f]	Ag ₂ CO ₃ (1.5 mol%)	PPh ₃ (6 mol%)	100	–	–
16^[g]	Ag₂CO₃ (1.5 mol%)	PPh₃ (6 mol%)	100	84 (82)^[h]	–
17 ^[g]	Ag ₂ CO ₃ (3 mol%)	PPh ₃ (12 mol%)	100	83	–

[a] Reaction conditions: **3.E** (0.20 mmol), CH₃CN (0.40 mL), room temperature, 24 h. [b] Determined by ¹H NMR using mesitylene as an internal standard. [c] Using DCM as solvent. [d] Using MeOH as solvent. [e] Using toluene as solvent. [f] Using DMF as solvent. [g] Under 20 bar CO₂ atmosphere. [h] Isolated yield. Y stands for yield. * An unidentified, unstable byproduct (~45% NMR yield) was formed, which after silica gel purification gave rise to a mixture of components.

3.5.4 Experimental procedures and characterization data for the substrates

The known 1-(2-aminophenyl) propargylic alcohols **3.1Ea**,²⁴ **3.1Ec**,²⁵ **3.1Ed**,²⁴ **3.1Ee**,²⁴ **3.1Ef**,²⁵ **3.1Eg**,²⁶ **3.2Ea**,²⁴ **3.2Ec**,²⁴ **3.3Ea**²⁷ and **3.3Eb**²⁷ were synthesized as reported in the literature. Below, the preparation of new substrates is detailed.

General Procedure A for synthesis of 1-(2-aminophenyl) propargyl alcohols:



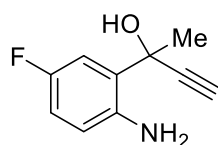
Substrates **3.1Eb**, **3.1Eh**, **3.1Ei**, **3.1Ej**, **3.2Eb** and **3.2Ed-3.2Eh** were prepared according to a literature procedure.²⁴ In an oven-dried Schleck flask conditioned under a nitrogen atmosphere was introduced the appropriate 1-(2-aminophenyl)ethanone compound (5.0 mmol, 1.0 equiv.) in anhydrous THF (40 mL). The solution was cooled down to 0 °C (ice/water) and ethynyl magnesium bromide (0.5 M in THF, 3.0 equiv, 30 mL) was added dropwise via a syringe. The reaction mixture was allowed to warm to room temperature and further stirred for 16 h. Then, the reaction mixture was quenched with saturated aqueous NH₄Cl. The organic phase was extracted with EtOAc (3 × 50 mL). All the organic fractions were combined, dried with anhydrous Na₂SO₄, filtered and concentrated. The crude products were purified by flash chromatography on silica gel (eluent: hexane/ EtOAc = 6/1 + 0.1% of Et₃N) to afford the corresponding 1-(2-aminophenyl) propargyl alcohols.

²⁴ Y. K. Kumar, G. R. Kumar, T. J. Reddy, B. Sridhar, M. S. Reddy, *Org. Lett.* **2015**, *17*, 2226–2229.

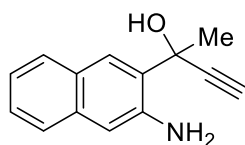
²⁵ W. Song, M. Li, Y. Zheng, *Org. Biomol. Chem.* **2019**, *17*, 2663–2669.

²⁶ M. R. Gannarapu, J. Zhou, N. Shibata, *iScience* **2020**, *23*, 100994.

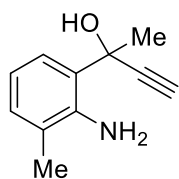
²⁷ J. Chaturvedi, C. Haldar, R. Bisht, G. Pandey, B. Chattopadhyay, *J. Am. Chem. Soc.* **2021**, *143*, 7604–7611.

2-(2-Amino-5-fluorophenyl)but-3-yn-2-ol (3.1Eb)

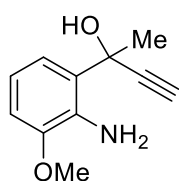
Brown solid (535.3 mg, 60% yield). Eluent hexanes/EtOAc = 6/1 + 0.1% of Et₃N. **¹H NMR** (400 MHz, CDCl₃) δ 7.23 – 7.20 (m, 1H), 6.86 – 6.81 (m, 1H), 6.65 – 6.62 (m, 1H), 4.23 (brs, 2H), 2.71 (s, 1H), 1.88 (s, 3 H); **¹³C NMR** (101 MHz, CDCl₃) δ 156.5 (d, *J* = 236.6 Hz), 140.1 (d, *J* = 2.3 Hz), 130.0 (d, *J* = 6.0 Hz), 119.36 (d, *J* = 7.6 Hz), 115.4 (d, *J* = 22.3 Hz), 113.2 (d, *J* = 24.5 Hz), 86.5, 73.5, 69.46 (d, *J* = 1.8 Hz), 28.3; **¹⁹F NMR** (376 MHz, CDCl₃) δ -125.38; **HRMS** (ESI/TOF) *m/z* Calcd for C₁₀H₁₁FNO [M + H]⁺ 180.0819; Found 180.0817.

2-(3-Aminonaphthalen-2-yl)but-3-yn-2-ol (3.1Eh)

Brown solid (707.5 mg, 67% yield). Eluent hexanes/EtOAc = 10/1 + 0.1% of Et₃N. **¹H NMR** (400 MHz, CDCl₃) δ 7.96 (s, 1H), 7.74 – 7.71 (m, 1H), 7.60 – 7.57 (m, 1H), 7.40 – 7.36 (m, 1H), 7.28 – 7.24 (m, 1H), 7.05 (s, 1H), 4.57 (brs, 2 H), 3.85 (brs, 1H), 2.77 (s, 1H), 2.03 (s, 3 H); **¹³C NMR** (101 MHz, CDCl₃) δ 142.4, 134.5, 131.0, 128.3, 128.0, 126.9, 125.7, 125.3, 123.3, 112.8, 87.1, 73.7, 70.0, 28.6; **HRMS** (ESI/TOF) *m/z* Calcd for C₁₄H₁₂N [M - OH]⁺ 194.0964; Found 194.0965.

2-(2-Amino-3-methylphenyl)but-3-yn-2-ol (3.1Ei)

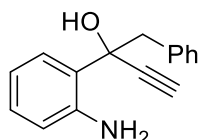
Yellow solid (498.7 mg, 57% yield). Eluent hexanes/EtOAc = 6/1 + 0.1% of Et₃N. **¹H NMR** (400 MHz, CDCl₃) δ 7.40 – 7.38 (m, 1H), 7.07 – 7.04 (m, 1H), 6.72 – 6.68 (m, 1H), 2.70 (s, 1H), 2.20 (s, 3H), 1.93 (s, 3 H); **¹³C NMR** (101 MHz, CDCl₃) δ 142.7, 130.6, 127.2, 124.5, 124.2, 118.0, 87.2, 73.3, 70.4, 28.7, 17.8; **HRMS** (ESI/TOF) *m/z* Calcd for C₁₁H₁₄NO [M + H]⁺ 176.1070; Found 176.1070.

2-(2-Amino-3-methoxyphenyl)but-3-yn-2-ol (3.1Ej)

Brown solid (573.2 mg, 60% yield). Eluent hexanes/EtOAc = 6/1 + 0.1% of Et₃N. **¹H NMR** (400 MHz, CDCl₃) δ 7.13 – 7.11 (m, 1H), 6.80 – 6.71 (m, 2H), 3.86 (s, 3H), 2.68 (s, 1H), 1.91 (s, 3 H); **¹³C NMR** (101 MHz, CDCl₃) δ 148.4,

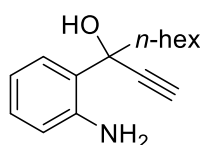
134.2, 128.4, 118.3, 117.8, 110.2, 87.1, 73.0, 69.9, 55.9, 28.4; **HRMS** (ESI/TOF) m/z Calcd for C₁₁H₁₄NO₂ [M + H]⁺ 192.1019; Found 192.1020.

2-(2-Aminophenyl)-1-phenylbut-3-yn-2-ol (3.2Eb)



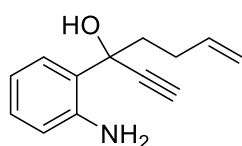
Obtained at 50 °C, yellow oil (579.5 mg, 49% yield). Eluent hexanes/EtOAc = 10/1 + 0.1% of Et₃N. **¹H NMR** (400 MHz, CDCl₃) δ 7.46 – 7.43 (m, 1H), 7.27 – 7.20 (m, 5H), 7.13 – 7.09 (m, 1H), 6.73 – 6.69 (m, 2H), 3.39 (dd, $J = 41.7, 13.2$ Hz, 2H), 2.75 (s, 1H); **¹³C NMR** (101 MHz, CDCl₃) δ 144.2, 135.8, 131.2, 129.3, 128.1, 128.0, 127.2, 126.1, 118.5, 118.1, 85.3, 76.6, 74.8, 45.9; **HRMS** (ESI/TOF) m/z Calcd for C₁₆H₁₄N [M – OH]⁺ 220.1121; Found 220.1126.

3-(2-Aminophenyl)non-1-yn-3-ol (3.2Ed)

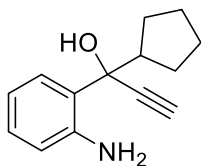


Brown oil (624.7 mg, 54% yield). Eluent hexanes/EtOAc = 6/1 + 0.1% of Et₃N. **¹H NMR** (400 MHz, CDCl₃) δ 7.54 – 7.51 (m, 1H), 7.12 – 7.08 (m, 1H), 6.76 – 6.72 (m, 1H), 6.66 – 6.64 (m, 1H), 2.75 (s, 1H), 2.14 – 2.09 (m, 2H), 1.59 – 1.49 (m, 1 H), 1.39 – 1.27 (m, 7 H), 0.88 – 0.85 (m, 3 H); **¹³C NMR** (101 MHz, CDCl₃) δ 144.6, 129.1, 127.7, 126.7, 118.1, 117.9, 86.1, 74.9, 74.8, 39.7, 31.9, 29.4, 24.9, 22.7, 14.2; **HRMS** (ESI/TOF) m/z Calcd for C₁₅H₂₀N [M – OH]⁺ 214.1590; Found 214.1597.

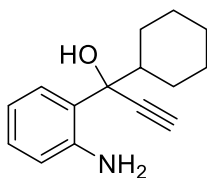
3-(2-Aminophenyl)hept-6-en-1-yn-3-ol (3.2Ee)



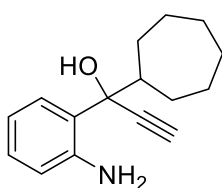
Brown oil (351.6 mg, 35% yield). Eluent hexanes/EtOAc = 6/1 + 0.1% of Et₃N. **¹H NMR** (400 MHz, CDCl₃) δ 7.54 – 7.52 (m, 1H), 7.13 – 7.09 (m, 1H), 6.77 – 6.73 (m, 1H), 6.67 – 6.65 (m, 1H), 5.90 – 5.80 (m, 1H), 5.08 – 4.94 (m, 2 H), 2.78 (s, 1H), 2.40 – 2.32 (m, 1 H), 2.25 – 2.13 (m, 3 H); **¹³C NMR** (101 MHz, CDCl₃) δ 144.5, 138.2, 129.2, 127.7, 126.5, 118.3, 118.0, 114.9, 85.7, 75.4, 74.6, 38.8, 29.4; **HRMS** (ESI/TOF) m/z Calcd for C₁₃H₁₆NO [M + H]⁺ 202.1226; Found 202.1225.

1-(2-Aminophenyl)-1-cyclopentylprop-2-yn-1-ol (3.2Ef)

Obtained at 50 °C, yellow oil (516.3 mg, 48% yield). Eluent hexanes/EtOAc = 6/1 + 0.1% of Et₃N. **¹H NMR** (400 MHz, CDCl₃) δ 7.56 – 7.55 (m, 1H), 7.10 – 7.07 (m, 1H), 6.73 – 6.70 (m, 1H), 6.64 – 6.61 (m, 1H), 4.52 (brs, 2 H), 2.99 – 2.93 (m, 2H), 2.72 (s, 1H), 1.88 – 1.76 (m, 2 H), 1.74 – 1.69 (m, 1 H), 1.66 – 1.56 (m, 2 H), 1.52 – 1.47 (m, 1 H), 1.43 – 1.34 (m, 2 H); **¹³C NMR** (101 MHz, CDCl₃) δ 144.7, 128.9, 128.4, 126.6, 117.79, 117.76, 84.8, 78.8, 75.7, 46.1, 29.5, 28.2, 26.2, 25.9; **HRMS** (ESI/TOF) *m/z* Calcd for C₁₄H₁₈NO [M + H]⁺ 216.1383; Found 216.1380.

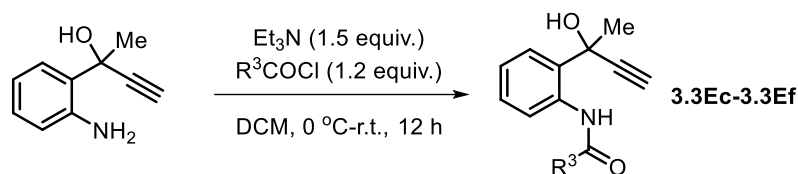
1-(2-Aminophenyl)-1-cyclohexylprop-2-yn-1-ol (3.2Eg)

Obtained at 50 °C, yellow solid (583.2 mg, 51% yield). Eluent hexanes/EtOAc = 6/1 + 0.1% of Et₃N. **¹H NMR** (400 MHz, CDCl₃) δ 7.55 – 7.52 (m, 1H), 7.11 – 7.07 (m, 1H), 6.73 – 6.69 (m, 1H), 6.64 – 6.61 (m, 1H), 2.77 (s, 1H), 2.31 – 2.25 (m, 1H), 2.07 – 2.03 (m, 1 H), 1.84 – 1.80 (m, 1 H), 1.68 – 1.63 (m, 2 H), 1.41 – 1.25 (m, 3 H), 1.21 – 1.11 (m, 3 H); **¹³C NMR** (101 MHz, CDCl₃) δ 144.7, 129.4, 128.9, 125.5, 117.8, 117.5, 84.8, 79.2, 76.2, 43.6, 28.8, 27.2, 26.4, 26.3, 26.2; **HRMS** (ESI/TOF) *m/z* Calcd for C₁₅H₁₉NNaO [M + Na]⁺ 252.1359; Found 252.1357.

1-(2-Aminophenyl)-1-cycloheptylprop-2-yn-1-ol (3.2Eh)

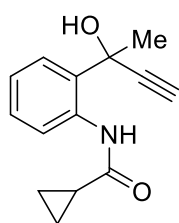
Obtained at 50 °C, brown oil (461.5 mg, 38% yield). Eluent hexanes/EtOAc = 6/1 + 0.1% of Et₃N. **¹H NMR** (400 MHz, CDCl₃) δ 7.57 – 7.56 (m, 1H), 7.10 – 7.07 (m, 1H), 6.73 – 6.70 (m, 1H), 6.63 – 6.61 (m, 1H), 4.47 (brs, 2 H), 2.76 (brs, 1H), 2.73 (s, 1H), 2.53 – 2.48 (m, 1 H), 2.13 – 2.07 (m, 1 H), 1.84 – 1.78 (m, 1 H), 1.60 – 1.54 (m, 3 H), 1.53 – 1.45 (m, 4 H), 1.39 – 1.30 (m, 3 H); **¹³C NMR** (101 MHz, CDCl₃) δ 144.7, 129.4, 128.9, 126.0, 117.8, 117.5, 85.0, 79.3, 75.9, 44.8, 30.6, 28.6, 28.4, 28.0, 27.3, 27.0; **HRMS** (ESI/TOF) *m/z* Calcd for C₁₆H₂₀N [M – OH]⁺ 226.1590; Found 226.1592.

General Procedure B for synthesis of 1-(2-aminophenyl) propargyl alcohols:



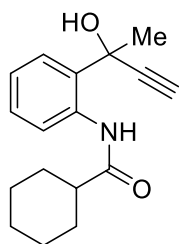
Substrates **3.3Ec-3.3Ef** were prepared according to a literature procedure.²⁷ In a 50 mL round-bottom flask, the respective 1-(2-aminophenyl) propargyl alcohol (5.0 mmol, 1.0 equiv), 20 mL dry DCM and dry Et₃N (7.5 mmol, 1.5 equiv) were added. The reaction mixture was cooled down to 0 °C and stirred for 15 minutes. Then, R³COCl (6.0 mmol, 1.2 equiv) was added slowly to the reaction mixture and stirred at room temperature overnight (typically 16-18 h). When the starting material was consumed (judged by TLC), the resulting reaction mixture was extracted with DCM (3 × 30 mL). All the organic fractions were combined, dried with anhydrous Na₂SO₄, filtered and concentrated. The crude product were purified by flash chromatography on silica gel (eluent: hexane/EtOAc = 10/1) to afford the corresponding propargylic alcohol.

N-(2-(2-hydroxybut-3-yn-2-yl)phenyl)cyclopropanecarboxamide (3.3Ec)



Brown solid (617.3 mg, 54% yield). Eluent hexanes/EtOAc = 10/1. **¹H NMR** [400 MHz, (CD₃)₂CO] δ 9.96 (brs, 1H), 8.26 – 8.24 (m, 1H), 7.68 – 7.65 (m, 1H), 7.28 – 7.24 (m, 1H), 7.07 – 7.03 (m, 1H), 6.02 (s, 1H), 3.28 (s, 1H), 1.88 (s, 3 H), 1.65 – 1.58 (m, 1H), 0.93 – 0.89 (m, 2H), 0.83 – 0.79 (m, 2H); **¹³C NMR** [101 MHz, (CD₃)₂CO] δ 171.7, 138.2, 129.0, 127.1, 123.7, 123.3, 87.4, 75.1, 71.1, 31.1, 16.5, 7.6, 7.5; **HRMS** (ESI/TOF) *m/z* Calcd for C₁₄H₁₅NNaO₂ [M + Na]⁺ 252.0995; Found 252.0995.

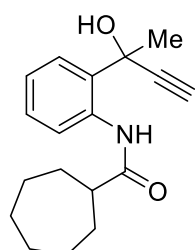
N-(2-(2-hydroxybut-3-yn-2-yl)phenyl)cyclohexanecarboxamide (3.3Ed)



White solid (772.3 mg, 57% yield). Eluent hexanes/EtOAc = 10/1. **¹H NMR** [400 MHz, (CD₃)₂CO] δ 9.79 (brs, 1H), 8.32 – 8.30 (m, 1H), 7.66 – 7.63 (m, 1H), 7.29 – 7.25 (m, 1H), 7.06 – 7.02 (m, 1H), 6.01 (s, 1H), 3.27 (s, 1H), 2.30 – 2.23 (m, 1H), 2.01 – 1.95 (m, 2H), 1.87 (s, 3 H), 1.82 – 1.77 (m, 2H), 1.71 – 1.65 (m, 1H), 1.56 – 1.46 (m, 2H), 1.41 – 1.19 (m, 3H); **¹³C NMR** [101 MHz,

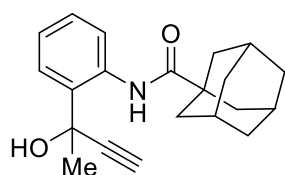
(CD₃)₂CO] δ 173.8, 138.3, 132.6, 129.0, 127.0, 123.6, 123.1, 87.4, 75.0, 71.0, 47.5, 31.0, 30.4, 30.3, 26.6, 26.4; **HRMS** (ESI/TOF) m/z Calcd for C₁₇H₂₁NNaO₂ [M + Na]⁺ 294.1465; Found 294.1461.

N-(2-(2-hydroxybut-3-yn-2-yl)phenyl)cycloheptanecarboxamide (3.3Ee)



Brown solid (783.3 mg, 55% yield). Eluent hexanes/EtOAc = 10/1. **¹H NMR** (400 MHz, CDCl₃) δ 9.44 (brs, 1H), 8.17 – 8.14 (m, 1H), 7.63 – 7.60 (m, 1H), 7.28 – 7.24 (m, 1H), 7.06 – 7.02 (m, 1H), 4.10 (brs, 1H), 2.71 (s, 1H), 2.39 – 2.32 (m, 1H), 1.99 – 1.93 (m, 2H), 1.86 (s, 3 H), 1.79 – 1.65 (m, 4H), 1.60 – 1.43 (m, 6H); **¹³C NMR** (101 MHz, CDCl₃) δ 175.7, 136.6, 131.4, 128.9, 126.4, 123.6, 123.2, 86.2, 74.3, 71.1, 49.1, 31.64, 31.61, 30.5, 28.3, 28.2, 26.69, 26.66; **HRMS** (ESI/TOF) m/z Calcd for C₁₈H₂₃NNaO₂ [M + Na]⁺ 308.1621; Found 308.1621.

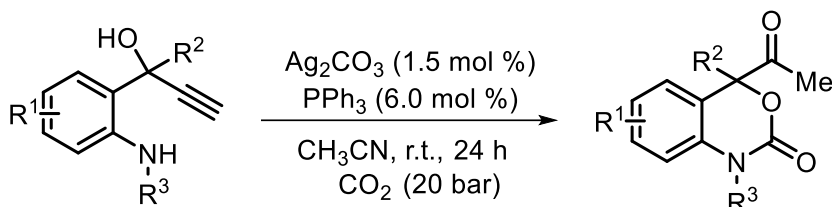
(3r,5r,7r)-N-(2-(2-hydroxybut-3-yn-2-yl)phenyl)adamantane-1-carboxamide (3.3Ef)



Yellow solid (904.5 mg, 56% yield). Eluent hexanes/EtOAc = 10/1. **¹H NMR** (400 MHz, CDCl₃) δ 9.54 (brs, 1H), 8.24 – 8.21 (m, 1H), 7.64 – 7.62 (m, 1H), 7.30 – 7.26 (m, 1H), 7.06 – 7.02 (m, 1H), 3.61 (brs, 1 H), 2.73 (s, 1H), 2.07 – 2.04 (m, 3H), 1.94 – 1.93 (m, 6H), 1.88 (s, 3H), 1.77 – 1.68 (m, 6H); **¹³C NMR** (101 MHz, CDCl₃) δ 176.5, 136.7, 131.4, 129.0, 126.4, 123.6, 123.5, 86.1, 74.5, 71.3, 41.8, 39.3, 36.6, 30.3, 28.3; **HRMS** (ESI/TOF) m/z Calcd for C₂₁H₂₅NNaO₂ [M + Na]⁺ 346.1778; Found 346.1779.

3.5.5 Procedures and characterization data for the cyclic carbamate products

General Procedure C for the synthesis of the cyclic carbamates:

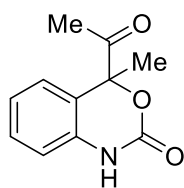


In a stainless-steel HEL-multireactor, the respective 1-(2-aminophenyl) propargylic alcohols **E** (0.20 mmol, 1.0 equiv.), Ag₂CO₃ (0.0030 mmol, 1.5 mol%), PPh₃ (0.012 mmol, 6.0 mol%) were dissolved in MeCN (0.30 mL). The reactor was purged three times with CO₂ (20 bar) and then charged with CO₂ (20 bar). The reaction mixture was stirred at room temperature for 24 h. The mixture was then transferred to a round-bottom flask, concentrated and purified by flash column chromatography on silica to afford the corresponding carbamate products. **Note:** *only the characteristic carbonyl/carbonate IR frequencies are provided in the analytical data descriptions.*

NB: The 5-membered cyclic carbonate **3.H** was also formed according to the **General Procedure C** at 50 °C.

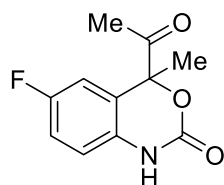
Scale-up reaction: In a 30 mL stainless steel reactor, the propargylic alcohol **3.1Ea** (3.0 mmol, 1.0 equiv) was dissolved in MeCN (4.5 mL), Ag₂CO₃ (0.045 mmol, 1.5 mol %) and PPh₃ (0.18 mmol, 6.0 mol%) were added. Three cycles of pressurization and depressurization of the reactor with 20 bar of CO₂ were carried out before finally stabilizing at 20 bar. The reaction mixture was stirred at room temperature for 24 h. Then the mixture was transferred to a round-bottom flask, concentrated and purified by flash column chromatography on silica to afford the corresponding cyclic carbonate product **3.1a** with a 67% isolated yield.

4-Acetyl-4-methyl-1,4-dihydro-2H-benzo[d][1,3]oxazin-2-one (3.1a)



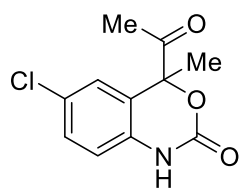
White solid (34.8 mg, 84% yield). Eluent hexanes/EtOAc = 5/1. ¹H NMR (400 MHz, CDCl₃) δ 9.37 (brs, 1H), 7.31 – 7.27 (m, 1H), 7.20 – 7.18 (m, 1H), 7.11 – 7.07 (m, 1H), 6.93 – 6.90 (m, 1H), 2.28 (s, 3H), 1.85 (s, 3H); ¹³C NMR (101 MHz, CDCl₃) δ 203.8, 152.0, 134.5, 130.3, 124.8, 124.1, 119.7, 115.1, 89.0, 25.1, 23.4; IR (neat, C=O, cm⁻¹): ν = 1712; HRMS (ESI/TOF) *m/z* Calcd for C₁₁H₁₂NO₃ [M + H]⁺ 206.0812; Found 206.0811. This compound was further characterized by X-ray crystallography.

4-Acetyl-6-fluoro-4-methyl-1,4-dihydro-2H-benzo[d][1,3]oxazin-2-one (3.1b)



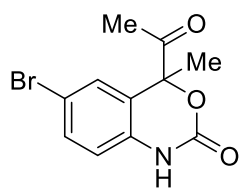
Brown solid (20.0 mg, 45% yield). Eluent hexanes/EtOAc = 5/1. ¹H NMR [400 MHz, (CD₃)₂CO] δ 9.28 (brs, 1H), 7.26 – 7.24 (m, 1H), 7.16 – 7.12 (m, 1H), 7.04 – 7.01 (m, 1H), 2.23 (s, 3H), 1.86 (s, 3H); ¹³C NMR [101 MHz, (CD₃)₂CO] δ 203.8, 159.5 (d, *J* = 240.0 Hz), 150.5, 133.3 (d, *J* = 2.4 Hz), 123.0 (d, *J* = 7.4 Hz), 117.4 (d, *J* = 23.1 Hz), 116.6 (d, *J* = 8.2 Hz), 113.1 (d, *J* = 25.3 Hz), 88.1 (d, *J* = 1.8 Hz), 24.6, 22.6; ¹⁹F NMR [376 MHz, (CD₃)₂CO] δ -121.42; IR (neat, C=O, cm⁻¹): ν = 1715; HRMS (ESI/TOF) *m/z* Calcd for C₁₁H₁₁FNO₃ [M + H]⁺ 224.0717; Found 224.0717.

4-Acetyl-6-chloro-4-methyl-1,4-dihydro-2H-benzo[d][1,3]oxazin-2-one (3.1c)



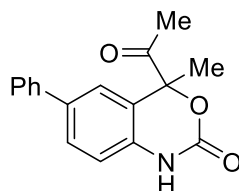
White solid (27.7 mg, 58% yield). Eluent hexanes/EtOAc = 5/1. ¹H NMR [400 MHz, (CD₃)₂CO] δ 9.36 (brs, 1H), 7.46 (d, *J* = 2.3 Hz, 1H), 7.36 (dd, *J* = 8.5, 2.3 Hz, 1H), 7.02 (d, *J* = 8.5 Hz, 1H), 2.24 (s, 3H), 1.88 (s, 3H); ¹³C NMR [101 MHz, (CD₃)₂CO] δ 203.8, 150.3, 135.9, 130.7, 128.4, 126.0, 123.2, 116.8, 88.2, 24.6, 22.6; IR (neat, C=O, cm⁻¹): ν = 1724; HRMS (ESI/TOF) *m/z* Calcd for C₁₁H₁₀ClNNaO₃ [M + Na]⁺ 262.0241; Found 262.0246. Elemental analysis (duplicate): Calcd. for C₁₁H₁₀ClNO₃: C 55.13, H 4.21, N 5.84; Found: C 54.73/54.93, H 3.80/3.76, N 5.89/6.13.

4-Acetyl-6-bromo-4-methyl-1,4-dihydro-2H-benzo[d][1,3]oxazin-2-one (3.1d)



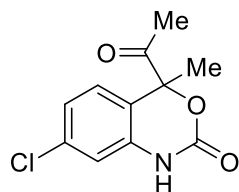
White solid (39.3 mg, 69% yield). Eluent hexanes/EtOAc = 5/1. ¹H NMR [400 MHz, (CD₃)₂CO] δ 9.37 (brs, 1H), 7.59 – 7.58 (m, 1H), 7.51 – 7.48 (m, 1H), 6.98 – 6.96 (m, 1H), 2.24 (s, 3H), 1.88 (s, 3H); ¹³C NMR [101 MHz, (CD₃)₂CO] δ 203.8, 150.2, 136.3, 133.7, 128.8, 123.5, 117.2, 115.6, 88.1, 24.6, 22.6; IR (neat, C=O, cm⁻¹): ν = 1720; HRMS (ESI/TOF) *m/z* Calcd for C₁₁H₁₀BrNNaO₃ [M + Na]⁺ 305.9736; Found 305.9737.

4-Acetyl-4-methyl-6-phenyl-1,4-dihydro-2H-benzo[d][1,3]oxazin-2-one (3.1e)



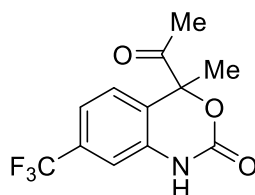
Obtained at 60 °C, yellow solid (38.6 mg, 68% yield; 59% yield, at 50 °C). Eluent hexanes/EtOAc = 5/1. ¹H NMR [400 MHz, (CD₃)₂CO] δ 9.32 (brs, 1H), 7.69 – 7.63 (m, 4H), 7.48 – 7.43 (m, 2H), 7.37 – 7.33 (m, 1H), 7.10 (d, *J* = 8.7 Hz, 1H), 2.25 (s, 3H), 1.95 (s, 3H); ¹³C NMR [101 MHz, (CD₃)₂CO] δ 203.9, 150.5, 140.9, 137.0, 136.3, 129.8, 129.4, 128.1, 127.5, 124.4, 121.8, 115.7, 88.7, 24.6, 22.7; IR (neat, C=O, cm⁻¹): ν = 1737, 1721; HRMS (ESI/TOF) *m/z* Calcd for C₁₇H₁₅NNaO₃ [M + Na]⁺ 304.0944; Found 304.0953.

4-Acetyl-7-chloro-4-methyl-1,4-dihydro-2H-benzo[d][1,3]oxazin-2-one (3.1f)



Obtained at 50 °C, brown solid (29.3 mg, 63% yield; 30% yield at room temperature). Eluent hexanes/EtOAc = 5/1. ¹H NMR (400 MHz, CDCl₃) δ 9.66 (brs, 1H), 7.15 – 7.13 (m, 1H), 7.07 – 7.05 (m, 1H), 6.96 – 6.95 (m, 1H), 2.28 (s, 3H), 1.84 (s, 3H); ¹³C NMR (101 MHz, CDCl₃) δ 203.5, 152.0, 136.2, 135.6, 126.1, 124.2, 118.2, 115.3, 88.7, 25.0, 23.4; IR (neat, C=O, cm⁻¹): ν = 1717; HRMS (ESI/TOF) *m/z* Calcd for C₁₁H₁₀ClNNaO₃ [M + Na]⁺ 262.0241; Found 262.0233.

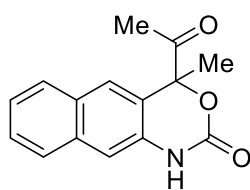
4-Acetyl-4-methyl-7-(trifluoromethyl)-1,4-dihydro-2H-benzo[d][1,3]oxazin-2-one (3.1g)



Obtained at 50 °C, white solid (33.3 mg, 60% yield). Eluent hexanes/EtOAc = 5/1. ¹H NMR (400 MHz, CDCl₃) δ 9.85 (brs, 1H), 7.36 – 7.35 (m, 2H), 7.18 (s, 1H), 2.31 (s, 3H), 1.89 (s, 3H); ¹³C NMR (101

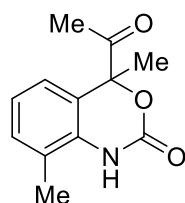
MHz, CDCl₃) δ 203.3, 151.8, 135.1, 132.8 (q, $J = 33.2$ Hz), 125.7, 123.35 (q, $J = 272.5$ Hz), 123.31, 120.8 (q, $J = 3.8$ Hz), 112.2 (q, $J = 3.9$ Hz), 88.8, 25.1, 23.4; **¹⁹F NMR** (376 MHz, CDCl₃) δ -63.14; **IR** (neat, C=O, cm⁻¹): $\nu = 1723$; **HRMS** (ESI/TOF) m/z Calcd for C₁₂H₁₀F₃NNaO₃ [M + Na]⁺ 296.0505; Found 296.0510. Elemental analysis (duplicate): Calcd. for C₁₂H₁₀F₃NO₃: C 52.75, H 3.69, N 5.13; Found: C 52.77/53.13, H 3.44/3.50, N 5.03/5.16.

4-Acetyl-4-methyl-1,4-dihydro-2H-naphtho[2,3-d][1,3]oxazin-2-one (3.1h)



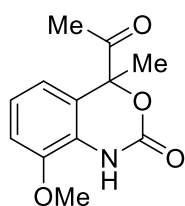
White solid (32.1 mg, 63% yield). Eluent hexanes/EtOAc = 5/1. **¹H NMR** [400 MHz, (CD₃)₂CO] δ 8.02 (s, 1H), 7.94 – 7.91 (m, 1H), 7.80 – 7.78 (m, 1H), 7.52 – 7.48 (m, 1H), 7.44 – 7.39 (m, 2H), 2.24 (s, 3H), 1.98 (s, 3H); **¹³C NMR** [101 MHz, (CD₃)₂CO] δ 203.9, 150.8, 135.1, 134.7, 130.9, 129.2, 128.3, 127.5, 126.1, 125.7, 122.8, 110.5, 88.6, 24.4, 22.9; **IR** (neat, C=O, cm⁻¹): $\nu = 1719$; **HRMS** (ESI/TOF) m/z Calcd for C₁₅H₁₄NO₃ [M + H]⁺ 256.0968; Found 256.0966.

4-Acetyl-4,8-dimethyl-1,4-dihydro-2H-benzo[d][1,3]oxazin-2-one (3.1i)

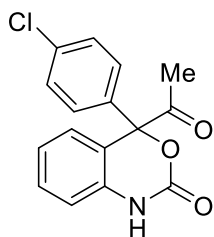


White solid (22.5 mg, 51% yield). Eluent hexanes/EtOAc = 5/1. **¹H NMR** (400 MHz, CDCl₃) δ 8.33 (brs, 1H), 7.16 – 7.14 (m, 1H), 7.05 – 6.98 (m, 2H), 2.31 (s, 3H), 2.26 (s, 3H), 1.84 (s, 3H); **¹³C NMR** (101 MHz, CDCl₃) δ 203.8, 151.4, 133.0, 131.6, 123.6, 123.3, 122.5, 119.8, 88.7, 25.0, 23.2, 16.8; **IR** (neat, C=O, cm⁻¹): $\nu = 1726, 1715$; **HRMS** (ESI/TOF) m/z Calcd for C₁₂H₁₄NO₃ [M + H]⁺ 220.0968; Found 220.0969. Elemental analysis (duplicate): Calcd. for C₁₂H₁₃NO₃: C 65.74, H 5.98, N 6.39; Found: C 65.92/66.15, H 5.77/5.86, N 6.42/6.51.

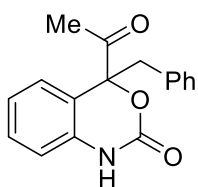
4-Acetyl-8-methoxy-4-methyl-1,4-dihydro-2H-benzo[d][1,3]oxazin-2-one (3.1j)



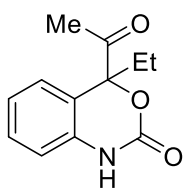
Brown solid (36.2 mg, 76% yield). Eluent hexanes/EtOAc = 5/1. **¹H NMR** (400 MHz, CDCl₃) δ 7.53 (brs, 1H), 7.04 – 7.00 (m, 1H), 6.86 – 6.76 (m, 1H), 6.78 – 6.76 (m, 1H), 3.88 (s, 3H), 2.26 (s, 3H), 1.80 (s, 3H); **¹³C NMR** (101 MHz, CDCl₃) δ 204.0, 149.8, 145.4, 124.0, 123.7, 120.2, 116.4, 111.1, 88.9, 56.1, 25.2, 23.4; **IR** (neat, C=O, cm⁻¹): $\nu = 1736, 1715$; **HRMS** (ESI/TOF) m/z Calcd for C₁₂H₁₄NO₄ [M + H]⁺ 236.0917; Found 236.0927.

4-Acetyl-4-(4-chlorophenyl)-1,4-dihydro-2H-benzo[d][1,3]oxazin-2-one (3.2a)

White solid (23.2 mg, 40% yield). Eluent hexanes/EtOAc = 5/1. **¹H NMR** (400 MHz, CDCl₃) δ 9.07 (brs, 1H), 7.39 – 7.31 (m, 3H), 7.23 – 7.19 (m, 3H), 7.16 – 7.12 (m, 1H), 6.96 – 6.94 (m, 1H), 2.45 (s, 3H); **¹³C NMR** (101 MHz, CDCl₃) δ 203.2, 151.7, 135.6, 135.5, 135.1, 130.6, 129.0, 128.5, 126.2, 123.9, 118.7, 115.5, 91.0, 26.8; **IR** (neat, C=O, cm⁻¹): ν = 1717; **HRMS** (ESI/TOF) *m/z* Calcd for C₁₆H₁₂ClNNaO₃ [M + Na]⁺ 324.0398; Found 324.0396. Elemental analysis (duplicate): Calcd. for C₁₆H₁₂ClNO₃: C 63.69, H 4.01, N 4.64; Found: C 63.54/63.45, H 4.24/4.36, N 4.53/4.60.

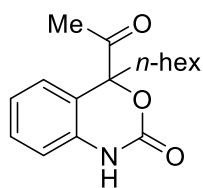
4-Acetyl-4-benzyl-1,4-dihydro-2H-benzo[d][1,3]oxazin-2-one (3.2b)

Obtained at 50 °C, white solid (21.3 mg, 39% yield; 19% yield at room temperature). Eluent hexanes/EtOAc = 5/1. **¹H NMR** (400 MHz, CDCl₃) δ 8.56 (s, 1H), 7.31 – 7.24 (m, 2H), 7.17 – 7.08 (m, 4H), 7.02 – 7.00 (m, 2H), 6.72 – 6.70 (m, 1H), 3.40 (dd, *J* = 18.3, 14.2 Hz, 2H), 2.26 (s, 3H); **¹³C NMR** (101 MHz, CDCl₃) δ 204.7, 150.5, 134.8, 133.7, 130.8, 130.2, 128.3, 127.4, 125.0, 123.9, 117.1, 114.9, 91.9, 44.4, 26.7; **IR** (neat, C=O, cm⁻¹): ν = 1714; **HRMS** (ESI/TOF) *m/z* Calcd for C₁₇H₁₅NNaO₃ [M + Na]⁺ 304.0944; Found 304.0943.

4-Acetyl-4-ethyl-1,4-dihydro-2H-benzo[d][1,3]oxazin-2-one (3.2c)

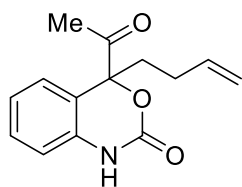
Brown solid (21.2 mg, 48% yield). Eluent hexanes/EtOAc = 5/1. **¹H NMR** (400 MHz, CDCl₃) δ 9.43 (brs, 1H), 7.29 – 7.25 (m, 1H), 7.20 – 7.19 (m, 1H), 7.10 – 7.06 (m, 1H), 6.92 – 6.90 (m, 1H), 2.27 – 2.22 (m, 5H), 1.00 (t, *J* = 7.3 Hz, 3H); **¹³C NMR** (101 MHz, CDCl₃) δ 204.2, 152.1, 135.0, 130.1, 125.1, 124.0, 117.9, 115.1, 92.4, 30.0, 25.8, 7.5; **IR** (neat, C=O, cm⁻¹): ν = 1715; **HRMS** (ESI/TOF) *m/z* Calcd for C₁₂H₁₄NO₃ [M + H]⁺ 220.0968; Found 220.0966.

4-Acetyl-4-hexyl-1,4-dihydro-2H-benzo[d][1,3]oxazin-2-one (3.2d)



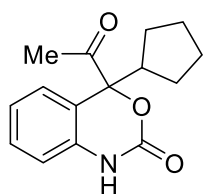
Yellow oil (31.2 mg, 56% yield). Eluent hexanes/EtOAc = 5/1. **¹H NMR** (400 MHz, CDCl₃) δ 7.29 – 7.24 (m, 1H), 7.21 – 7.18 (m, 1H), 7.09 – 7.05 (m, 1H), 6.92 – 6.90 (m, 1H), 2.27 (s, 3H), 2.20 – 2.16 (m, 2H), 1.45 – 1.23 (m, 8H), 0.85 (t, *J* = 6.9 Hz, 3H); **¹³C NMR** (101 MHz, CDCl₃) δ 204.2, 152.2, 134.9, 130.1, 125.1, 124.0, 118.1, 115.2, 92.1, 36.9, 31.6, 29.3, 25.8, 23.0, 22.6, 14.1; **IR** (neat, C=O, cm⁻¹): ν = 1712; **HRMS** (ESI/TOF) *m/z* Calcd for C₁₆H₂₂NO₃ [M + H]⁺ 276.1594; Found 276.1592.

4-Acetyl-4-(but-3-en-1-yl)-1,4-dihydro-2H-benzo[d][1,3]oxazin-2-one (3.2e)

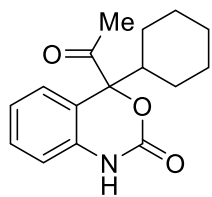


Brown solid (25.4 mg, 52% yield). Eluent hexanes/EtOAc = 5/1. **¹H NMR** (400 MHz, CDCl₃) δ 9.41 (s, 1H), 7.30 – 7.26 (m, 1H), 7.21 – 7.19 (m, 1H), 7.11 – 7.06 (m, 1H), 6.92 – 6.90 (m, 1H), 5.83 – 5.73 (m, 1H), 5.06 – 4.96 (m, 2H), 2.33 – 2.26 (m, 5H), 2.24 – 2.13 (m, 2H); **¹³C NMR** (101 MHz, CDCl₃) δ 204.0, 151.8, 136.9, 134.8, 130.3, 125.1, 124.1, 117.8, 115.8, 115.2, 91.7, 36.1, 27.4, 25.8; **IR** (neat, C=O, cm⁻¹): ν = 1719; **HRMS** (ESI/TOF) *m/z* Calcd for C₁₄H₁₅NNaO₃ [M + Na]⁺ 268.0944; Found 268.0945.

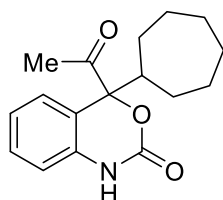
4-Acetyl-4-cyclopentyl-1,4-dihydro-2H-benzo[d][1,3]oxazin-2-one (3.2f)



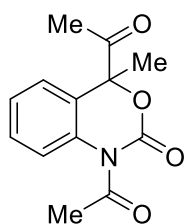
Obtained at 50 °C, white solid (22.2 mg, 44% yield). Eluent hexanes/EtOAc = 5/1. **¹H NMR** [400 MHz, (CD₃)₂CO] δ 9.15 (brs, 1H), 7.51 – 7.49 (m, 1H), 7.33 – 7.29 (m, 1H), 7.12 – 7.08 (m, 1H), 6.98 – 6.96 (m, 1H), 3.31 – 3.23 (m, 1H), 2.16 (s, 3H), 1.74 – 1.53 (m, 7H), 1.48 – 1.41 (m, 1H); **¹³C NMR** [101 MHz, (CD₃)₂CO] δ 203.5, 150.7, 137.6, 130.6, 126.7, 123.8, 119.6, 115.1, 93.0, 44.5, 27.6, 26.9, 26.43, 26.35, 25.2; **IR** (neat, C=O, cm⁻¹): ν = 1718; **HRMS** (ESI/TOF) *m/z* Calcd for C₁₅H₁₈NO₃ [M + H]⁺ 260.1281; Found 260.1272.

4-Acetyl-4-cyclohexyl-1,4-dihydro-2H-benzo[d][1,3]oxazin-2-one (3.2g)

Obtained at 50 °C, white solid (29.2 mg, 53% yield). Eluent hexanes/EtOAc = 5/1. **¹H NMR** [400 MHz, (CD₃)₂CO] δ 9.18 (brs, 1H), 7.44 – 7.42 (m, 1H), 7.32 – 7.28 (m, 1H), 7.12 – 7.08 (m, 1H), 6.98 – 6.96 (m, 1H), 2.63 – 2.55 (m, 1H), 2.17 (s, 3H), 1.82 – 1.66 (m, 3H), 1.58 – 1.47 (m, 3H), 1.40 – 1.28 (m, 2H), 1.23 – 1.13 (m, 2H); **¹³C NMR** [101 MHz, (CD₃)₂CO] δ 204.4, 150.3, 137.8, 130.5, 126.5, 123.8, 118.0, 115.3, 94.4, 44.0, 27.1, 26.87, 26.85, 26.84, 26.81, 25.7; **IR (neat, C=O, cm⁻¹):** ν = 1721; **HRMS (ESI/TOF) m/z** Calcd for C₁₆H₁₉NNaO₃ [M + Na]⁺ 296.1257; Found 296.1253.

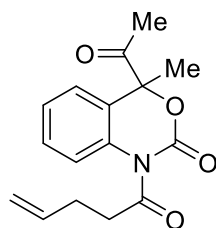
4-Acetyl-4-cycloheptyl-1,4-dihydro-2H-benzo[d][1,3]oxazin-2-one (3.2h)

Obtained at 60 °C, yellow solid (20.2 mg, 34% yield; 32% yield, at 50 °C). Eluent hexanes/EtOAc = 5/1. **¹H NMR** (400 MHz, CDCl₃) δ 7.27 – 7.22 (m, 2H), 7.09 – 7.05 (m, 1H), 6.90 – 6.87 (m, 1H), 2.65 – 2.59 (m, 1H), 2.24 (s, 3H), 1.78 – 1.66 (m, 3H), 1.61 – 1.46 (m, 7H), 1.44 – 1.34 (m, 2H); **¹³C NMR** (101 MHz, CDCl₃) δ 204.7, 152.0, 135.4, 130.0, 125.4, 124.0, 117.6, 115.1, 96.7, 45.4, 28.6, 28.2, 28.1, 27.9, 27.3, 27.2, 26.4; **IR (neat, C=O, cm⁻¹):** ν = 1720; **HRMS (ESI/TOF) m/z** Calcd for C₁₇H₂₂NO₃ [M + H]⁺ 288.1594; Found 288.1598.

1,1'-(4-Methyl-2-oxo-2H-benzo[d][1,3]oxazine-1,4(4H)-diyl)bis(ethan-1-one) (3.3a)

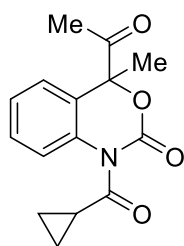
Yellow solid (25.9 mg, 53% yield). Eluent hexanes/EtOAc = 5/1. **¹H NMR** (400 MHz, CDCl₃) δ 7.76 – 7.73 (m, 1H), 7.47 – 7.43 (m, 2H), 7.37 – 7.33 (m, 1H), 2.65 (s, 3H), 2.10 (s, 3H), 1.94 (s, 3H); **¹³C NMR** (101 MHz, CDCl₃) δ 200.8, 170.3, 151.7, 133.9, 129.8, 127.6, 127.0, 124.8, 123.8, 87.5, 25.8, 23.9, 20.4; **IR (neat, C=O, cm⁻¹):** ν = 1754, 1718, 1703; **HRMS (ESI/TOF) m/z** Calcd for C₁₃H₁₄NO₄ [M + H]⁺ 248.0917; Found 248.0916.

4-Acetyl-4-methyl-1-(pent-4-enoyl)-1,4-dihydro-2H-benzo[d][1,3]oxazin-2-one (3.3b)



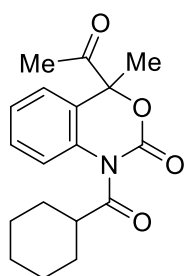
Yellow oil (30.7 mg, 53% yield). Eluent hexanes/EtOAc = 5/1. ¹H NMR (400 MHz, CDCl₃) δ 7.74 – 7.71 (m, 1H), 7.46 – 7.42 (m, 2H), 7.36 – 7.32 (m, 1H), 5.93 – 5.83 (m, 1H), 5.13 – 4.99 (m, 2H), 3.35 – 3.27 (m, 1H), 3.07 – 2.98 (m, 1H), 2.53 – 2.41 (m, 2H), 2.10 (s, 3H), 1.93 (s, 3H); ¹³C NMR (101 MHz, CDCl₃) δ 200.9, 172.7, 151.4, 137.0, 134.0, 129.7, 127.6, 126.9, 124.7, 123.8, 115.6, 87.5, 36.5, 28.7, 23.9, 20.4; **IR** (neat, C=O, cm⁻¹): ν = 1755, 1716; **HRMS** (ESI/TOF) *m/z* Calcd for C₁₆H₁₇NNaO₄ [M + Na]⁺ 310.1050; Found 310.1062.

4-Acetyl-1-(cyclopropanecarbonyl)-4-methyl-1,4-dihydro-2H-benzo[d][1,3]oxazin-2-one (3.3c)



Brown solid (30.0 mg, 56% yield). Eluent hexanes/EtOAc = 5/1. ¹H NMR (400 MHz, CDCl₃) δ 7.80 – 7.77 (m, 1H), 7.44 – 7.39 (m, 2H), 7.34 – 7.30 (m, 1H), 2.83 – 2.77 (m, 1H), 2.13 (s, 3H), 1.94 (s, 3H), 1.22 – 1.10 (m, 3H), 1.04 – 0.99 (m, 1H); ¹³C NMR (101 MHz, CDCl₃) δ 201.1, 174.8, 151.6, 134.4, 129.8, 127.0, 126.6, 123.9, 123.7, 87.6, 24.0, 20.7, 15.6, 11.7, 11.3; **IR** (neat, C=O, cm⁻¹): ν = 1718; **HRMS** (ESI/TOF) *m/z* Calcd for C₁₅H₁₅NNaO₄ [M + Na]⁺ 296.0893; Found 296.0904.

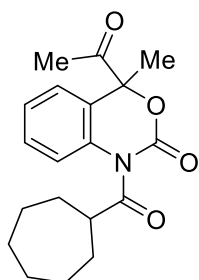
4-Acetyl-1-(cyclohexanecarbonyl)-4-methyl-1,4-dihydro-2H-benzo[d][1,3]oxazin-2-one (3.3d)



Obtained at 50 °C, 72 h reaction time, yellow solid (35.8 mg, 56% yield; 49% yield at 50 °C, 24 h). Eluent hexanes/EtOAc = 3/1. ¹H NMR (400 MHz, CDCl₃) δ 7.68 – 7.65 (m, 1H), 7.44 – 7.39 (m, 2H), 7.33 – 7.29 (m, 1H), 3.41 – 3.36 (m, 1H), 2.23 – 2.20 (m, 1H), 2.11 (s, 3H), 1.92 (s, 3H), 1.85 – 1.70 (m, 4H), 1.55 – 1.36 (m, 4H), 1.31 – 1.23 (m, 1H); ¹³C NMR (101 MHz, CDCl₃) δ 201.0, 177.4, 151.0, 134.4, 129.8, 127.2, 126.6, 123.9, 123.8, 87.5, 45.1, 30.2, 29.5, 25.9, 25.7, 25.6, 24.1, 20.7; **IR** (neat, C=O, cm⁻¹): ν = 1764, 1716, 1700; **HRMS** (ESI/TOF) *m/z* Calcd for C₁₈H₂₁NNaO₄ [M + Na]⁺ 338.1363; Found 338.1375.

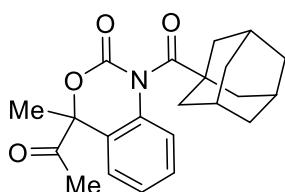
4-Acetyl-1-(cycloheptanecarbonyl)-4-methyl-1,4-dihydro-2H-benzo[d][1,3]oxazin-2-one

(3.3e)



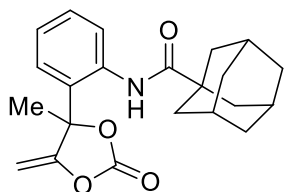
Obtained at 75 °C, 50 bar CO₂ pressure, white solid (55.8 mg, 84% yield; 42% yield at 75 °C, 20 bar CO₂ pressure). Eluent hexanes/EtOAc = 3/1. **¹H NMR** (400 MHz, CDCl₃) δ 7.68 – 7.66 (m, 1H), 7.44 – 7.39 (m, 2H), 7.33 – 7.29 (m, 1H), 3.55 – 3.48 (m, 1H), 2.24 – 2.18 (m, 1H), 2.11 (s, 3H), 1.92 (s, 3H), 1.86 – 1.75 (m, 3H), 1.71 – 1.54 (m, 8H); **¹³C NMR** (101 MHz, CDCl₃) δ 201.1, 178.5, 151.1, 134.5, 129.8, 127.1, 126.6, 123.9, 123.6, 87.4, 46.1, 32.0, 31.5, 28.31, 28.26, 26.8, 26.5, 24.1, 20.7; **IR** (neat, C=O, cm⁻¹): ν = 1757, 1715; **HRMS** (ESI/TOF) *m/z* Calcd for C₁₉H₂₃NNaO₄ [M + Na]⁺ 352.1519; Found 352.1523.

4-Acetyl-1-((3r,5r,7r)-adamantane-1-carbonyl)-4-methyl-1,4-dihydro-2H-benzo[d][1,3]oxazin-2-one (3.3f)



Obtained at 75 °C, colorless solid (45.4 mg, 62% yield). Eluent hexanes/EtOAc = 5/1. **¹H NMR** (400 MHz, CDCl₃) δ 7.32 – 7.25 (m, 2H), 7.18 – 7.14 (m, 1H), 6.72 – 6.70 (m, 1H), 2.27 (s, 3H), 2.06 – 1.98 (m, 8H), 1.89 (s, 3H), 1.78 – 1.67 (m, 7H); **¹³C NMR** (101 MHz, CDCl₃) δ 203.1, 183.3, 149.4, 134.9, 130.2, 125.1, 124.5, 121.1, 114.5, 87.9, 47.4, 38.6, 36.3, 27.9, 24.8, 22.7; **IR** (neat, C=O, cm⁻¹): ν = 1726; **HRMS** (ESI/TOF) *m/z* Calcd for C₂₂H₂₅NNaO₄ [M + Na]⁺ 390.1676; Found 390.1672.

(3r,5r,7r)-N-(2-(4-methyl-5-methylene-2-oxo-1,3-dioxolan-4-yl)phenyl)adamantane-1-carboxamide (3.H)



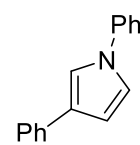
White solid (58.1 mg, 79% yield). Eluent hexanes/EtOAc = 5/1. **¹H NMR** (400 MHz, CDCl₃) δ 8.00 (brs, 1H), 7.90 – 7.88 (m, 1H), 7.53 – 7.51 (m, 1H), 7.43 – 7.38 (m, 1H), 7.17 – 7.13 (m, 1H), 5.20 (d, *J* = 4.1 Hz, 1H), 4.60 (d, *J* = 4.1 Hz, 1H), 2.12 – 2.09 (m, 3H), 1.99 – 1.98 (m, 6H), 1.95 (s, 3H), 1.80 – 1.72 (m, 6H); **¹³C NMR** (101 MHz, CDCl₃) δ 176.4, 155.3, 150.3, 136.4, 130.6, 128.8, 127.6, 125.5, 125.1, 91.3, 88.7, 41.7, 39.2, 36.5, 28.2, 26.5; **IR** (neat, C=O,

cm⁻¹): $\nu = 1824, 1811$; **HRMS** (ESI/TOF) m/z Calcd for C₂₂H₂₆NO₄ [M + H]⁺ 368.1856; Found 368.1852. This compound was further characterized by X-ray crystallography.

Note: This 5-membered cyclic carbonate (**3.H**) was the only product isolated while attempting the synthesis of cyclic carbamate **3.3f**.

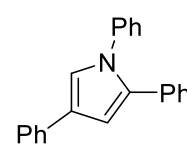
Analytical data for the non-targeted products

1,3-Diphenyl-1H-pyrrole (3.A)

 Yellow solid (52.9 mg, 98% yield, 0.3 mmol scale). Eluent hexanes/EtOAc = 100/1. **¹H NMR** (400 MHz, CDCl₃) δ 7.60 – 7.57 (m, 2H), 7.46 – 7.44 (m, 4H), 7.40 – 7.35 (m, 3H), 7.29 – 7.25 (m, 1H), 7.23 – 7.19 (m, 1H), 7.14 – 7.12 (m, 1H), 6.67 – 6.66 (m, 1H); **¹³C NMR** (101 MHz, CDCl₃) δ 140.7, 135.5, 129.8, 128.8, 127.1, 125.99, 125.95, 125.4, 120.52, 120.48, 116.0, 108.9.

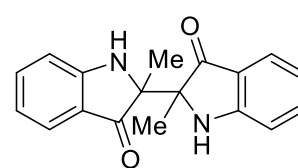
Note: product **3.A** was isolated using the conditions reported in Table 3.2, entry 2.²⁸

1,2,4-Triphenyl-1H-pyrrole (3.B)

 White solid (86.5 mg, 98% yield, 0.3 mmol scale). Eluent hexanes/EtOAc = 100/1. **¹H NMR** (400 MHz, CDCl₃) δ 7.62 – 7.60 (m, 2H), 7.40 – 7.29 (m, 5H), 7.26 – 7.19 (m, 9H), 6.76 (d, *J* = 2.0 Hz, 1H); **¹³C NMR** (101 MHz, CDCl₃) δ 140.5, 135.3, 134.9, 132.9, 129.2, 128.9, 128.5, 128.3, 126.9, 126.7, 126.0, 125.8, 125.7, 125.3, 121.0, 108.9.

Note: product **3.B** was isolated using the conditions reported in Table 3.3, entry 7.²⁹

2,2'-Dimethyl-[2,2'-biindoline]-3,3'-dione (3.D)

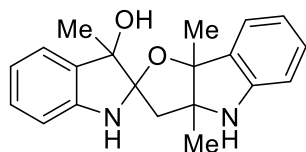
 Yellow solid (12.5 mg, 29% yield, 0.3 mmol scale). Eluent hexanes/EtOAc = 3/1. **¹H NMR** (400 MHz, CDCl₃) δ 7.62 – 7.59 (m, 2H), 7.51 – 7.47 (m, 2H), 6.95 – 6.92 (m, 2H), 6.82 – 6.78 (m, 2H), 6.07 (brs, 2H), 1.14 (s, 6H); **¹³C NMR** (101 MHz, CDCl₃) δ 204.3, 161.1, 138.3, 124.9, 120.0, 118.7, 112.4, 68.7, 18.4. This compound was further characterized by X-ray crystallography.

Note: product **3.D** was isolated using the conditions reported in Table 3.4, entry 7.³⁰

²⁸ A. Bunrit, S. Sawadjoon, S. Tšupova, P. J. R. Sjöberg, J. S. M. Samec, *J. Org. Chem.* **2016**, *81*, 1450–1460.

²⁹ B. B. Thompson, J. Montgomery, *Org. Lett.* **2011**, *13*, 3289–3291.

³⁰ X. Jiang, B. Zhu, C. Yu, *Org. Biomol. Chem.* **2019**, *17*, 2199–2203.

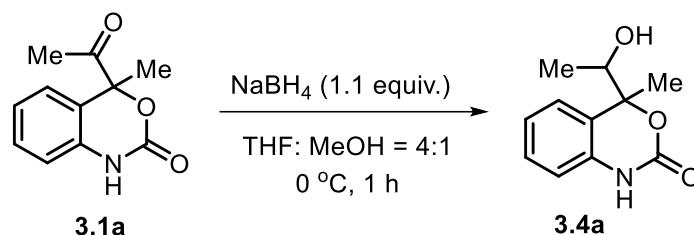
Coupling product from two molecules of 3-hydroxy-2,3-dimethylindolenine (3.F)

Yellow solid (39.4 mg, 82% yield, 0.3 mmol scale). Eluent hexanes/EtOAc = 3/1. ¹H NMR (400 MHz, CDCl₃) δ 7.24 – 7.15 (m, 3H), 6.99 – 6.94 (m, 1H), 6.78 – 6.71 (m, 3H), 6.40 – 6.38 (m, 1H), 5.02 (brs, 1H), 3.88 (brs, 1H), 3.22 (brs, 1H), 2.42 (dd, *J* = 15.1, 13.3 Hz, 2H), 1.52 (s, 3H), 1.41 (s, 3H), 1.33 (s, 3H); ¹³C NMR (101 MHz, CDCl₃) δ 149.0, 146.8, 134.2, 131.4, 130.0, 128.5, 124.4, 122.7, 119.5, 119.4, 110.5, 109.8, 105.9, 91.7, 78.7, 74.3, 42.2, 24.3, 22.0, 19.9. This compound was further characterized by X-ray crystallography.

Note: product **3.F** was isolated using the condition reported in Table 3.6, entry 11.³¹

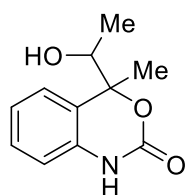
³¹ V. Dave, E. W. Warnhoff, *Canadian Journal of Chemistry*, **1971**, *49*(11), 1911–1920.

3.5.6 Experimental procedures for the product diversification

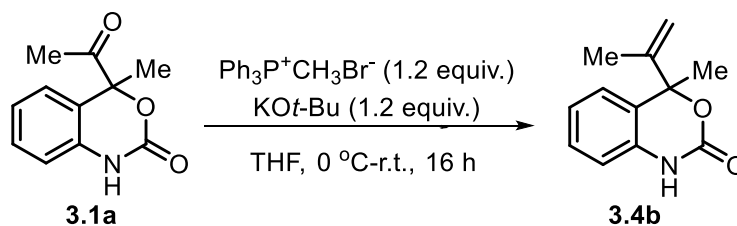


To a stirred solution of **3.1a** (0.20 mmol, 1.0 equiv) in a 4:1 mixture of tetrahydrofuran and methanol (1 mL) was added NaBH₄ (0.22 mmol, 1.1 equiv) under an argon atmosphere at 0 °C. Then the reaction mixture was stirred for 1 h. When the starting material had disappeared (judged by TLC), the solvent was removed by evaporation and the residue was quenched by addition of a saturated ammonium chloride (5 mL) solution. Ethyl acetate (5 mL) was added to it and the aqueous layer was separated. Further extraction was carried out of the aqueous layer with ethyl acetate (3 × 5 mL). The combined organic layer was dried over anhydrous Na₂SO₄, filtered, and concentrated in *vacuo*. The crude product was purified by flash chromatography on silica gel to obtain the corresponding product **3.4a**.

4-(1-Hydroxyethyl)-4-methyl-1,4-dihydro-2H-benzo[d][1,3]oxazin-2-one (3.4a)

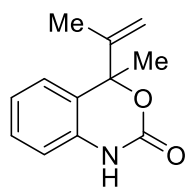


White solid (40.3 mg, 94% yield, 3:2 *dr*). Eluent hexanes/EtOAc = 5/1. ¹H NMR (400 MHz, CD₃OD) δ 7.28 – 7.17 (m, 2H), 7.06 – 7.03 (m, 1H), 6.86 – 6.82 (m, 1H), 3.98 – 3.91 (m, 1H), 1.67 (s, 1.8H), 1.65 (s, 1.2H), 1.17 (t, *J* = 6.6 Hz, 3H); ¹³C NMR (101 MHz, CD₃OD) δ 154.0, 153.8, 136.44, 136.37, 130.0, 129.9, 126.7, 126.4, 124.1, 123.9, 123.7, 115.2, 115.0, 88.72, 88.70, 74.0, 73.8, 24.1, 23.4, 17.5, 17.2; IR (neat, C=O, cm⁻¹): ν = 1682; HRMS (ESI/TOF) *m/z*. Calcd for C₁₁H₁₃NNaO₃ [M + Na]⁺ 230.0788; Found 230.0787.

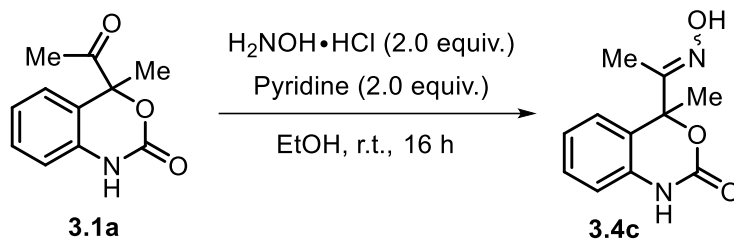


Methyl triphenylphosphonium bromide (0.24 mmol, 1.2 equiv) was dissolved in THF (0.40 mL) in a dried round bottom flask equipped with an ice water bath. Then $\text{KO}t\text{-Bu}$ (0.24 mmol, 1.2 equiv), the yellow suspension was stirred at 0 °C for 45 min. To this suspension was added a solution of the corresponding ketone **3.1a** (0.20 mmol, 1.0 equiv) in THF (0.3 mL) dropwise and the resulting mixture was stirred for 16 h at room temperature. The mixture was concentrated under reduced pressure and filtered. The solid was washed with ethyl acetate (3 × 5 mL) and the combined organic layer was concentrated in *vacuo*. The crude product was purified by flash chromatography on silica gel to obtain the corresponding product **3.4b**.

4-Methyl-4-(prop-1-en-2-yl)-1,4-dihydro-2H-benzo[d][1,3]oxazin-2-one (3.4b)

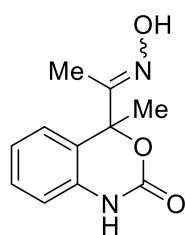


White solid (31.4 mg, 77% yield). Eluent hexanes/EtOAc = 6/1. ¹H NMR (400 MHz, CDCl₃) δ 8.66 (brs, 1H), 7.27 – 7.23 (m, 1H), 7.13 – 7.11 (m, 1H), 7.08 – 7.04 (m, 1H), 6.86 – 6.84 (m, 1H), 5.04 – 4.92 (m, 2H), 1.84 (s, 3H), 1.79 – 1.78 (m, 3H); ¹³C NMR (101 MHz, CDCl₃) δ 152.9, 145.4, 134.7, 129.3, 125.0, 124.1, 123.4, 114.7, 113.8, 86.7, 25.3, 18.8; IR (neat, C=O, cm⁻¹): ν = 1723; HRMS (ESI/TOF) *m/z* Calcd for C₁₂H₁₄NO₂ [M + H]⁺ 204.1019; Found 204.1010.



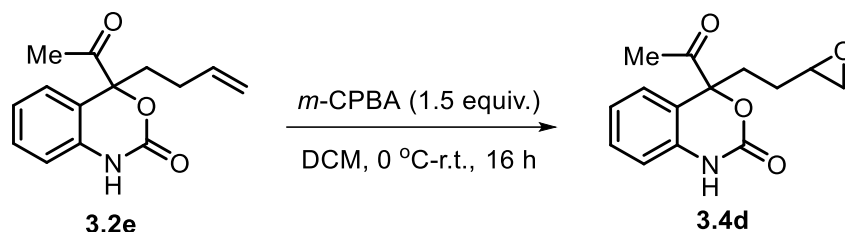
To a stirred solution of hydroxylamine hydrochloride (0.40 mmol, 2.0 equiv), pyridine (0.40 mmol, 2.0 equiv) in ethanol (2.0 mL) maintained at room temperature was added the compound **3.1a** (0.20 mmol, 1.0 equiv) dissolved in ethanol (2 mL). After the substrate was completely consumed (judged by TLC), the solvent was removed under reduced pressure. To the residue was added water and the product was extracted twice with methylene chloride (2×5 mL) and washed with a 0.10 M HCl solution. The organic layer was dried over anhydrous Na_2SO_4 , filtered and concentrated in *vacuo*. The crude product was purified by flash chromatography on silica gel to obtain the final product.

4-(1-Hydroxyprop-1-en-2-yl)-4-methyl-1,4-dihydro-2H-benzo[d][1,3]oxazin-2-one (3.4c)



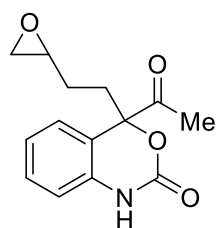
White solid (41.4 mg, 92% yield). Eluent hexanes/EtOAc = 6/1. ¹H NMR [400 MHz, (CD₃)₂CO] δ 10.29 (brs, 1H), 9.20 (brs, 1H), 7.31 – 7.26 (m, 1H), 7.11 – 6.99 (m, 3H), 1.83 (s, 3H), 1.76 (s, 3H); ¹³C NMR [101 MHz, (CD₃)₂CO] δ 156.3, 150.8, 136.6, 130.1, 125.4, 123.9, 123.6, 115.1, 86.0, 24.9, 10.3; IR (neat, C=O, cm⁻¹): ν = 1719; HRMS (ESI/TOF) *m/z* Calcd for C₁₁H₁₂N₂NaO₃

[M + Na]⁺ 243.0740; Found 243.0739.



To a solution of **3.2e** (0.20 mmol, 1.0 equiv) in DCM (3 mL) was added *m*-CPBA (0.30 mmol, 1.5 equiv) at 0 °C. The mixture was allowed to warm to room temperature and was stirred for an additional 16 h. The reaction mixture was washed with saturated Na₂CO₃ (3 × 5 mL). The combined organic layer was dried over anhydrous Na₂SO₄, filtered, and concentrated in *vacuo*. The crude product was purified by flash chromatography on silica gel to obtain the corresponding product.

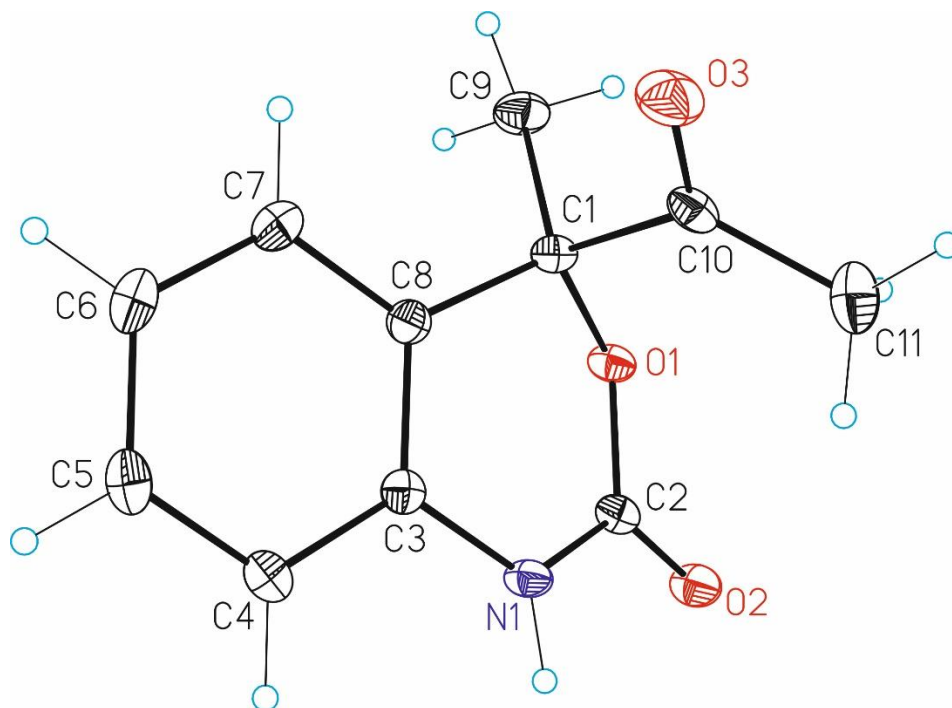
4-Acetyl-4-(2-(oxiran-2-yl)ethyl)-1,4-dihydro-2H-benzo[d][1,3]oxazin-2-one (3.4d)



White solid (36.4 mg, 68% yield, 1:1 *dr*). Eluent hexanes/EtOAc = 5/1. **¹H NMR** (400 MHz, CDCl₃) δ 7.29 – 7.26 (m, 1H), 7.20 – 7.17 (m, 1H), 7.10 – 7.06 (m, 1H), 6.91 – 6.89 (m, 1H), 2.95 – 2.92 (m, 1H), 2.76 – 2.72 (m, 1H), 2.47 – 2.28 (m, 3H), 2.27 (s, 1.5H), 2.26 (s, 1.5H), 1.87 – 1.71 (m, 1H), 1.60 – 1.49 (m, 1H); **¹³C NMR** (101 MHz, CDCl₃) δ 203.55, 203.51, 151.71, 151.68, 134.9, 130.4, 125.0, 124.9, 124.21, 124.17, 117.6, 117.4, 115.3, 91.39, 91.36, 51.69, 51.67, 47.3, 47.1, 32.8, 32.7, 26.5, 26.2, 25.6, 25.5; **IR** (neat, C=O, cm⁻¹): ν = 1714; **HRMS** (ESI/TOF) *m/z* Calcd for C₁₄H₁₅NNaO₄ [M + Na]⁺ 284.0893; Found 284.0893.

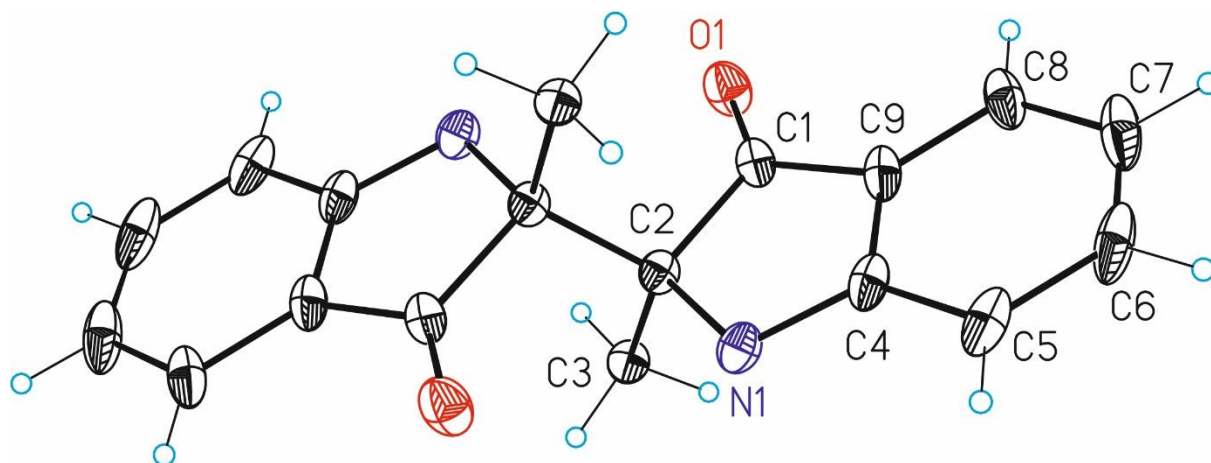
3.5.7 X-ray details

For the experimental procedure of the X-ray crystallographic analysis, please refer to Experimental Section of Chapter 2.



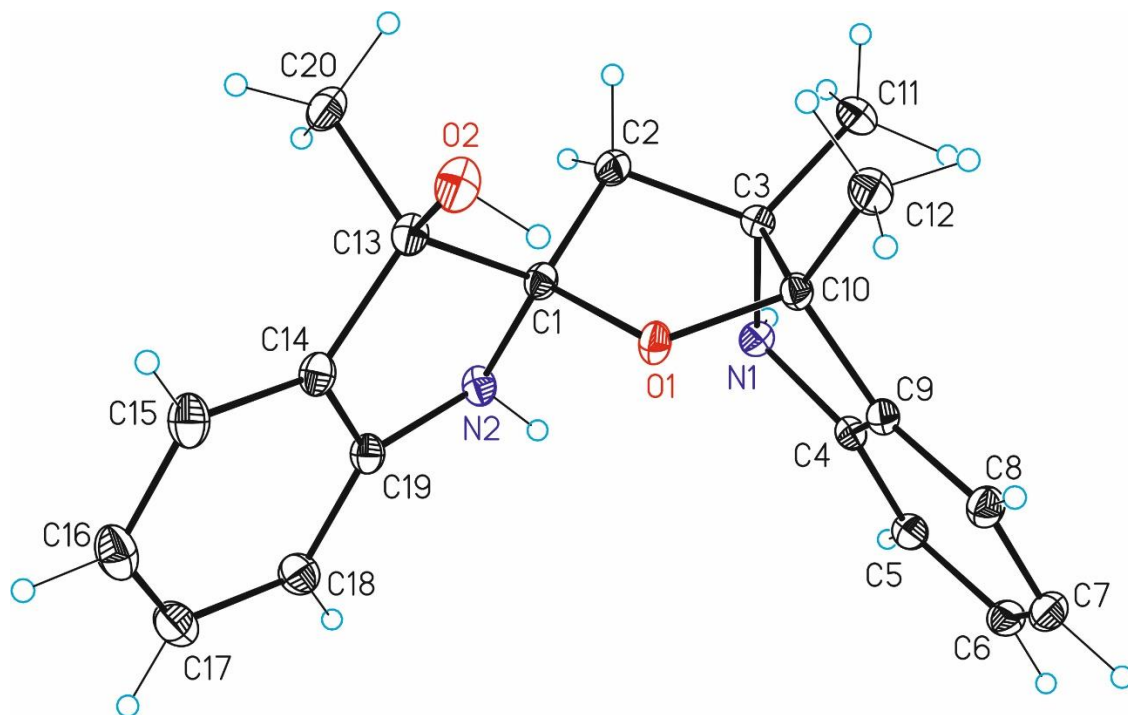
X-ray molecular structure for compound **3.1a**. CCDC-2208331

Crystallographic data for 3.1a: C₁₁H₁₁NO₃, *M_r* = 205.21, monoclinic, *C*2/*c*, *a* = 18.365(2) Å, *b* = 7.5643(9) Å, *c* = 14.0171(17) Å, α = 90°, β = 94.936(2)°, γ = 90°, *V* = 1940.0(4) Å³, *Z* = 8, ρ = 1.405 mg·M⁻³, μ = 0.103 mm⁻¹, λ = 0.71073 Å, *T* = 100(2) K, *F*(000) = 864, θ (min) = 2.226°, θ (max) = 31.013°, 11588 reflections collected, 3006 reflections unique (*R*_{int} = 0.0268), GoF = 1.038, *R*₁ = 0.0406, *wR*₂ = 0.1076 [*I* > 2σ(*I*)], *R*₁ = 0.0471, *wR*₂ = 0.1127 (all indices), min/max residual density = -0.477/0.490 [e·Å⁻³], Completeness to θ (31.013°) = 97.2 %.

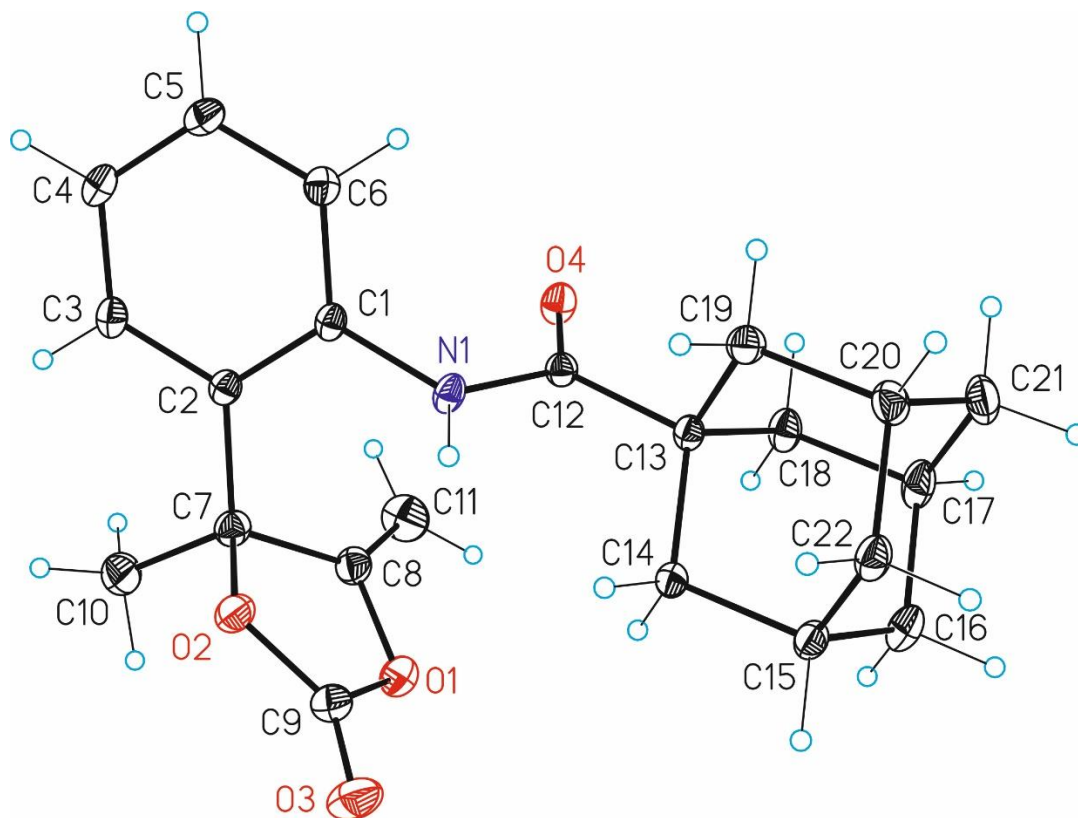


X-ray molecular structure for compound **3.D**. CCDC-2208330

Crystallographic data for 3.D: C₁₈H₁₄N₂O₂, *M*_r = 290.31, monoclinic, *P*2₁/*n*, *a* = 6.0854(5) Å, *b* = 20.0396(16) Å, *c* = 6.4992(6) Å, α = 90°, β = 116.085(2)°, γ = 90°, *V* = 711.84(11) Å³, *Z* = 2, ρ = 1.354 mg·M⁻³, μ = 0.090 mm⁻¹, λ = 0.71073 Å, *T* = 100(2) K, *F*(000) = 304, θ (min) = 2.032°, θ (max) = 29.994°, 12693 reflections collected, 2077 reflections unique (*R*_{int} = 0.0277), GoF = 1.073, *R*₁ = 0.0745, *wR*₂ = 0.1970 [*I* > 2σ(*I*)], *R*₁ = 0.0865, *wR*₂ = 0.2067 (all indices), min/max residual density = -0.329/0.951 [e·Å⁻³], Completeness to θ (29.994°) = 99.8 %.

X-ray molecular structure for compound **3.F**. CCDC-2208332

Crystallographic data for 3.F: C₂₀H₂₂N₂O₂, *Mr* = 322.39, monoclinic, *P*2₁/*c*, *a* = 10.04830(10) Å, *b* = 11.1949(2) Å, *c* = 15.1007(2) Å, α = 90°, β = 101.2810(10)°, γ = 90°, *V* = 1665.85(4) Å³, *Z* = 4 ρ = 1.285 mg·M⁻³, μ = 0.084 mm⁻¹, λ = 0.71073 Å, *T* = 100(2) K, *F*(000) = 688, θ (min) = 2.281°, θ (max) = 32.122°, 24644 reflections collected, 5381 reflections unique (*R*_{int} = 0.0193), GoF = 1.055, *R*₁ = 0.0371, *wR*₂ = 0.1014 [*I* > 2σ(*I*)], *R*₁ = 0.0400, *wR*₂ = 0.1032 (all indices), min/max residual density = -0.241/0.449 [e·Å⁻³], Completeness to θ (32.122°) = 92.0 %.

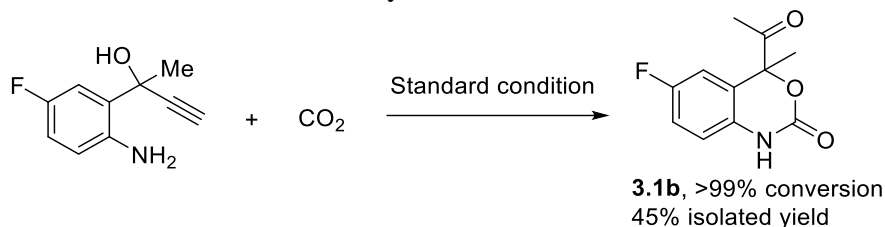


X-ray molecular structure for compound **3.H**. CCDC-2208333

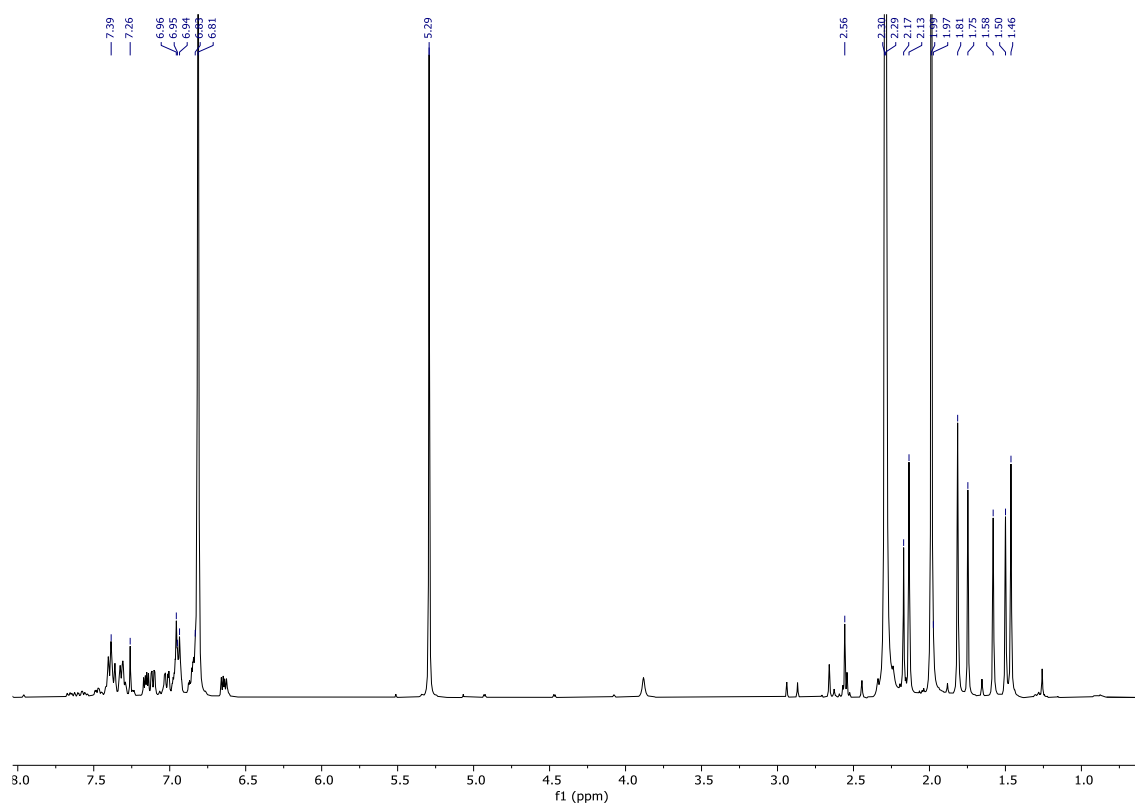
Crystallographic data for 3.H: C₂₂H₂₅NO₄, *M*_r = 367.43, monoclinic, *P*2₁/*c*, *a* = 10.0439(12) Å, *b* = 10.1689(12) Å, *c* = 18.381(2) Å, $\alpha = 90^\circ$, $\beta = 100.450(2)^\circ$, $\gamma = 90^\circ$, *V* = 1846.2(4) Å³, *Z* = 4, $\rho = 1.322 \text{ mg}\cdot\text{M}^{-3}$, $\mu = 0.091 \text{ mm}^{-1}$, $\lambda = 0.71073 \text{ \AA}$, *T* = 100(2) K, *F*(000) = 784, $\theta(\text{min}) = 2.062^\circ$, $\theta(\text{max}) = 32.595^\circ$, 46385 reflections collected, 6566 reflections unique ($R_{\text{int}} = 0.0572$), GoF = 1.053, $R_1 = 0.0516$, $wR_2 = 0.1332$ [$I > 2\sigma(I)$], $R_1 = 0.0719$, $wR_2 = 0.1455$ (all indices), min/max residual density = -0.489/0.697 [$\text{e}\cdot\text{\AA}^{-3}$], Completeness to $\theta(32.595^\circ) = 97.4\%$.

3.5.8 Additional control experiments and data

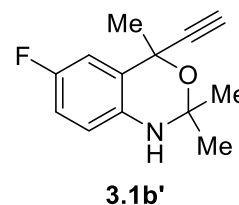
Analysis of crude reaction mixture in the synthesis of **3.1b**:



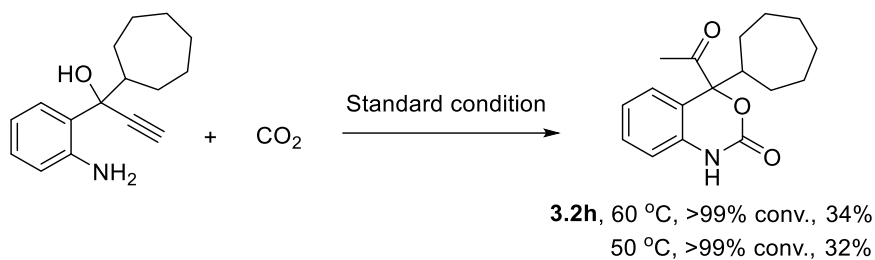
¹H NMR spectrum (400 MHz, CDCl₃) of “crude” **3.1b**



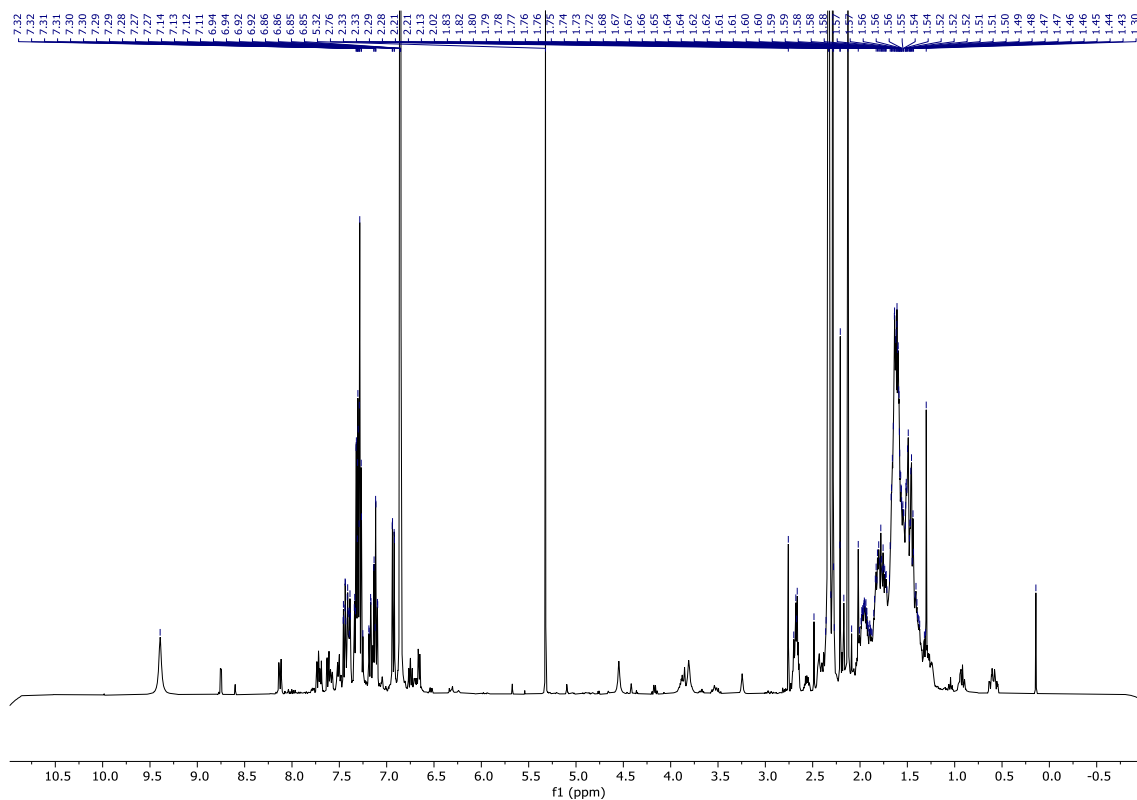
From the above-provided NMR spectrum with mesitylene as internal standard through signal integration we observe the following: >99% substrate conversion, about 43% NMR yield of product **3.1b** and 31% of a product (**3.1b'**) that we tentatively assign to the structure at the right-hand side. At this stage, the formation pathway of **3.1b'** is not clear but it shows that parasitic conversion of this substrate is possible.



Analysis of crude reaction mixture in the synthesis of **3.2h**:



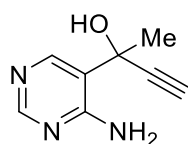
¹H NMR spectrum (400 MHz, CDCl₃) of “crude” **3.2h**



From the above complex ¹H NMR (CDCl₃) spectrum, we were unable to identify the formed byproducts (substrate conversion was >99%).

Control experiments using heterocycle-substituted propargylic substrates

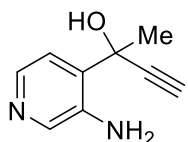
2-(4-Aminopyrimidin-5-yl)but-3-yn-2-ol



Prepared using the optimized procedure determined for **3.1a**. At 60 °C, yellow solid (513.7 mg, 63% yield). DCM/MeOH = 100/1. **¹H NMR** (400 MHz, CD₃OD) δ 8.38 (s, 1H), 8.30 (s, 1H), 3.23 (s, 1H), 1.78 (s, 3H); **¹³C NMR** (101 MHz, CD₃OD) δ 162.4, 158.0, 152.1, 121.0, 86.2, 75.7, 68.3, 29.4; **IR (neat, C=O, cm⁻¹)**: 3404, 3286, 3123, 2788, 1645, 1591 cm⁻¹. **HRMS** (ESI/TOF) m/z Calcd for C₈H₁₀N₃O [M + H]⁺ 164.0824; Found 164.0819.

Result: No product could be observed when trying to convert this substrate under the optimized conditions. In addition, upon increasing the reaction temperature to 100 °C and pressure to 50 bar no change was noted.

2-(3-Aminopyridin-4-yl)but-3-yn-2-ol



Prepared using the optimized procedure determined for **3.1a**. At 60 °C, pale yellow solid (461.9 mg, 57% yield). DCM/MeOH = 100/1. **¹H NMR** (400 MHz, CD₃OD) δ 8.34 (brs, 1H), 7.97 (s, 1H), 7.80 (d, *J* = 5.21 Hz, 1H), 7.52 (d, *J* = 5.21 Hz, 1H), 7.34 (brs, 2H), 3.20 (s, 1H), 1.78 (s, 3H); **¹³C NMR** (101 MHz, CD₃OD) δ 143.8, 138.5, 137.7, 137.0, 122.3, 86.7, 75.3, 70.2, 28.7.

Result: No product could be observed when trying to convert this substrate under the optimized conditions. In addition, upon increasing the reaction temperature to 100 °C and pressure to 50 bar no change was noted.

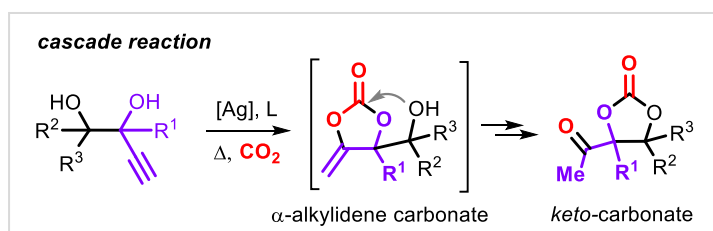
Chapter 4.

Summary and General Conclusions

UNIVERSITAT ROVIRA I VIRGILI
SILVER-CATALYZED CASCADE CONVERSIONS OF CO₂ INTO HETEROCYCLES
Xuetong Li

The main research objective of this thesis was the development of novel catalytic cascade approaches using propargyl alcohol derivatives and CO₂ as principal substrates. Such procedures could amplify the use of CO₂ as a renewable carbon reagent in multi-step processes leading to more complex compounds that are potentially useful as fine-chemical and pharmaceutical intermediates. The typically observed chemo-selectivity in the coupling of propargylic alcohols with carbon dioxide allows to establish α -alkylidene carbonates, and with the proper instalment of additional pro-nucleophilic groups (i.e., NH₂, OH) intramolecular isomerization/ring expansion can be induced. In this regard, a Ag/phosphine based catalytic system plays a crucial role in these cascade processes promoting the transformation of intermediate α -alkylidene carbonates to heterocyclic structures. Another key to success has been an efficient combination of a proper substrate design, reaction routes and rational ligand engineering. This allowed for a high control over the chemo-, regio-, stereo-selectivity features of the involved conversions. In the end, we have been able to design conceptually new processes by transforming propargylic alcohols into useful and functionally dense five-, six-, and seven-membered heterocycles.

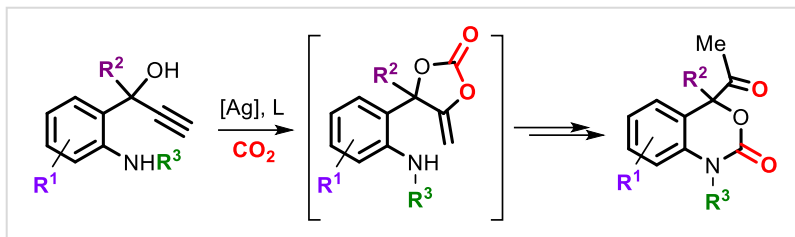
In **Chapter 2**, a new Ag-catalyzed process is reported for the cascade conversion of synthetically modular alkyne-1,*n*-diols and carbon dioxide allowing for the selective formation of *keto*-functionalized cyclic carbonates. The protocol is characterized by operational simplicity, excellent scope of carbonate-based heterocycles, and mild reaction conditions. In situ IR studies, control experiments, and detailed computational analysis of these manifolds support the intermediacy of an



α -alkylidene carbonate that can be intercepted by an intramolecular alcohol pro-nucleophile. The inherent synthetic potential of this conceptually attractive CO₂ transformation is demonstrated in the preparation of larger ring carbonates and their thermal rearrangement to sterically crowded, five-membered bicyclic carbonate products.

Inspired by the work discussed in chapter 2 of this thesis, the research described in **Chapter 3** focused on a conceptually novel catalytic domino approach for the synthesis of highly functional 1,4-dihydro-2*H*-1,3-benzoxazine-2-one (i.e., six-membered cyclic carbamate) derivatives. Key to the chemo-selectivity is a proper design of the precursor to override thermodynamically favored parasitic cyclization processes and empower the

formation of the desired product through Thorpe–Ingold effects (i.e., angle compression in the substrate is a main driver towards product formation). The synthetic diversity of these CO₂-based heterocycles was further demonstrated through the introduction of various substituents and



functional groups at different positions in the product. The isolation of a reaction intermediate supports our unusual ring-expansion sequence from an α -alkylidene, five-membered cyclic carbonate to a six-membered cyclic carbamate by *N*-induced isomerization. Access to a wider diversity of CO₂-based heterobicycles can further inspire the design of new biologically active compounds from a simple, cheap and readily available carbon reagent.

As a **General Conclusion** for the work presented in this thesis, the results suggest that that propargylic alcohols are highly versatile substrates for the design of multi-step synthetic sequences based on CO₂. This does not only expand the repertoire of functional heterocyclic compounds, but also showcases that more complex compounds are accessible through a judicious combination of cyclizative carboxylation and intramolecular isomerization by a nucleophilic present in the intermediate species. Such tandem sequences may be helpful to create a wider pallet of novel transformations expanding from a two- to multi-step cascades thereby increasing molecular complexity. In addition, the two-step cascades demonstrated in this thesis may provide a blueprint to combine with a multi-catalyst approach allowing to create more advanced derivatives from the final products without the requirement to isolate the intermediates. Crucial to success will be to determine a suitable operational window that permits to execute all these steps without comprising the individual efficiencies of each separate conversion. With the advancements made over the year in carboxylative cyclization and isomerization chemistry, we predict a bright future for cascade transformations that build on carbon dioxide utilization.

UNIVERSITAT ROVIRA I VIRGILI
SILVER-CATALYZED CASCADE CONVERSIONS OF CO₂ INTO HETEROCYCLES
Xuetong Li

UNIVERSITAT ROVIRA I VIRGILI
SILVER-CATALYZED CASCADE CONVERSIONS OF CO₂ INTO HETEROCYCLES
Xuetong Li

UNIVERSITAT ROVIRA I VIRGILI
SILVER-CATALYZED CASCADE CONVERSIONS OF CO₂ INTO HETEROCYCLES
Xuetong Li

